Mechanism of Lassa Virus Entry and Identification of Low Molecular Weight Drugs with Potential to Inhibit both Lassa and Ebola Virus Entry

Christine Elizabeth Hulseberg
Madison, Wisconsin

B.S. University of Illinois, 2007
M.S. University of Wisconsin, 2011

A Dissertation presented to the Graduate Faculty
of the University of Virginia in Candidacy for the Degree of
Doctor of Philosophy

Department of Microbiology

University of Virginia
August, 2018

Abstract

The arenavirus family has seven members that are considered Category A pathogens capable of causing severe hemorrhagic fever in humans. Lassa virus is by far the most clinically relevant virus in this family, causing tens or hundreds of thousands of infections in West Africa each year. Despite this tremendous public health burden, there are no specific licensed antiviral therapies for Lassa hemorrhagic fever, nor are there effective and approved vaccines. To develop the best possible drugs against Lassa virus, particularly those that intervene at an early stage of the viral infectious cycle, a detailed knowledge of its entry mechanism, particularly where and how host cell factors are involved, is required. The discovery that Lassa uses an endosomal receptor, Lamp1, during entry has opened a new field of inquiry about its role in facilitating viral entry. We show multiple lines of cell-based evidence that Lamp1 promotes entry of Lassa virus from compartments within the endocytic pathway by shifting the pH at which it fuses with the endosomal membrane. Our model for Lamp1's role proposes that, in its absence, pH-sensitive fusion proteins on the surface of Lassa virions are not activated, which prevents the viruses from escaping from endosomal compartments before inactivation. Noting many similar features between Lassa and Ebola virus entry, including that both viruses use a different endosomal receptor, we then asked whether a number of Ebola entry inhibitors also inhibit Lassa virus entry. After showing that six out of nine of these drugs were equally effective at blocking Lassa entry, one compound in particular, the anti-influenza drug, arbidol, was selected for further mechanistic studies. Our results are consistent with the proposal that arbidol impairs fusion of Lassa virus with host cells endosomes.

Table of Contents

List of Figures and Tables

Chapter 1

Chapter 3

List of Abbreviations

α-DG	Alpha dystroglycan
6HB	Six helix bundle
Ab	Antibody
ACE	Angiotensin-converting enzyme
AHF	Argentine hemorrhagic fever
APC	Antigen presenting cell
ASM	American Society for Microbiology / acid sphingomyelin
ATCC	American Type Tissue Culture Collection
β-DG	Beta dystroglycan
BHF	Bolivian hemorrhagic fever
BHK	Baby hamster kidney fibroblasts
βlaM	Beta lactamase
BMH	Bingham Memorial Hospital
BSL	Biosafety level
CAD	Cationic amphiphilic drug
CC	Cytotoxic concentration
CCHF	Crimean-Congo hemorrhagic fever
CCF	Cell-cell fusion
CDC	Centers for Disease Control and Prevention
CFR	Case fatality rate
CHHF	Chapare hemorrhagic fever

CHIKV	Chikungunya virus
CHPV	Chapare virus
CHO	Chinese hamster ovary
CME	Clathrin-mediated endocytosis
CRISPR	Clusters of regularly interspaced palindromic repeats
CPE	Cytopathic effect
DAA	Direct-acting antiviral
DC	Dendritic cell
DC-SIGN	DC-specific ICAM-3-grabbing non-integrin
DSHB	Developmental Studies Hybridoma Bank
DIC	Disseminated intravascular coagulation
DMEM	Dulbecco's modified Eagle's medium
DMSO	Dimethyl sulfoxide
DSP	Dual split protein
DTT	Dithiothreitol
DV	Dengue virus
EBOV	Ebola virus
EC	Effective concentration
ECM	Extracellular matrix
ER	Endoplasmic reticulum
ERGIC-53	Endoplasmic reticulum-Golgi intermediate compartment 53 kDa protein
ESCRT	Endosomal sorting complexes required for transport
EVD	Ebola virus disease

FACS	Fluorescence activated cell sorting
FBS	Fetal bovine serum
FFPM	Forced fusion at the plasma membrane
FIASMA	Functional inhibitor of acid sphingomyelinase
FIC	Fusion inhibitory concentration
GFP	Green fluorescent protein
GP	Glycoprotein
GPC	Glycoprotein precursor OR complex
GPd	Glycoprotein delta
gRNA	Guide RNA
GTOV	Guanarito virus
HA	Hemagglutinin
HCV	Hepatitis C virus
HEK	Human embryonic kidney
HIV	Human immunodeficiency virus
HMS	HEPES MES succinate
HR	Heptad repeat
HPI	Hours postinfection
HPT	Hours posttransfection
HSV	Herpes simplex virus
hTfR	Human transferrin receptor
IAV	Influenza A virus
IC	Inhibitory concentration

ICW	In-cell Western
ICU	Intensive care unit
IFITM	Interferon-induced transmembrane
IFN	Interferon
Ig	Immunoglobulin
IGR	Intergenic region
IL	Interleukin
IRF	Integrated Research Facility
ISG	Interferon stimulating gene
JUNV	Junín virus
kb	Kilobase
KD	Knockdown
kDa	Kilodalton
KGH	Kenema Government Hospital
KO	Knockout
L	Late domain OR arenavirus polymerase OR large RNA segment
LACV	La Crosse encephalitis virus
LAMP	Lysosomal associated membrane protein
LARGE	Like-acetylglucosaminyltransferase
LASV	Lassa virus
LCMV	Lymphocytic choriomeningitis virus
LHF	Lassa hemorrhagic fever
LLOV	Lloviu virus

LRN	Laboratory Response Network
LSECtin	Liver and lymph node sinusoidal endothelial calcium-dependent lectin
LTR	Long terminal repeat
LUJV	Lujo virus
mAb	Monoclonal antibody
MACV	Machupo virus
MARV	Marburg virus
MDA	Melanoma differentiation-associated protein
MERS-CoV	Middle East respiratory syndrome coronavirus
MES	Morpholineethanesulfonic acid
MLV	Murine leukemia virus
MOA	Mechanism of action
MoH	Ministry of Health
MOI	Multiplicity of infection
MORV	Morogoro virus
mRNA	Messenger RNA
MRU	Mano River Union
MRU-LFN	Mano River Union Lassa Fever Network
MS	Mass spectrometry
MVB	Multivesicular body
MWCO	Molecular weight cutoff
nAb	Neutralizing antibody
NAG	N-acetylglucosamine

NK	Natural killer cell
NHE	Sodium hydrogen exchanger
NP	Nucleoprotein
NPC1	Niemann-Pick C1
NR	Neutral red
NRP	Neuropilin
OMEM	Opti-MEM
O/N	Overnight
ORF	Open reading frame
PAM	Protospacer adjacent motif
PAMP	Pathogen-associated molecular patterns
PBS	Phosphate buffered saline
PFAM	Paraformaldehyde
PEI	Poly(ethylenimine)
PFU	Plaque forming unit
PM	Plasma membrane
RBR	Receptor binding region
RBS	Receptor binding site
RdRp	RNA-dependent RNA polymerase
RIG-I	Retinoic acid-inducible gene I
RING	Really Interesting New Gene
RIPA	Radioimmunoprecipitation assay
RLU	Relative light unit

RME	Receptor mediated endocytosis
RNP	Ribonucleoprotein complex
RSV	Respiratory syncytial virus
RT-PCR	Reverse transcriptase polymerase chain reaction
S	Small RNA segment OR Spike protein
SABV	Sabiá virus
SARS	Severe acute respiratory syndrome
SCS	Supplemented calf serum
SDS-PAGE	Sodium dodecyl sulfate-polyacrylamide gel electrophoresis
SFV	Semliki Forest virus
shRNA	Short hairpin RNA
siRNA	Small interfering RNA
SKI-1/S1P	Subtilisin kexin isozyme-1/site-1 protease
SNHL	Sudden-onset sensorineural hearing loss
SPR	Surface plasmon resonance
SSP	Stable signal peptide
TACV	Tacaribe virus
TAM	Tyro3, Axl, Mer
TCID	Tissue culture infectious dose
TfR	Transferrin receptor
TGN	Trans-Golgi network
TIM	T cell immunoglobulin mucin domain
TLR	Toll-like receptor

TM	Transmembrane
TMD	Transmembrane domain
TNF	Tissue necrosis factor
TSA	Thermal shift assay
TSG	Tumor susceptibility gene
USAMRIID	United States Army Medical Research Institute for Infectious Disease
UTR	Untranslated region
UUKV	Uukeniemi virus
VCF	Virus-cell fusion
VHF	Venezuelan hemorrhagic fever
VLP	Virus-like particle
VOPBA	Viral overlay protein blot assay
VSV	Vesicular stomatitis virus
VV	Vaccinia virus
YARU	Yale Arbovirus Research Unit
WT	Wildtype
WWAV	Whitewater Arroyo virus
WWS	Walker-Warburg syndrome
Z	Arenavirus matrix protein

Acknowledgements

When I began my doctoral studies at the University of Virginia almost exactly three years ago, I had just completed a two-year tour with the Walter Reed Project in Kericho, a rural town located in the highlands of western Kenya. Having spent over 18 years in the Army, I was no stranger to abrupt transitions, but the move from overseas laboratory director to new graduate student was particularly extreme. During my first semester here, which was spent surrounded by the bright minds and youthful faces of my fellow first year graduate students in the notoriously rigorous Core Course, it felt almost inconceivable that I would be able to fulfill my contractual obligation to finish this dissertation within 36 months. And yet thanks largely to the tremendous support from the academic community at the University of Virginia, this mandate was not only satisfied, but these few years in Charlottesville have also been some of the happiest of my life.

At the very top of the long list of people to whom I am indebted is, of course, my mentor, Dr. Judy White. Slight incarnate, but towering in her field, Judy is a remarkable scientist and person - someone who I have regarded as an exemplary role model. Her focused attention-to-detail, impeccable judgement, and organizational skills have led me to reflect - on many a wistful occasion - that she would have made a fine Colonel in the Army Medical Department. Beyond the scientific mentorship and guidance Judy has provided, I am also most grateful for her generosity and for always making herself accessible. I cannot imagine thriving under any other mentor as I have with Judy and am so proud to have been her student.

Next to Judy, I credit our lab manager, Elizabeth Nelson (Liz), as an Indispensable. Having scarcely held a pipet during the roughly seven-year interim between my Master's

and doctoral studies, I doubt whether I could have made it through this program without her patient supervision while I recovered and developed my bench skills. Liz has also been my closest friend at UVA; I will deeply miss her cheerful companionship and sunny disposition. I am inordinately grateful to (and fond of) my other coworkers and friends in the White Lab. Lucie Fénéant, Kasia Szymańska, Kelly Drews, and Maya Cabot have each made their own ineffable contribution to sustain the productive, but always convivial, atmosphere in our close-knit lab. I was particularly fortunate to have had the opportunity to mentor a very talented undergraduate, Natalie Kessler, who has always been a bright star in my eyes. Other individuals outside the lab I would like to thank for their friendship, support, and encouragement are: Christina Rodriguez, Brian McKenna, Laurie Gray, Becky Stanhope, Pedro Pinheiro, Alex Kreutzberger, Laura Odongo, Amanda Ward, Patrick Seelheim, Ryan D'Souza, Adam Greene, Jeff Romano, Pooja Sonavane, and Megan Harris.

I thank the members of my academic advisory committee for their outstanding support and guidance: Drs. Dean Kedes (my very patient committee chair), Jim Casanova, Dan Engel, David Rekosh, and Lukas Tamm. Drs. Amy Bouton and Lucy Pemberton were both instrumental in accommodating my special circumstances here at UVA. Other faculty members to whom I am grateful are Drs. David Castle, Barb Mann, Doug DeSimone, Mazhar Adlii, Cem Kuscu, and Barry Hinton. The program administrators, Sandy Weirich and Amy Andersen, have both been terrific; every graduate student in the department is lucky to have them. Drs. Stephen Polyak at the University of Washington, Seattle, and Connie Schmaljohn and Charles (Jason) Shoemaker, both at the Virology Division at the US Army Medical Research Institute of Infectious Diseases, our collaborators for the work

presented in Chapter 4, have worked tirelessly in support of the associated manuscript. In addition to performing the live Lassa virus experiments for this study, my future colleague (and a former White Lab member), Jason, has been incredibly helpful in smoothing the way for my transition back to Army life at my next assignment in Fort Detrick, Maryland.

The Army's Long Term Health Education and Training (LTHET) program has provided the financial support for my studies. I appreciate the administrative support provided by my unit, the 187th Medical Battalion, 32d Medical Brigade at the Army Medical Department Center and School in Fort Sam Houston, Texas. Colonel Rodney Coldren, a mentor and close personal friend, played a large part in my selection for the LTHET program.

Lastly, I thank my family for never leaving my side no matter how far away I am. To my parents, Don and Sandy, my brother, Paul, and my sister-in-law, Orathai: I love you very much.

Chapter 1

Introduction

1.A. Overview of Arenaviruses

Lassa virus is a member of the *Arenaviridae*, a diverse family of enveloped RNA viruses. Until recently the family was comprised of a single genus of rodent-borne viruses, but with the recent discoveries of a two additional genera of reptile-borne viruses, the 25-member taxon has been reordered to now include the rodent-borne *Mammarenavirus*, the *Reptarenavirus*, and the *Hartmanivirus* [1-3]. *Mammarenavirus* is further divided into two groups based upon antigenicity, geographical distribution and phylogenetic relatedness. Pathogenic Old World arenaviruses include the Lassa and Lujo viruses, both found in Africa, and lymphocytic choriomeningitis virus, which has worldwide distribution. The New World arenaviruses are found mainly in Central and South America (**Figure 1.1**) [4]. The discovery of the major pathogenic arenaviruses is overviewed chronologically, with the exception of Lassa virus which follows in a more detailed section.

1.A.1. Brief History of Pathogenic Arenaviruses and Major Outbreaks

Lymphocytic choriomeningitis virus (LCMV), the first arenavirus identified from a human isolate, was discovered adventitiously during an outbreak of encephalitis in the 1930s [5]. During the investigation into the encephalitis epidemic, Charles Armstrong, a surgeon with the US Public Health Service, collected cerebrospinal fluid of a woman who was determined upon autopsy to have succumbed to a primary infection with St. Louis encephalitis virus, a flavivirus, [6].

FIG 1.1. Phylogeny of arenaviruses. Clustering based upon the GPC sequences of Old and New World mammarenaviruses. The pathogenic members (indicated by an asterisk) of the New World arenaviruses of South America are in Clade B, while LASV and LCMV are pathogenic Old World arenaviruses. LUJV, also pathogenic, does not cluster with Old World arenaviruses, but is more closely related to them. Obtained from Zong et al. [4] with permission from American Society for Microbiology (ASM) (license 435724124931).

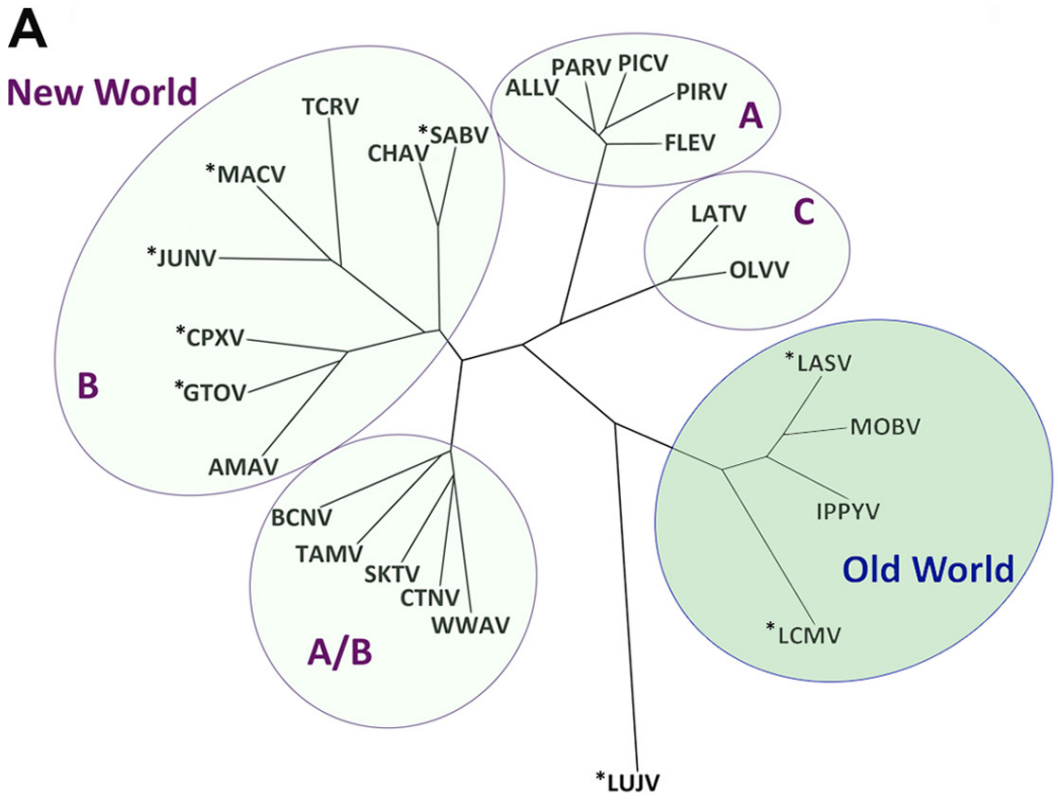
A
New World
TCRV
*SABV
CHAV
*MACV
*JUNV
*CPXV
*GTOV
AMAV
B
ALLV
PARV
PICV
PIRV
FLEV
A
LATV
C
OLVV
*LASV
MOBV
IPPYV
Old World
*LCMV
BCNV
TAMV
SKTV
CTNV
WWAV
A/B
*LUJV

Hoping to cultivate St. Louis encephalitis virus by transferring the inoculum into monkeys and mice, Armstrong instead isolated LCMV[1].

The following year in 1936, Rivers and Scott isolated and identified LCMV as the etiologic agent of several cases of acute nonbacterial meningitis; this strain became known as WE, after the initials of one of the patients [7, 8]. That same year, Erich Traub serologically linked LCMV isolates from his mouse colonies (the Traub strain) to Armstrong's LCMV isolates [9-11], providing the initial evidence of the virus's zoonosis from rodents to humans. Much of the LCMV-related research in last the 80 years has involved these three strains isolated in the 1930s.

Following its discovery, LCMV became a model virus to study chronic versus acute viral infections as well as the prototypical virus for the emerging pathogens of the arenavirus family. A major advantage to working with this virus – arguably one of the most well-studied of all viruses – was that it was considered relatively safe and could be handled in BSL2 laboratories. However, when it became known in the 1960s and 70s that passaging the virus through hamsters could increase its virulence, advisory boards upgraded the precautions for handling clinical, uncharacterized, or hamster-passaged LCMV isolates to BSL3 conditions [12-14]. Despite increased awareness of the potential for laboratory-acquired LCMV infection, high profile outbreaks have occurred. Of the most notable was in 1973, when 21 out of a total of 48 infected workers involved in using Syrian hamsters for tumor research became ill (with no lethal cases) [15]. To date, there have only been five

[1] Armstrong named the virus after describing the resulting pathologies in his animals. This strain of LCMV isolated from monkeys was, in turn, named after Armstrong.

reported fatal cases from laboratory infections, most of which involve direct handling of infected animals [15-19]. Hemorrhagic symptoms are rare but have been reported [20].

As with many arenavirus infections, LCMV infections are usually acquired via inhalation of excreta from infected mice and hamsters, which can shed high titers of the virus in saliva, nasal secretions, urine, and feces regardless of whether the animals are healthy or sick [21]. Thus sporadic cases occur worldwide after exposure to wild rodent excreta, but the primary outbreak risk is posed by the pet industry, particularly since sales and distribution of pet rodents is not federally regulated. One such large multi-state outbreak occurred in 1974, when 181 people across 21 states fell ill after contact with LCMV-infected pet store hamsters [22, 23]. In a 2012 outbreak of LCMV, 32% of workers employed at several rodent breeding facilities were infected; four of these otherwise healthy workers developed aseptic meningitis [24]. Infection among immunocompromised individuals is more common, particularly among transplant recipients. A 2005 outbreak among several organ transplant recipients was traced to a common donor who had purchased an infected hamster [25]. Similar clusters of transplant-acquired LCMV infections stemming from common donors have also been reported in recent years [26].

In the early 1950s, reports of hemorrhagic fever of an unknown etiology emerged from a densely populated area of Buenos Aires [27]. Parodi et al. managed to identify the viral etiologic agent of the outbreak in 1958, and named it Junín after the city and county of its discovery [28]. The disease caused by Junín virus (JUNV), Argentine hemorrhagic fever (AHF), is classically associated with male agricultural workers who likely contract the virus by inhaling rodent-contaminated aerosols near mechanical grain harvesters [29].

Outbreaks of AHF are infrequent, but the disease seasonally spikes during the

harvesting months of May and June[2]. The incidence of AHF peaked in Argentina in 1964 with over 3000 cases and a case fatality rate (CFR) of 20% [29]. Prior to the deployment of the first – and only – arenavirus vaccine, Candid #1, AHF was the most clinically significant arenavirus in the Western hemisphere [32, 33]. Owing to the success of Candid #1, there are usually under 50 cases of AHF reported per annum, despite an at-risk population of approximately 5 million people [34].

In the late 1950s / early 1960s, pockets of hemorrhagic fever began to occur in rural areas of northern Bolivia [35]. Hundreds of cases of what was called "black typhus" were reported in Bolivia from 1959 – 1962 alone [36]; one small town affected during this period lost nearly 10% of its entire population (CFR = 41%) [37]. In 1963, Machupo virus (MACV) (named after a nearby river) emerged as the etiologic agent of the newly described Bolivian hemorrhagic fever (BHF) after it was isolated from the spleen of one of the victims of the outbreak [38]. As with AHF in neighboring Argentina, BHF disproportionately affected male agricultural workers and occurred most frequently during harvest times. Indeed, an outbreak of BHF in 1962 that spread into an urban area was largely attributed to an uptick in the rodent population following a sudden decline in the city's cat population. Effective rodent control programs implemented in the mid 1960s were highly successful in reducing transmission of MACV [39]. In fact, after an outbreak in 1971 (which involved a rare case of person-to-person transmission of a MACV

[2] Interestingly, it has been speculated that a hemorrhagic fever virus, possibly JUNV, caused the great epidemic in 16th century Mesoamerica that decimated native populations [**30**. Marr, J.S. and J.B. Kiracofe, *Was the huey cocoliztli a haemorrhagic fever?* Med Hist, 2000. **44**(3): p. 341-62, 31. **31**. Acuna-Soto, R., L.C. Romero, and J.H. Maguire, *Large epidemics of hemorrhagic fevers in Mexico 1545-1815.* Am J Trop Med Hyg, 2000. **62**(6): p. 733-9].

infection) [40], twenty years elapsed before sporadic cases began to reemerge in the mid 1990s [36]. Notable clusters of BHF following this mysterious period of dormancy include: 19 cases in 1994, eight cases in 1999, 18 cases in 2000, and 20 cases in 2007 (CFR = 20%), and 200 suspected cases in 2008 [36, 41-43].

Severe hemorrhagic fever broke out again in the Venezuelan town of Guanarito during the fall of 1989 [44]. Initially suspected as dengue fever, which is common throughout much of Venezuela, most patients presented with fever, arthralgia, nausea/vomiting, diarrhea, and cough; others presented with bleeding gums and mouth, thrombocytopenia, facial edema, hematemesis, and petechial hemorrhaging. Despite intensive supportive care for 15 hospitalized patients, nine of the patients died within six days of admission. Recognizing similarities to AHF and BHF, clinical or autopsy samples sent to the CDC for virus isolation and serology were handled under special precautions [44]. The isolated virus, Guanarito (GTOV), was found to the etiologic agent of Venezuelan hemorrhagic fever (VHF), the third arenavirus-caused South American hemorrhagic fever [45]. Given the restrictive range of GTOV's rodent vector, area researchers were able to closely study the 165 suspected cases of VHF that occurred during the eight-year period from 1989-1997 [46]. The CFR for VHF-confirmed cases during this period was 33.3%. Of five reported VHF outbreaks, the most recent was in 2016, when there were 142 suspected cases and a CFR of 14.7% [47].

Sabiá virus (SABV), the causative agent of Brazilian hemorrhagic fever or São Paulo hemorrhagic fever, was discovered in 1990 [48]. Blood samples from the index case, a lethal case originally diagnosed as yellow fever, were sent to the US Army Medical Research Institute for Infectious Disease (USAMRIID) and the Yale Arbovirus Research

Unit (YARU) for isolation and characterization. Two additional cases of SABV-related illness, both involving non-lethal laboratory accidents, occurred in 1992 and 1994 [49-51]. An exceedingly rare disease in humans, the most recently confirmed case of Brazilian hemorrhagic fever was a lethal case in a male coffee-grain machine operator in 1999 [52]. Chapare virus (CHPV) is the most recently identified pathogenic New World arenavirus. Chapare hemorrhagic fever (CHHF), like Brazilian hemorrhagic fever, is quite rare and has so far only been reported in a single lethal case in 2003 involving a male farmer near Cochabamba, Bolivia [53]. This case also presented with symptoms indistinguishable from yellow fever or dengue hemorrhagic fever. After the patient's specimens tested negative for yellow fever, dengue fever, and MACV, samples had to be sent to the CDC's BSL4 containment laboratory for virus isolation and characterization.

The most recently identified Category A arenavirus is the Old World arenavirus, LUJV[3] [54]. To date, the only human LUJV infections occurred during a small outbreak in Zambia and South Africa that occurred 40 years after LASV's discovery in West Africa [55]. The index case was a tour guide living outside of Lusaka who was airlifted to Johannesburg, South Africa after she fell ill. The original source of the infection was never determined, but, as her condition worsened, the arduous diagnoses evolved from food poisoning to influenza to tick-borne disease. She died from acute respiratory distress two days after arriving in South Africa (and ten days after the onset of symptoms) without having been tested for viral hemorrhagic fever. Her body was not autopsied. Seventeen days after the tour guide's death, the Zambian paramedic who treated her en route to South

[3] The name Lujo is a portmanteau of Lusaka (Zambia) and Johannesburg (South Africa).

Africa developed flu-like symptoms and was admitted to the same hospital in Johannesburg as the tour guide. The next day, a South African nurse who had treated the tour guide in the ICU became ill. The results from liver biopsies from both the second and third cases showed necrosis and vasculitis, confirming viral hemorrhagic fever and prompting the hospital to coordinate epidemiological investigations and adopt full precautions. The fourth confirmed case was a custodian who had cleaned the room of the index patient, and who had been identified through contact tracing. She died on the day of her admission (three weeks after exposure) from a comorbidity. The fifth and final case was another nurse who became infected after treating the Zambian medic. She was the only patient who was treated with ribavirin and cared for under full special infection control measures throughout. She was discharged 51 days after her admission after multiple negative blood and urine results from RT-PCR. The CFR for this sole LUJV outbreak in 2008 was 80% [56, 57].

1.A.2. Origins and Outbreaks of Lassa Hemorrhagic Fever

Although LASV was only been scientifically described in the last half a century, it is not a new virus. Molecular dating of LASV isolates indicates that it has been circulating in Nigeria since ~900-1300 AD [58, 59]. Furthermore, haplotyping of geographically diverse groups indicates a strong selective pressure for LASV-resistant alleles in Nigerian populations, suggesting a long history of transmission and co-evolution with humans [60-63].

Nigeria has three distinct LASV lineages currently circulating (I-III). Movement of the virus out of Nigeria began 300-500 years ago, but a fourth extant LASV lineage (IV)[4] did not become established in the Mano River Union (MRU) region of Guinea, Sierra Leone, and Liberia until 150-250 years ago, probably during the diaspora of the colonial period in West Africa [59, 64, 65]. A fifth LASV lineage from Mali and Côte d'Ivoire may have emerged as a consequence of the refugees from the Sierra Leonean civil war of 1991-2002 [59, 66, 67].

Cases suggestive of Lassa hemorrhagic fever (LHF) reported by French researchers in West Africa began to appear the 1930s and 40s [68, 69]. Described as a "savanna typhus', the febrile illnesses were characterized by severe headache, neurological impairments, terminal hypotension, rash, uremia, and shock. Notably occurring among hunters of small rodents, the mortality rate was estimated to be 50%. Although it is likely not possible to definitively reconcile whether these cases were actual LHF or murine typhus, stronger epidemiological evidence of LHF emerged in the mid 1950s in Sierra Leone where an outbreak of 45 LHF-like cases occurred (CFR = 29%) [70, 71]. Years later, serum samples collected from hundreds of missionaries stationed in Africa were tested to determine exposures to LASV [72]. LASV neutralizing antibodies (nAbs) were evident in individuals who had worked in Nigeria as far back as the early 1950s [73]; clinical histories from the seropositive missionaries involve both symptomatic and asymptomatic recollections [72].

[4] Josiah, the prototypical strain used in most LASV vaccine studies (and the work for this dissertation), belongs to lineage IV.

On January 25th, 1969, physicians at Bingham Memorial Hospital (BMH) in Jos, Nigeria received what would become the first case of LHF to be described in the literature [74]. A 69-year-old nurse had been airlifted from the mission hospital in Lassa, Nigeria after her condition had worsened precipitously. Initially treated for oral ulcerations, sore throat, aches, fever, she soon manifested hemorrhagic and neurological symptoms. After going into cardiac arrest, she was given digoxin and steroids and her physicians were forced to apply tourniquets to her extremities in an attempt to maintain her blood pressure. She ultimately died the day after admission to BMH, and her body was returned to Lassa for autopsy. Days after her death, a nurse who had cared for her reported having chills, sore throat, and body aches. She too went on to develop features of vascular and neurologic impairment – with significant respiratory distress – and died ten days after the onset of illness. By the time a third nurse (who had treated both of the initial patients at BMH and assisted in their autopsies) presented with fever, sore throat, and other minor symptoms, the hospital's medical team decided the situation warranted sending her back to the US for treatment. Although biosafety standards were comparatively lax at the time, she was nevertheless put into an isolation ward upon arrival at the Columbia-Presbyterian Medical Center in New York [75]. After three months of acute illness and gradual recovery, she was deemed well enough to be discharged with relatively minor sequela (despite lack of laboratory-based evidence that she had cleared the virus) [73].

The next year, Frame et al. published clinical and pathological findings from these three cases [74]. They described a litany of diseases considered in the differential, as well as the difficulty of proving the epidemiologic linkages between the cases. Despite the multitude of diagnostic challenges, they were remarkably astute in noting similarities

between LHF and severe LCMV infection. Another prescient observation was that, given the severity of the disease, LASV was likely maintained in an animal reservoir and probably not "well-adapted" to humans. It was also apparent (from the second case in particular, where the nurse in BMH contracted LHF after treating the patient transported from Lassa) that the pathogen could nonetheless be transmitted person-to-person. When YARU pathologists Jordi Casals and Sonja Buckley reported that they had isolated a virus from the blood specimens of all three patients, Frame was finally able to diagnose the cases as Lassa fever, naming the virus and disease after the unfortunate town in Borno State where the first nurse presumably contracted the virus [74, 76]. Dr. Casals, who nearly died from LHF himself while handling these specimens that summer in 1969, was credited with discovering the virus. One of his colleagues helping him at Yale did in fact die from laboratory-acquired LHF (the first lethal case in the US) [69]. These two back-to-back cases of LHF on US soil elicited an abrupt end to the LASV-related work at YARU. It also permanently changed the biosafety landscape in the US, codifying new biosafety regulations requiring that infectious agents like LASV be sent to either the CDC or USAMRIID (the only two maximum security BSL4 facilities in the Laboratory Response Network) [77-79].

Less than a year after the first case cluster of LHF, a much larger outbreak of LHF occurred in Jos [80-82]. Out of 28 cases there were at least 14 deaths (CFR = 52%) [83]. One of the lethal cases included Jeanette Troup, a well-known pathologist also involved in the 1969 outbreak who was infected while performing autopsies on victims of this second outbreak [81, 84].

From 1970-1972, an area of eastern Sierra Leone over 1400 miles from Nigeria experienced an epidemic of LHF involving 63 cases [85, 86]. Based on the number of hospitalized cases, the CFR was initially assessed as 38%. However, given the high seropositivity to LASV IgG in this area (10%-52% of the population, frequently cited as the highest in the world) [85, 87-89], it became clear that subclinical LASV infections in humans were quite common as well. Fraser et al. therefore adjusted the CFR to <5% based on seroconversion rather than symptomatic infections [85]. Another early and oft-cited epidemiologic study conducted in the 1980s based its annual LASV morbidity and mortality statistics for West Africa on data gathered from this hyperendemic area of Sierra Leone; the extrapolated figures suggest there are 100,000-300,000 LASV infections and 5,000 deaths per year in West Africa [87].

After the prolonged 1970s Sierra Leone outbreak, the CDC partnered with Sierra Leone's Ministry of Health (MoH) to establish several regional treatment and research centers for LHF in the heart of the MRU countries [89-91]. The director of the largest of these facilities, Dr. Aniru Conteh, continued to maintain the Lassa ward at Kenema Government Hospital (KGH) throughout the Blood Diamond civil war in Sierra Leone from 1991-2002, even after the CDC suspended its in-country activities in 1993. However, after Dr. Conteh's death from LHF in 2004 (and in combination with waning financial support from the CDC and the destruction of much of Sierra Leone's own healthcare infrastructure) the LASV program became largely defunct. Several years later researchers at Tulane University secured substantial post-9/11 bioterrorism funding from the NIH to develop control and prevention strategies for LHF. Upon partnering with the WHO, UN, USAMRIID, and the MRU governments, they formed the Mano River Union Lassa Fever

Network (MRU-LFN) and relaunched the Lassa program at KGH and several other sites [90-92]. With a primary focus on LASV diagnostics, the LASV program at KGH was also charged with running the LASV treatment ward, performing much of the epidemiologic surveillance work across the MRU, implementing rodent control measures, and providing community education [91]. It also became a critical center for Ebola virus (EBOV) testing and treatment during the 2013-2016 epidemic [88, 90-92].

In a relatively short period of time following the initial reports of LHF, the Lassa fever belt in West Africa became defined as a noncontiguous, barbell-shaped region stretching from Guinea in the west to Nigeria in the east (**Figure 1.2**). The strongest areas of LHF endemicity are in forested areas of Sierra Leone, Guinea, Liberia, and Nigeria, but seroprevalence – and sometimes even outbreaks – has been reported in Mali, Togo, Benin, Burkina Faso, Senegal, Côte d'Ivoire, Guinea-Bissau, Cameroon, Niger, and Ghana [93-98]. Unlike the hemorrhagic fevers caused by the filoviruses, the South American arenaviruses, and other hemorrhagic fever viruses, LHF is not a rare disease. LASV's long incubation period (of up to three weeks) also makes it one of the most commonly imported hemorrhagic fever viruses. Indeed, the cumulative number of imported LHF cases documented (including the US, the UK, Germany, Sweden, Canada, Israel, South Africa, and Japan) has been considerable over the past few decades [99-112].

FIG 1.2. Map of arenavirus distribution. The distribution of the pathogenic members of the South American New World arenaviruses is indicated on the map on the left. On the right, endemic areas for LHF are in blue while EBOV endemic areas are in green. Regions of West Africa which are endemic for both LASV and EBOV are colored in turquoise. Image generated from mapchart.net.


Pathogenic New World Arenaviruses
Junín (1958)
Machupo (1963) / Chapare (2008)
Sabiá (1990)
Guanarito (1990)
VENEZUELA
COLOMBIA
ECUADOR
PERU
BRAZIL
BOLIVIA
PARAGUAY
CHILE
ARGENTINA
URUGUAY
GUYANA
SURINAME
FRENCH GUIANA
TRINIDAD AND TOBAGO
PANAMA
FALKLAND ISLANDS


Filoviruses and Pathogenic Old World Arenaviruses
Lassa
Ebola/Marburg
Lassa and Ebola
Lujo
TUNISIA
MOROCCO
ALGERIA
LIBYA
EGYPT
WESTERN SAHARA
MAURITANIA
MALI
NIGER
CHAD
SUDAN
ERITREA
DJIBOUTI
CAPE VERDE
SENEGAL
THE GAMBIA
GUINEA-BISSAU
GUINEA
BURKINA FASO
BENIN
NIGERIA
SIERRA LEONE
LIBERIA
COTE D' IVOIRE
GHANA
TOGO
CAMEROON
CENTRAL AFRICAN REPUBLIC
SOUTH SUDAN
ETHIOPIA
SOMALIA
EQ. GUINEA
SÃO TOMÉ AND PRÍNCIPE
GABON
CONGO
UGANDA
KENYA
RWANDA
DR CONGO
BURUNDI
TANZANIA
SEYCHELLES
ANGOLA
ZAMBIA
MALAWI
MOZAMBIQUE
COMOROS
MAYOTTE
MADAGASCAR
MAURITIUS
RÉUNION
ZIMBABWE
NAMIBIA
BOTSWANA
SWAZILAND
LESOTHO
SOUTH AFRICA

Despite the lower adjusted CFR and its entrenched endemicity, LHF is still considered a disease with epidemic potential [113]. In recent years, there has been a steady increase in the incidence of LHF cases. With nearly 1,000 suspected cases, the 2012 outbreak in Nigeria was, up until then, one of the largest documented LHF outbreaks [114, 115]. However, the 2018 LHF epidemic (also in Nigeria) has dwarfed the 2012 outbreak [116, 117]: from January 1st 2018 until the end of the emergency phase was declared May 9th, 2018, there were 1894 suspected cases, 423 confirmed cases, and 106 deaths [118], making it the largest LHF recorded outbreak [119]. The precise reasons for the size and scale of this outbreak are not clear, but changing ecological niches for LASV's rodent reservoir and weak, destabilized healthcare infrastructure are likely factors.

1.A.3. Arenavirus Reservoirs

Rodents are the natural reservoirs of all mammarenaviruses, with the exception of two viruses: the nonpathogenic bat-borne New World Tacaribe virus (TACV) in the Caribbean, and the newly identified shrew-borne Old World Wēnzhōu virus in South East Asia [120]. Healthy rodent carriers typically shed high titers of virus in their excreta throughout their lifespan. Transmission of arenaviruses to humans occurs primarily by contact with infected rodent excreta, inhalation of aerosolized virus, and consumption of rodent meat. In heavily endemic areas, spillover from peridomestic rodents in close contact with rural populations is usually the cause of infection. Rodent control efforts, particularly those implemented in Bolivia to reduce MACV transmission, have been highly effective in curbing incidence of human arenavirus infections but require sustained commitment to be successful [29, 121]. Generally, the area of endemicity for each arenavirus is restricted by the range of its

respective rodent reservoir. Accordingly, LCMV is the only arenavirus with worldwide distribution since it is carried by the ubiquitous house mouse, *Mus musculus*. For a more thorough review on the animal reservoirs for the reptarenaviruses and New World mammarenaviruses, see the review articles by Sarute et al. and Charrel et al. [122, 123]. LASV's primary natural host species is the Natal multimammate mouse *Mastomysis natalensis* [85, 124, 125], but LASV has recently been detected in at least two other rodent species: the African wood mouse, *Hylomyscus pamfi* in Nigeria and the Guinea mouse, *Mastomys erythroleucus* [126]. Multimammate mice are common throughout Africa, and have a role in the transmission and spread of a number of other important diseases, including leptospirosis, leishmaniasis, bartonellosis, and plague [64]. It is not clearly understood why the endemic area of LHF in West Africa is confined to a smaller region relative to the broad range of its host, which extends across much of the continent.

In contrast to EBOV, which can be maintained for long periods of time in human-to-human transmission chains, LASV is sustained mainly by rodent-to-rodent transmission. Rodents are usually infected *in utero* and carry the virus throughout life, but horizontal transmission in rodent colonies is also common [124]. Analysis of the phylogenetic relatedness of LASV isolates from both *M. natalensis* and humans has confirmed that infections in humans are usually the result of multiple separate rodent-to-human transmission events [58]. Person-to-person transmission of LASV contributes to as much as ~20% of LHF cases [127], but this mode of transmission is likely supported mostly in nosocomial settings. Besides humans, other mammals susceptible to secondary LASV infections include primates, bats, dogs, guinea pigs, hamsters, rabbits, and squirrels [13, 128-133]. Notably, birds appear to be resistant to LASV infection [134, 135].

1.A.4. Clinical Presentation of Lassa Hemorrhagic Fever

An estimated 80% of human LASV infections are either too mild to require medical attention or altogether asymptomatic [136]. When an infection is established, however, incubation periods can be very long, sometimes up to 21 days after exposure [137]. Of the constellation of symptoms reported in the literature, no one sign (even fever, the most common) is omnipresent in LHF, and thus the symptoms that listed in **Table 1.1** are inclusive but not highly specific. The earliest complaints are often fever, headache, and malaise, shortly followed by dysphagia (difficulty and painful swallowing), exudative pharyngitis (painful swelling near the back of the throat), elevated heart rate, and chest pain. Over 50% of patients develop joint and back pain. If the illness advances, gastrointestinal problems such as diarrhea, vomiting, and abdominal pain may follow. Respiratory involvement, such as rales (a crackling noise during respiration), pleural effusion/edema (the accumulation of fluids in the chest cavity), cyanosis (a bluish discoloration of the skin associated with inadequate oxygenation), and adult respiratory distress syndrome occurs in ~20% of cases [138]. Some form of neurological impairment, including mania, insomnia, confusion/delirium, dementia, encephalopathy, ataxia, and tremors, occurs in 10% of cases [139]. Sudden-onset sensorineural hearing loss (SNHL),

TABLE 1.1. Symptoms of Lassa hemorrhagic fever. Incubation periods for LHF range from one to three weeks. Differential diagnosis is difficult during early stages, when flu-like symptoms present. Involvement of hemorrhagic dysfunction and/or neurologic involvement is associated with a poor prognosis for survival. Material from the open access article by Yun et al. [93].

Clinical signs and symptoms	Day of illness		Duration, days
	Start day	End day	
Fever	1	11	10
Weakness	3	14	11
Cough	3	14	11
Chest pain	4	13	9
Back pain	4	12	8
Joint pain	4	12	8
Sore throat	4	11	7
Dysuria	4	10	6
Headache	4	11	7
Abdominal pain	5	8	3
Vomiting	5	9	4
Diarrhea	5	9	4
Pharyngitis	7	12	5
Conjunctivitis	7	12	5
Bleeding	7	11	4
Abdominal	9	14	5
Rales	9	14	5
Facial edema	9	16	7

which typically does not manifest until convalescence, is common even in mild and otherwise asymptomatic cases, afflicting nearly a third of those infected[5] [140, 141]. Although most infections resolve within one to three weeks, fatal cases tend to deteriorate suddenly and unexpectedly one to two weeks after onset of illness [20]. The precise reason for the sudden clinical deterioration associated with LHF is not well understood, but is could be related to a pivotal point in the infection when the immune responses fail to control levels of viremia. In contrast to the pathognomonic hemorrhaging caused by filoviruses and South American arenaviruses, signs of vascular and hemostatic dysfunction in LHF – hematemesis, facial edema, prolonged bleeding from venipuncture sites, bleeding of the gums, nose and other mucosal surfaces, hypotension, and hypovolemic shock – may not manifest at all, even in cases with a fatal outcome [20]. The differential diagnosis for febrile illnesses in the Lassa fever belt (**Figure 1.2**) is vast, including influenza, Ebola virus disease (EVD), dengue fever, yellow fever, malaria, and a host of other viral, rickettsial, parasitic, and bacterial etiologies [90]. Thus, the difficulty in making an empirical diagnosis of LHF, coupled with insufficient diagnostic support from laboratories, complicates the clinical management of LHF cases. McCormick et al. have suggested, however, that febrile cases presenting with a triad of chest pain, vomiting, and pharyngitis in a LASV endemic area has an 80% likelihood of having LHF [138]. High levels of viremia and hemorrhage are the best predictors of fatal outcomes [93].

[5] Although recognized as a major sequela of LHF since the 1970s, SNHL places heavy public health, social, and economic burdens in West Africa, where the WHO has ranked as having among the highest prevalence of deafness in the world. This impact has only recently been appreciated.

1.A.5. Pathogenesis of Lassa Hemorrhagic Fever

The various routes of LASV infection (inhalation, ingestion, or entry through abrasions, mucosa, etc.) do not seem determinative of disease severity or outcome, although needle stick injuries are associated with an extremely high risk of mortality because of the more direct route of entry into the bloodstream [98]. LASV entry requires access to basolateral surfaces [142], and since LASV is neither cytopathic to epithelial cells [143] nor disruptive to the barrier function of cells, cuts and abrasions are probably important for epithelial sites of entry. It is not clear how LASV crosses gastrointestinal epithelial lining, but the virus has been shown to be resistant to low pH [144].

Both mucosal and subcutaneous inoculation permits virus entry into peripheral capillaries. Dendritic cells (DCs), macrophages, and other antigen-presenting cells (APCs) are early targets for LASV as they are present throughout peripheral entry sites. Infected APCs, which have impaired abilities to further activate the adaptive immune response, support the initial rounds of replication during the establishment of LASV infection. Recruitment of additional DCs serves to amplify the viral load and helps disseminate virus to the lymphatics and other tissues throughout the body [145, 146]. Effective suppression of the host's cellular immune responses allows for replication and virus release to become rampant, as hepatocytes and secondary lymphoid organs, fibroblasts, epithelial cells, and endothelial cells can all produce high titers of virus without eliciting cell death [147, 148]. It is controversial whether the etiology of LASV-associated SNHL is due to cellular immune responses or to direct viral damage to inner ear or the VIII cranial nerve [139]. Both LASV antigen and $CD3^+$ T cells have been detected in damaged regions of the ear, but the development of SNHL in patients with low levels of viremia, as well as the frequent

causality between immune response and deafness, tend to favor the latter [20, 149]. Further supporting an immunologic etiology for SNHL, LASV can be present or absent in CSF from patients exhibiting neurological symptoms or sequelae [20, 150].

Further unchecked systemic spread leads to tissue damage in a number of organs, particularly in the lungs and the liver, with the latter displaying particular LASV tropism [93, 151, 152]. Damage to the liver is a notable feature during autopsy; it may also devastate the organ's ability to produce many blood-clotting proteins, contributing to vascular leakage and hemorrhage [153]. Upon autopsy, however, tissue and organ damage is seldom severe enough to cause death, which is instead caused by sepsis-like conditions [147]. Terminal viremia in fatal cases can reach 10^3 to 10^8 $TCID_{50}$/ml [149].

1.A.6. Immune Response to LASV Infection

Replicating arenaviruses generate a number of pathogen-associated molecular patterns (PAMPs) in host cells. Single- and double-stranded RNA, uncapped 5'-triphosphates, and short RNA fragments are all targets of recognition by RIG-I and MDA5, which, if detected, can lead to the activation of the JAK/STAT signaling pathway. Activation of JAK/STAT in turn induces expression of hundreds of interferon stimulated genes (ISGs) [154, 155]. In order to sustain persistent infections in mice (particularly in LCMV infections), the viral nucleoprotein (NP) is able to effectively antagonize interferon-I (IFN-I) responses [156-158]. Furthermore, the matrix protein (Z) of some arenaviruses can bind directly to RIG-I and MDA5, blocking induction of the IFN pathway [149]. Since Z-mediated suppression of IFN induction has only been described in pathogenic arenaviruses, this ability seems to be an important determinant in virulence [159, 160].

Cytokine expression is among the most important host defenses to LASV infection as activated DCs, macrophages, and T cells are crucial for clearing the viruses. In particular, the early proliferative T cells are central to controlling LASV infection. Indeed, the uncontrolled viremia associated with lethal outcomes is largely determined by the critical early stages of infection, when the successful suppression of antiviral defenses allows the virus to efficiently replicate and spread [161]. Although patients recovering from LHF may have high antibody titers, more typically, survivors will mount only a weak antibody response during infection[6]; strong and long-lived $CD4^+$ and $CD8^+$ T cell responses are much more highly associated with positive outcomes [162, 163]. The opposite is true for EVD, where the dominant protective immune response stems from early expression of antigen-specific IgM and IgG, and early transient T cell responses (especially anti-inflammatory responses) are associated with lethal outcomes [163].

1.B. Structure and Molecular Characteristics of Arenaviruses

The arenaviruses are pleomorphic, enveloped, negative sense RNA viruses that are 50 to 300 nm in diameter. The family name was derived from the Latin *arenosus,* meaning "sandy", because of the distinctive granular appearance of its ribosome-filled interior (ribosomes and other host proteins are thought to be incidentally incorporated into the virus particle during assembly). Glycoprotein (GP) spikes covering the surface of the virus are also easily seen in electron micrographs. The four-gene genome of arenaviruses is carried on two RNA segments, the large (L) and small (S) strands (**Figure 1.3**). The two open

[6] However, nAb titers often steadily rise after recovery, suggesting that subclinical, but persistent, viremia continues to stimulate humoral immunity (Reference 93).

reading frames on each segment are coded in opposite orientations and are separated by a noncoding intergenic region (IGR) that serves as a transcription termination signal [164]. The 7.3kb L strand encodes the 250 kDa viral RNA-dependent RNA polymerase (RdRp), L, and a small 11 kDa matrix protein-like Z protein. The 3.5kb S segment encodes the structural proteins: the 63 kDa NP and the 75 kDa GP precursor (GPC)[7] protein. Sequence complementarity on the highly conserved untranslated regions (UTRs) at the 5' and 3' termini of both RNAs panhandles the ends, circularizing each segment and serving as binding sites for L [165]. The RNAs are encapsidated by protective NPs and have at least one L protein per RNA; this structure is the ribonucleoprotein (RNP) complex [166]. NP, the most abundant viral protein, is the key structural element of the RNP and, along with L, is requisite for viral genome replication and transcription [167]. NP also plays a prominent role in immunosuppression by directly binding to RIG-I, MDA5, and other effectors in the IFN pathway that are important for a robust immune response [168]. Known to contribute to Z protein-mediated assembly, NP appears to have a YxxL late (L) domain that is important for interactions with cellular machinery involved during assembly [169]. L protein, in addition to its function in transcription and genome synthesis, is a central factor in the virulence of arenaviruses [170]. Recent proteomic analyses of LCMV have also revealed a number of previously unappreciated interactions between L protein and cellular factors involved in signal transduction, cytoskeletal rearrangement, protein

[7] Throughout most of the text, the abbreviation "GP" will be used generally to refer to LASV glycoprotein. As "GPC" can refer to either the mature glycoprotein complex or the precursor protein, this abbreviation will be reserved for more specific contexts.

FIG 1.3. Arenavirus structure and genome organization. The pleomorphic shape, variable size (ranging from 50 – 300 nm), grainy interior, and GP spikes are characteristic features of the arenaviruses, which can be seen electron microscopy images of LASV particles (**A**). The cartooned diagram depicts the virus's "club-shaped" GP surface spikes and GP's interactions with matrix protein (Z) on the interior of the virus. The bisegmented, circularized RNA genome is encapsidated by nucleoproteins (NP) and each segment has at least one polymerase (L) molecule associated with it (**B**). The non-overlapping open reading frames (ORFs) on each segment are of opposite polarity and are separated by a short hairpin intergenic region (IGR) (**C**). Figure is from an open access review article by Fehling et al. [164].

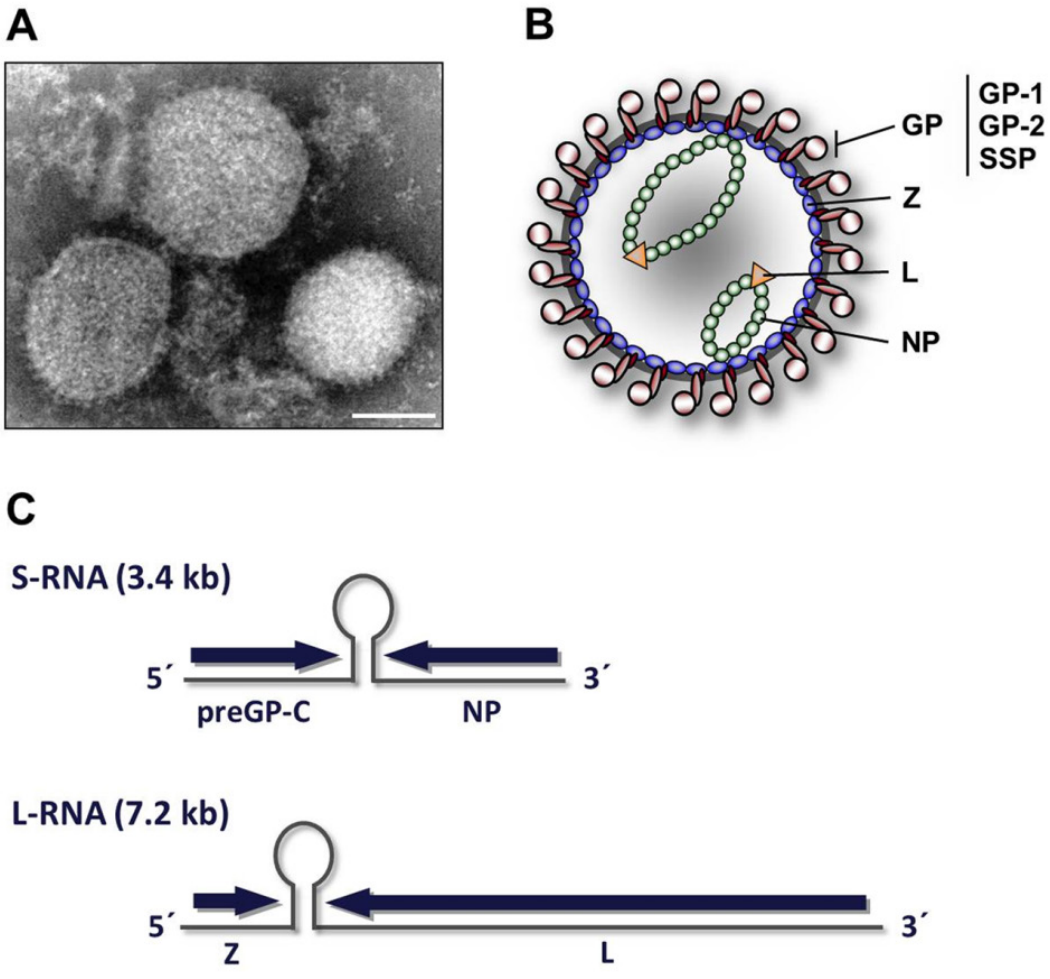
A
B
GP-1
GP-2
SSP
GP
Z
L
NP
C
S-RNA (3.4 kb)
5´
3´
preGP-C
NP
L-RNA (7.2 kb)
5´
3´
Z
L

trafficking, and translation [171]. I describe the function of GPC is described in detail in later sections.

As with other viral matrix proteins, Z lines the interior of the virus and fulfills an important structural role by bridging surface GP with RNP [172]. Z protein's lipid interactions, which provide structural integrity and facilitate budding at the plasma membrane (PM), require myristoylation of Z at its N terminus. Disruption of the myristoylation moiety (which is universally conserved in the arenavirus Z protein) has a drastic effect LASV replication, causing Z to disperse diffusely throughout the cytoplasm rather than organize in punctate clusters [173, 174]. In addition to interactions with GP, RNP, and lipid membranes, Z contains a zinc-binding RING finger that interacts with a number of cellular proteins [164]. The Z protein of all pathogenic arenaviruses species also binds to RIG-I and MDA5, counteracting IFN induction and preventing activation of macrophages in a manner similar to NP [168]. Z is the chief coordinator for assembly and budding, as evidenced by the fact that expression of Z protein alone is sufficient to drive budding of enveloped virus-like particles (VLPs) [175, 176]. LASV Z protein has two canonical C-terminus late (L) domains: the PPPY domain that interacts with Nedd4-like ubiquitin ligases and the PTAP L domain that interacts with Tsg101 [175].

1.B.1. Arenavirus Life Cycle

Arenavirus entry, which I will discuss in further detail in later sections, is primarily mediated by the GP on the surface of virus particles. Upon GP binding to host cell surface receptors, the virus is internalized into a vesicle and delivered into the endocytic pathway.

After GP is activated, it fuses with the endosomal membrane and the viral contents escape into the cytoplasm through the resulting pore [177].

Synthesis of progeny viruses commences immediately following endosomal escape (**Figure 1.4)**. In preparation for transcription, the L protein cap-snatch 5' caps from cellular mRNAs to prime mRNA synthesis [178, 179]. Since the RdRp activity of L is equipped for both transcription and replication, the primacy of initiating transcription over replication is thought to be regulated by low levels of NP that prevent L from reading through the IGR (as it does in replication mode). Thus, the negative sense replicative elements, L and NP, are first transcribed directly from promoter regions near the 3' UTR of the genomic RNA. As the L and NP mRNAs are translated into the first viral proteins of the infection, L senses the accumulation of NP and shifts into replication mode where it freely moves across the IGR, synthesizing full-length antigenomic RNA copies [180]. GPC and Z are then each transcribed separately from the antigenomic templates due to the secondary structure of the IGRs, which act as termination signals. As the GPC and Z mRNAs are translated, L finishes replicating progeny genomes which are quickly encapsidated by nascent NPs to reform RNP complexes. Cues for L protein to halt replication and transcription come from an accumulation of Z protein, which catalytically "locks" the polymerase in an inactive state and prevents it from further RNA synthesis; consequently, viral activities then transition to coordinated assembly and release [181, 182].

After the biosynthetic steps are completed, the progeny genomes and newly synthesized virus proteins (with the exception of GPC, which requires post-translational proteolytic cleavage and further modification before maturation) begin to assemble.

FIG 1.4. Arenavirus replication cycle. The cartoon overviews the complete lifecycle of the arenaviruses (**A**). The two-stage cleavage of GPC in the ER and Golgi is accomplished after expression in the producer cells (**B**). A mature virus buds from the cell surface with trimeric and fully glycosylated GPC spikes on its exterior (**C**). Figures were obtained from an open-access review article by Burri et al. [183].

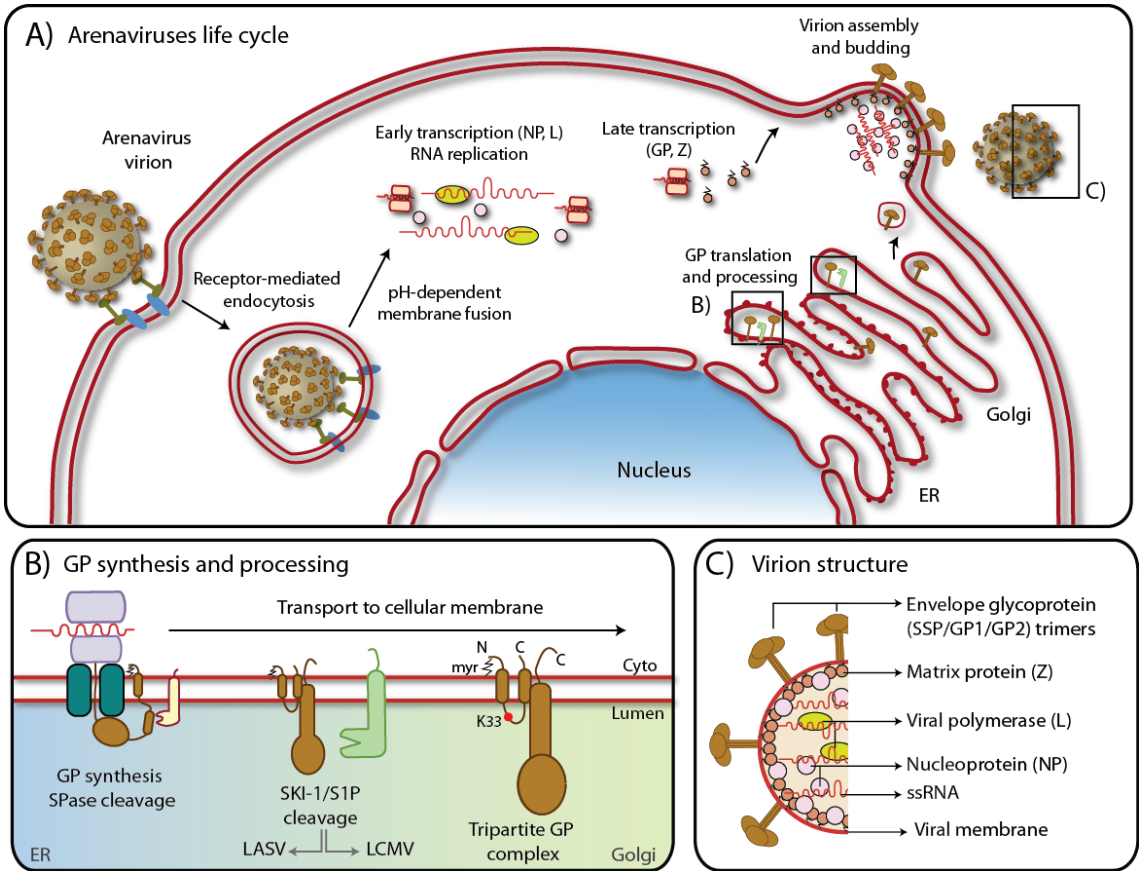
A) Arenaviruses life cycle
Virion assembly and budding
Arenavirus virion
Early transcription (NP, L) RNA replication
Late transcription (GP, Z)
C)
Receptor-mediated endocytosis
pH-dependent membrane fusion
GP translation and processing
B)
Golgi
Nucleus
ER
B) GP synthesis and processing
Transport to cellular membrane
N
C
myr
C
Cyto
Lumen
K33
GP synthesis SPase cleavage
SKI-1/S1P cleavage
LASV
LCMV
Tripartite GP complex
ER
Golgi
C) Virion structure
Envelope glycoprotein (SSP/GP1/GP2) trimers
Matrix protein (Z)
Viral polymerase (L)
Nucleoprotein (NP)
ssRNA
Viral membrane

Z begins packaging RNPs into a virus core while maturated subunits of GPC are trafficked to the PM for insertion at the budding site. Although the final stages of the arenaviral life cycle are not well understood, a model proposed by Urata et al. suggests that enriched patches of membrane-anchored GPC interact with Z protein and serve as assembly scaffolds for the final packaging of RNP cores [184]. With the assistance of cellular endosomal sorting complexes required for transport (ESCRT) machinery, the new viruses are released from host cell membrane [169, 183].

1.B.2. The LASV Glycoprotein

Tasked with ensuring the virus's genomic payload is delivered to the correct location in the correct cells, GPs are key determinants in viral tropism, infectivity, and fitness. In order to navigate incoming virus particles through every step in the formidable entry process, arenavirus GPs require extensive modifications during expression in producer cells.

1.B.3. Post-translational Modifications of LASV Glycoprotein

The full 498-amino-acid GPC of LASV is translated as a single polypeptide consisting of three subunits: a stable signal peptide (SSP), GP1, and GP2. A hydrophobic region within SSP directs the entire polypeptide to the endoplasmic reticulum (ER), where resident signal peptidases cleave the 58-amino-acid (6 kDa) subunit from the rest of the GP1/GP2 precursor [177]. Here, the cleaved SSPs oligomerize into trimeric complexes, which are myristoylated on the glycine residue at position 2 (a universally conserved residue among the arenaviruses). SSP is positioned within the ER membrane by a two-pass transmembrane domain (TMD) with it N- and C- termini oriented toward the cytoplasm [185]. Cleavage

and positioning of SSP is a critical checkpoint at this stage of GP maturation; without it, ER-retention signals on GP2 remain exposed and GP is prevented from exiting the ER [186, 187]. Unlike other viral signal peptides, arenaviral SSPs are required to stabilize GP and, thus, remain associated with GP throughout the infectious lifecycle [188-190].

The glycosylation of viral GP has been intensively studied for many years. Proper maturation of GP's glycan structure is of critical importance for a number of downstream functions; it is first required before GP even leaves the ER since chaperones do not correctly fold improperly glycosylated proteins. Misfolding of GP prevents the exposure of a second cleavage site on GP1/GP2 [191]. While these under-glycosylated and uncleaved GPs will still be transported and expressed at the cell surface, they may not be incorporated into budding viruses, resulting in either "bald" or defective virus particles with aggregates and other oligomeric forms of GPC on their surfaces [191-193].

In general, protein glycosylation involves several iterative modifications beginning with attachment of a high mannose core to the asparagine residue of N-X-S/T motifs [194]. The core mannose residues are sequentially cleaved in the Golgi and replaced with glucose, N-acetylglucosamine (NAG), and other sugars [195]. Glycosyltransferases are highly upregulated and overburdened in heavily infected cells, as they struggle to meet the demands of glycosylating viral GPs [196]. Complex trimming and remodeling of these oligosaccharides continues as GP is transported through the Golgi. Among the arenaviruses, GP1 is more heavily glycosylated than GP2; however, the number of N-linked glycans on GP1 varies widely from three (for Candid #1 live attenuated vaccine

strain JUNV) to eleven (for Pichinde virus)[8]. LASV has a total of seven N-linked glycans on GP1 and four on GP2 [199]. The finished carbohydrate shield on GP contributes to about 25% of the entire complex's mass [200-202].

En route through the ER via the secretory pathway, arenavirus GPs undergo a second proteolytic event to cleave GP1 from GP2. This effectively accomplishes the "priming" of arenavirus GP (to a fusion-competent form) while they are still in the producer cell, an action delayed in several viruses until they enter a target cell [203-208]. GPs from the arenaviruses and the bunyavirus, Crimean Congo hemorrhagic fever (CCHF) virus, are cleaved by subtilisin kexin isozyme-1 (SKI-1)/site-1 protease (S1P), which recognizes an RRLL motif [209]. Interestingly, while the normal cellular substrates for SKI-1/S1P are located in the medial Golgi, the majority of SKI-1/S1P-mediated cleavage of GP1/GP2 for LASV and CCHF occurs while still in the ER [192]. For reasons that are not clear, LCMV GP1/GP2 is not processed by SKI-1/S1P until reaching the trans-Golgi network (TGN) [192, 200, 210].

After GP1/GP2 cleavage, the tripartite GP complex (GPC) is trafficked through the final leg of its journey to the surface accompanied by the cargo receptor endoplasmic reticulum (ER)-Golgi intermediate compartment 53 kDa protein (ERGIC-53) [211].

[8] Importantly, the number of glycans on GP1 does appear to inversely correlate to the titers of nAbs, and partially deglycosylated GP1s will enhance the nAb response (References 197 and 198).

1.B.4. LASV Glycoprotein Structure

Virus particles released into the extracellular environment are covered with 250-300 GP spikes [212]. A single 230 kDa GP spike on a virus particle is made up of three tripartite (SSP-GP1-GP2) monomers which, based on computed tomograms, are spaced ~4 nm apart from one another and extend 5-10 nm up from the surface [201, 212]. The GP trimers are anchored onto the membrane by a total of nine TMDs (six from SSP and three from GP2) and are held together via the zinc-binding interactions between SSPs and the cytosolic tails of GP2 [189]. Intersubunit interactions between the GP1 subunits also play an important part in maintaining the structural integrity of the spike **(Figure 1.5)** [202, 213].

The fusogenic transmembrane subunit, GP2 (residues 260-491), features three prominent α-helices, each 20-40 residues, as well as two highly conserved hydrophobic heptad repeats (HRs) on the spike side of the TMD [201, 202]. The N terminus of GP2 also has two short, conserved hydrophobic regions that are reported to function as fusion peptides (FPs): the N-terminal FP (NFP, residues 260-266) and the internal FP (IFP, residues 283-294) [214-216]. Glycans pack against the FPs, providing concealment and stability. The amino acid sequences of SSP and GP2 are fairly highly conserved among the arenaviruses, with identities of 67.3% and 70.5% respectively [198]. Recently available crystal structures for the GP2 subunits of both LASV [202] and LCMV [217, 218] also show generally similar structural features. However, there are subtle distinctions that may explain functional differences between the fusion parameters of LASV and LCMV. Hastie et al. have pointed out that LCMV's FP is tucked more closely into the GP1/GP2 interface than LASV's FP [202].

FIG 1.5. Lassa virus glycoprotein schema and structure. Schema of major modification sites mapped onto a linear display of LASV GPC peptide (**A**). Gray areas indicate hydrophobic regions, including a total of three TMDs. The locations of N-linked glycosylation sites are indicated by the tree-like symbols [199]. **B** and **C** represent basic and complex schema, respectively, for LASV GPC. In **B**, the N- and C-terminal HRs on GP2 are shown by black boxes. The highly conserved lysine at position 33 of the SSP is important for expression, processing, and fusion [219, 220]. The zinc-binding motif between the C terminus of SSP and the C terminus of GP2 is indicated by blue circles. The myristolyated membrane anchor is shown with a zig-zag symbol. The dimensions of the fully glycosylated prefusion trimeric spike demonstrate the considerable bulk added to the structure by the carbohydrate shield (**C**). The cartoon in **A** is taken from Eichler et al. [199], **B** is taken from a review article by Jack Nunberg [177], and **C** is taken from Eschli et al. [201]. **A** and **B** are from open access articles and permission was obtained from ASM for **C** (license 4357270906005).

A

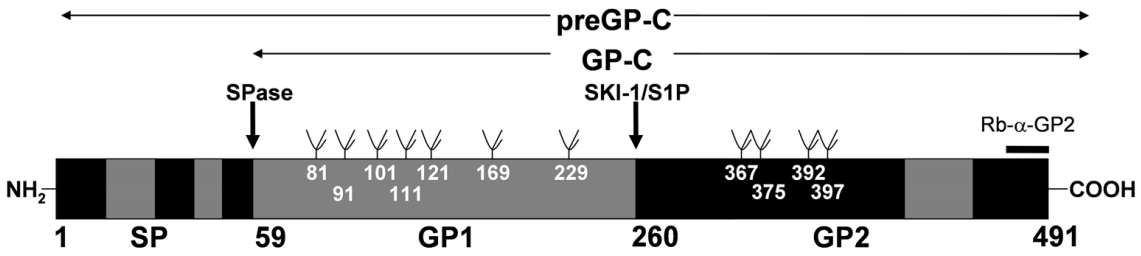
preGP-C
GP-C
SPase
SKI-1/S1P
Rb-α-GP2
81
91
101
111
121
169
229
367
375
392
397
NH2
COOH
1
SP
59
GP1
260
GP2
491

B

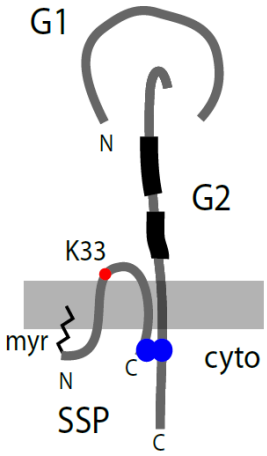
G1
N
G2
K33
myr
N
C
cyto
SSP
C

C

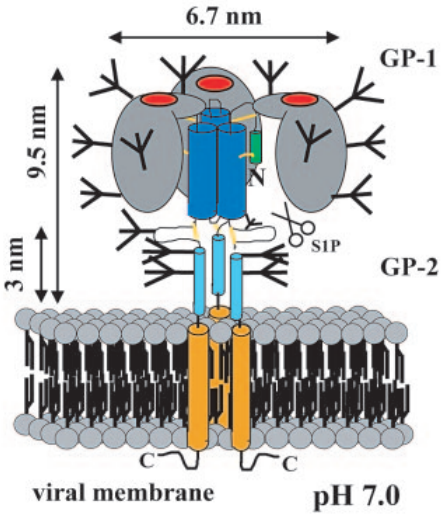
6.7 nm
GP-1
9.5 nm
3 nm
S1P
GP-2
C
C
viral membrane
pH 7.0

The globular, receptor-binding surface subunit, GP1 (residues 59-259), sits on top of GP2, fixated by ionic interactions with GP2's N terminus. GP1 has a fairly conserved membrane distal β-sheet face, a more variable membrane proximal helix-loop face, and an N-terminal β-strand that is important for interactions with GP2 [221]. The seven glycosylated residues of LASV GP1 (N79, N89, N99, N109, N119, N167, and N224) are located on the β-sheet face, shielding most of the subunit from antibody binding [202]. Important functional inferences can be made from comparing the crystal structures for the GP1s of the New World arenaviruses, JUNV [222, 223], GTOV [224], MACV [225, 226], and Whitewater Arroyo virus (WWAV) [227], and the Old World arenaviruses, LASV [202, 221], LCMV [218], and Morogoro virus (MORV) [202]. Although arenaviral GP1 cores share a unique α/β fold, the sequence identity between members of the New World and Old World arenaviruses is only ~33% [198]. Interestingly, LCMV GP1, which has 20% sequence identity with JUNV and MACV GP1 and 63% identity with LASV, is structurally more like the New World arenaviruses than it is LASV [218].

1.C. Virus Entry: General Considerations

Enveloped viruses enter target cells by engaging a vast array of cellular proteins, carbohydrates, and lipids, which can function as viral receptors, co-receptors, secondary receptors, or attachment factors. Host ranges and tissue tropisms can be restricted not only by whether a preferred receptor is expressed, but also by its density and distribution, responsive up-regulation during infection, or its glycosylation pattern (or addition of other tissue-specific moieties) [228]. The outcome and severity of disease can also be linked to

receptor affinity, as exemplified by severe acute respiratory coronavirus (SARS-CoV) and its receptor, ACE-2 [229, 230].

After attachment to the cell surface, a number of host factors are consequential to ensuring viral genomes are well placed before exposing them during the replication process. For viruses such as the murine leukemia virus (MLV), most herpes viruses, and some of the paramyxoviruses, virus-receptor contact triggers fusion directly at the PM [231]. However, the extensive crowding of cortical networks near the underside of the PM can make entry at the cell surface disadvantageous. The vast majority of viruses therefore opt for receptor contacts that will potentiate internalization into the endocytic pathway, where they can be delivered to sites more amenable to replication. Some viruses will stay tethered to their receptors in the membrane during internalization, while others uncouple and "float" within the vesicular lumen, as some larger cellular cargo does.

Once inside the endocytic pathway, viral GPs can theoretically fuse with endosomal membranes at any point depending upon exposure to specific cellular cues, which can be any combination of low pH, proteases, or receptors within the transitional environment of maturing endosomes [231, 232]. For example, vesicular stomatitis virus (VSV) and Semliki Forest virus (SFV) escape from an early endosomal compartment, where the pH is just above 6, within ten minutes of endocytosis [233-235]. EBOV GP and Middle East respiratory syndrome coronavirus (MERS-CoV) spike (S) protein, on the other hand, require priming from pH-activated endosomal cathepsins prior to gaining fusion-competence [236-238]; the half-times of endosomal escape for these viruses, which penetrate the endo-lysosomal membrane, can be over an hour [239].

The arenavirus GPs and many other viral fusion proteins can be triggered by low pH alone [144, 240]. Kinetic studies of LASV and LCMV entry have shown that, from the time of attachment to the time of penetration of the late endosomal membrane, the half-times for endosomal escape have been reported to be 20 – 30 minutes [233, 241-246]. This is the roughly same amount of time needed for New World arenavirus and influenza A virus (IAV) entry [239, 242], but faster than other late-penetrating viruses, such as EBOV and SARS (presumably owing more to additional GP priming requirements from endosomal cathepsins rather than later endosomal escape) [232, 239].

Kinetic studies such as these can be applied to bin viruses as either "early" or "late" penetrating; however, this can be misleading if viewed in isolation. A case in point is a comparison between two pH-dependent viruses: the bunyavirus, Uukuniemi (UUKV), and LASV. Live-cell microscopy studies with UUKV have shown it takes a "classical" entry route from attachment (to DC-SIGN), internalization into vesicles that carry it to early endosomes, and finally transit to late endosome, where fusion with the endosomal membrane occurs [246, 247]. However, the half-time to endosomal escape for UUKV is under 20 minutes, shorter than typically observed for LASV [246].

1.C.1. General Overview of LASV Entry

For LASV, upon binding to a principal PM receptor (see next section), particles are endocytosed into the cellular endocytic pathway via a "macropinocytosis-like" pathway [248]. Entry through classic macropinocytosis, which is adopted by vaccinia virus (VV), is characterized by sequential activation of GTPases, growth factor stimulation, actin rearrangements, membrane ruffling, and the formation of macropinosomes that internalize

receptor-virus complexes and a large volume of extracellular fluid [232, 249, 250]. While LASV entry does activate macropinocytosis-associated kinases and requires the sodium hydrogen exchanger (NHE1) protein (a marker for macropinocytosis), its internalization elicits negligible changes in cellular morphology and fails to use a number of cellular factors that are considered diagnostic markers for macropinocytosis [245, 248, 251].

Once internalized, LASV exhibits several other uncommon entry features. While the majority of inbound vesicular cargo is delivered into early $Rab5^+$ endosomes, LASV entry is Rab5-independent [233, 252]. This suggests that LASV may bypass these early endosomal compartments altogether, transiting instead directly to multivesicular bodies (MVBs) found later in the pathway[9] [233, 253]. As do a number of other viruses, LASV requires cholesterol for entry, which is thought to provide structural stability during fusion [193, 256, 257]. Microtubules are also critical for trafficking LASV through the endocytic pathway, which conveys them in the general direction of the perinuclear area [242, 253].

Much of the sorting in the endocytic pathway is accomplished in early endosomes, where cargo is routed to recycling endosomes, the PM, the TGN, or to lysosomes for degradation. LASV, like other so-called late-penetrating viruses such as EBOV, IAV, UUKV, and VV, travels deep within this pathway [231]. Endosomal escape must be timed to occur before virus particles are destroyed by lysosomal hydrolases and proteases, but after they have reached a location in the cell. LASV GP has intricately evolved pH-sensing

[9] It has been speculated that the bypass of early endosomes is a strategy employed by LASV to avoid detection by Toll-like receptors (TLRs) (Reference 253). TLR9 in particular is enriched in $Rab5^+$ early endosomes and recognizes incoming RNA viruses (References 254 and 255). The unusual entry route may be a key component in LASV's ability to evade host immune responses.

capabilities that are triggered by the acidic environment of late endosomes. Once the fusion cascade is triggered, GP mediates fusion between the viral and endosomal membranes, allowing for release of the viral contents into the cytosol.

One of the earliest steps in the LASV fusion cascade is the dissociation of GP1 from GP2. Data from crystal structures [202] and tomographic reconstructions [212] of LASV GP1 are in agreement that GP1 undergoes important destabilizing changes at endosomal pH, which are triggered by the protonation of a conserved pH-sensing histidine triad on GP1 [221, 258, 259]. Destabilization is thought to cause the GP1 subunits to slightly spread apart from one another near the apex of the trimer, deepening the crevices between them, altering the receptor binding site (RBS) of GP1, and ultimately driving the dissociation of the GP1 subunits from the rest of the spike (**Figure 1.6**). Hastie et al. have referred to the conformational changes in GP1 that precede its dissociation as a priming step for LASV GP. We view it as a secondary priming step, with the initial priming event being the cleavage of GP1/GP2 in producer cells [202, 260].

The dissociation of GP1 results in profound structural rearrangements within the GP2 subunits. Refolding of GP2 forms α-helices that unfurl out toward the target membrane [261-263]. Exposed hydrophobic FPs at the N-terminal tips of GP2's extended helices (which are buried in the prefusion complex) are thrust into the outer leaflet of the endosomal membrane, creating a physical tether between the virus particle and the endosome [264]. The N- and C-terminal HRs in GP2 then begin to collapse toward each other, folding the structure into the preferred low-energy state of the postfusion conformation. The spontaneous formation of the resulting six helical bundle structure (6HB; often described as a "trimer of hairpins") brings the membranes into close proximity

[265]. Insertion of the FPs into the target membrane destabilizes the lipid bilayer, allowing for lipid mixing between viral and endosomal membranes to occur. A lipid stalk is formed during this hemifusion step, which grows until the inner leaflets of both membranes begin to fuse. The widening pore in the endosomal membrane then permits the viral contents to enter into the cytosol.

Once the fusion cascade is triggered, the entire structural transition from prefusion to postfusion conformation is spontaneously driven to completion. If GPs are triggered by low pH before the virus particle is positioned near its target membrane, the HRs will still collapse into the thermodynamically favored 6HB structure, causing the FPs to bury themselves into the viral membrane of the virus particle. This irreversible process can therefore render the virus inactive and noninfectious.

FIG 1.6. Viral fusion cascade. Class I viral fusion proteins, such as arenavirus and filovirus GPs and influenza HAs, are converted from a fusion-incompetent state (**i**) to a fusion competent, metastable form (**ii**) by a proteolysis of the covalent bond between the receptor binding (rb) and fusion (f) subunits. Next, upon receiving a fusion trigger (which may be low pH, additional proteolysis, engagement of a receptor(s) or a combination thereof, the receptor binding (i.e., GP1 for arenaviruses) subunit (purple) moves away from, and thereby unclamps, the fusion subunit (GP2 for arenaviruses; shown in blue) allowing it to undergo structural changes that lead to fusion. The first of these changes (**iii**) involves formation of an extended pre-hairpin structure and insertion of a hydrophobic FP or fusion loop (red) into the target membrane. The HRs then begin to fold back on each other (**iv**), bringing the virus and target membranes into close apposition. As the HRs form the stable trimer of hairpins structure (the 6HB [**v**]), the outer leaflets of the membranes begin to mix and form a stalk leading to hemifusion. The final step in the fusion cascade involves the mixing of the inner membrane leaflets (**vi**), which leads to the formation of a fusion pore. Material is taken from an open access review article by Drs. Judith White and Gary Whittaker [231]. For LASV GP, the triggering step may occur in three steps: (**i**) at pH ~6.5, there are likely conformational changes to GP1 that cause it to move slightly, but not yet dissociate, from GP1. This then allows engagement with Lamp1 (**ii**), which at lower pH causes full dissociation of GP1 from GP2 (**iii**). This permits the subsequent steps in the fusion cascade to (**iii-vi**) to ensue.

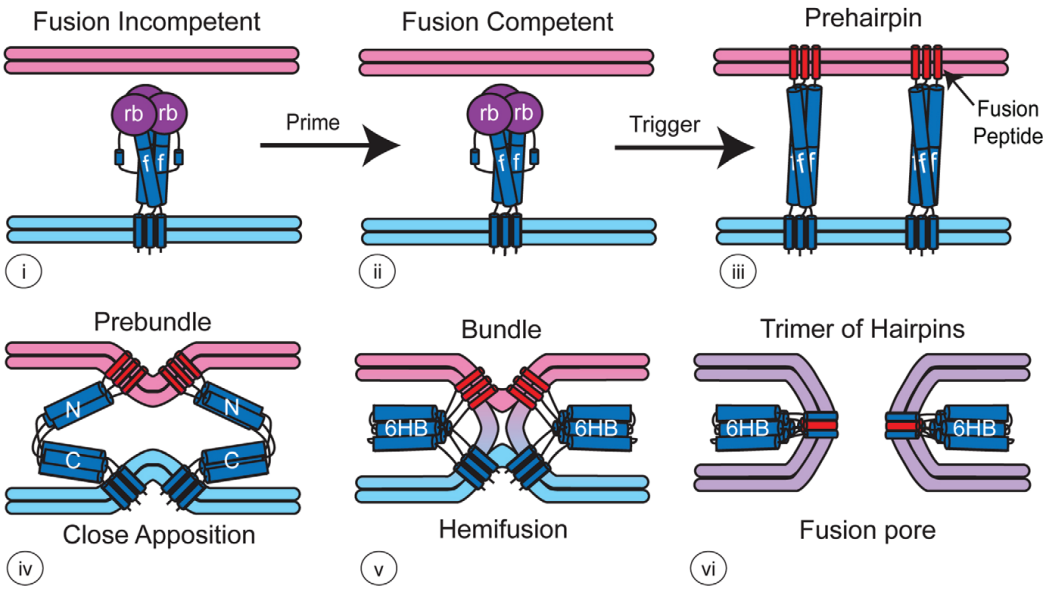
Fusion Incompetent
Fusion Competent
Prehairpin
Prime
Trigger
rb
rb
f
f
Fusion
Peptide
i
ii
iii
Prebundle
Bundle
Trimer of Hairpins
N
C
6HB
Close Apposition
Hemifusion
Fusion pore
iv
v
vi

1.C.2. Arenavirus Plasma Membrane Receptors

Initial contact of viruses with the host cell is often mediated by low affinity, electrostatic interactions with attachment factors, typically moieties such as gangliosides, sialic acid, and heparin sulfate [266, 267]. EBOV does not have a dedicated primary cell surface receptor and serves an example of a virus that can use a number of different attachment factors, including TIM/TAMs, glycosaminoglycans, and numerous C-type lectins to initiate endocytosis [268, 269]. On the other hand, the receptors for LASV and other arenaviruses discussed below are often cited examples of bona fide PM viral receptors.

In recent years, however, there have been several caveats describing various cell types and conditions in which both Old World and New World arenaviruses may, in lieu of engaging with their primary receptor, use low affinity attachment factors, e.g. DC-SIGN, Tyro3, Axl, Mer (TAM family), TIM-1, LSECTin, and heparan sulfate [135, 244, 246, 270-272], to gain access into the cell. Widely expressed on most cells (and highly expressed on the endothelial cells and activated immune cells favored by arenaviruses), the New World arenavirus receptor, transferrin receptor 1 (TfR1), is rapidly endocytosed and recycled through early endosomes [241]. It was identified as a primary New World arenavirus receptor by Radoshitzky et al. as they investigated cell line features that rendered them permissive to MACV, GTOV, JUNV, SABV, and CHPV infection [273]. These five pathogenic arenaviruses are members of the same clade (clade B of the New World arenaviruses) and all use the hTfR1 receptor. A deeper understanding of receptor usage came from the observation that hTfR1 is in fact only used by these pathogenic members of clade B New World arenaviruses.

Hence, viral GP compatibility with both hTfR1 and the TfR1 orthologues of their rodent host viruses is "absolutely predictive" of a New World arenavirus's potential to cause hemorrhagic disease in humans [4, 274, 275]. Furthermore, only modest differences exist between the hTfR1 receptor and its rodent orthologues [4], perhaps indicating that some of the nonpathogenic, clade B New World arenaviruses may require only minor evolutionary changes in their GP1 RBS to become emergent zoonotic human pathogens. Among the remaining New World arenavirus clades (which are considered nonpathogenic), clade C uses α-dystroglycan (α-DG) (the same receptor used by the Old World arenaviruses), and the North American clade D arenaviruses use rodent orthologues of TfR1 [276, 277]. The receptor for clade A arenaviruses is still unknown.

The Old World arenavirus receptor was identified using a viral overlay protein blot assay (VOPBA) on LCMV-bound cell lines originating from several mammalian species (including humans) [278, 279]. After subsequently solubilizing and separating membrane proteins by sequential column chromatography, the 156 kDa receptor was identified as α-DG by mass spectrometry (MS). It associated with the GP1s of LCMV, LASV, and two other (nonpathogenic) Old World arenaviruses, but not with the New World GTOV GP1. With the exception of LUJV, which was recently discovered to use the semaphorin receptor protein, NRP2 [280], the Old World (and clade C New World) arenaviruses use α-DG as their primary cell surface receptor (interestingly, *Mycobacterium leprae* also uses α-DG as its receptor) [281].

High affinity contacts are made between α-DG and ECM proteins, namely perlecan, neurexin, agrin, and laminin. The nonconvalently associated transmembrane β subunit interacts with a number of signal transduction proteins and actin-based cytoskeletal

adaptors in the cytoplasm [241]. As a ubiquitously expressed ECM receptor, dystroglycan has many important roles: in muscle fibers, it prevents excessive mechanical damage during contraction by anchoring cells to the underlying extracellular matrix (ECM) [282]. It supports polarity of signaling and activation of STAT5 in epithelial cells [283, 284]. It is important in the establishment of neuromuscular synapses, helps control growth and metastasis in cancer cells, and is required for the formation, assembly, and organization of basement membranes at the tissue level during embryogenesis [285, 286]. Loss of functional dystroglycan is associated with a number of clinically important human diseases[10].

As a foundational component of ECM organization and tissue architecture, α-DG has an inherently more static role at the PM than the frequently endocytosed TfR1. It nonetheless is involved in the turnover of EMC components, particularly during development and tissue repair [289, 290]. Of α-DG's ECM ligands, laminin is the most well-characterized. Live-cell imaging studies show colocalization of α-DG with laminin in $Rab7^{+}$ late endosomes. This finding supports the notion that α-DG is internalized along with its high affinity ECM ligands. [291]. Attachment to α-DG receptor occurs in < 5 minutes [245] and dynamin-dependent internalization of α-DG-laminin complexes can occur within one hour. Laminin destined for degradation presumably dissociates from α-DG as the pH decreases and is then trafficked to the lysosome. Owing to the common

[10] In addition to a range of dystroglycanopathies associated with loss of functional dystroglycan (most notably Walker-Warburg syndrome [WWS]), suppression of its modifying enzymes in cancerous cells correlates with aggressive subtypes and poor prognosis. Roughly 20-30% of all solid tumors have nonfunctional dystroglycan (References 287 and 288).

receptor usage between laminin and LASV GP, Oppliger et al. tested whether recombinant LASV-GP LCMV pseudoviruses (rLCMV-LASVGP) follow the same pathway as laminin [245]. Because LASV pseudoviruses are insensitive to dynamin inhibitors, LASV particles probably do not follow the same pathway as α-DG's endogenous ECM ligands do during internalization.

Although its protein core is highly conserved, the glycosylation pattern of the α subunit is exquisitely adapted to tissue type-dependent functional demands [246]. Analysis of the carbohydrate structure of α-DG shows an extremely complex pattern of O-mannosylation with abundant (and, again, highly tissue-specific) expression of sialylated O-linked sugar chains [292-295]. Over two dozen glycosyltransferases function as modifiers for the overall glycan structure of α-DG's mucin-like domain [289, 296, 297]. A particularly critical modifier among this cohort of enzymes is the like-acetylglucosaminyltransferase (LARGE) protein, which is responsible for installing 3-xylose-α1,3-glucoronic acid-β1 polysaccharides on the laminin binding site of α-DG [245, 298]. The laminin binding site overlaps with the LASV binding region near residues 313-408 of α-DG, putting the virus and laminin in direct competition for binding to α-DG. Under neutral pH conditions, α-DG's affinity for binding LASV GP1 is strong enough so as to be nearly irreversible [299]. Indeed, overexpression of LARGE increases α-DG's affinity for LASV GP1, which has implications for its role in viral pathogenesis since disruptions in the ECM may contribute to the vascular pathologies manifested in severe LHF [289].

An example of the consequential importance of LARGE in the context of LHF infections is illustrated by the findings from the International HapMap project. This study

showed that human populations living in the Lassa Belt of West Africa have been under intensive selective pressure to acquire polymorphisms in the LARGE gene [60, 62]. Although individuals with homozygous mutations in LARGE may suffer from severe muscular dystrophies [300], heterozygotes with a defective LARGE allele may have resistance – or at least reduced susceptibility – to LASV infection. The disproportionately high carriage of this genetic adaptation in endemic areas underscores the dramatic scale and impact of LHF burden.

1.C.3. Endosomal Receptors

In addition to the spotlight on LARGE's role in LASV pathogenesis from the HapMap Project, other important pro-virus cellular factors have been recently identified in a series of high-profile genetic screens from the Brummelkamp group, which specializes in genetic and metabolic diseases [135, 280, 300-302]. Their approach relies upon using transposon-mediated knockout (KO) haploid cell lines to identify the most robust phenotypic loss-of-function responses to virus infection [303]. Their methodology entails an initial screen, conducted using recombinant VSV particles pseudotyped with a viral GP (rVSV–LASV, LUJV, EBOV, or Marburg [MARV]-GP), to identify virus entry-specific genes. Hits from the pseudovirus interrogation are then "cross-checked" against gene trap-insertion sites identified via authentic virus infection. The findings from this approach have revealed an exciting new discovery: some viruses use secondary endosomal receptors.

The 2011 discovery of EBOV's entry requirement for the late endosomal cholesterol transporter, Niemann Pick C1 (NPC1), was the first example of an intracellular virus receptor [301]. As a critical host factor for EBOV, MARV, and Lloviu virus (LLOV)

entry, NPC1 appears to be universally required for filoviral entry [304]. The prevailing model for NPC1's role in EBOV infection is that it binds to EBOV GP during the endosome-lysosome transition and then, in a manner distinct from its role in cholesterol transport, facilitates GP-mediated fusion with the endosomal membrane [302, 305]. Although the mechanistic details of how NPC1 contributes to EBOV fusion are still unclear, the NPC1 requirement is plainly an additional determinant of viral tropism. In a fruit bat species and several species of reptiles, for example, a single amino acid change in NPC1 prevents EBOV GP binding and is responsible for conferring intrinsic resistance to EBOV infection to these species [306-308].

Soon after the discovery of the NPC1 requirement for filovirus entry, the observation that fibroblasts from WWS patients were resistant to LASV infection motivated an interest in better understanding how glycosylation defects contribute to both genetic disorders and LASV resistance [300]. Thus, a comparative screen for pro-LASV factors was executed in WT and α-DG-deficient cells, allowing for the discrimination of factors that were unrelated to α-DG binding, but important for LASV entry. The hit for the gene for lysosomal associated membrane protein (Lamp1) in both WT and α-DG-deficient screens was of great interest because Lamp1, and the small cohort of sialyltransferase hits that modify Lamp1's N-linked glycan structure, has no ontological relatedness to the glycosyltransferases involved in maintaining and modifying α-DG's O-linked glycan structure.

Recognizing that they had probably discovered another intracellular receptor for a major viral pathogen, the Brummelkamp group quickly followed-up with a *Science* paper in 2015 characterizing the virus-endosomal receptor relationship [135]. The study was

framed around the hypothesis that Lamp1, if indeed a functional virus receptor for LASV, might also restrict LASV's species tropism. This would then explain an obscure observation, published over 30 years ago, that chicken fibroblasts are resistant to LASV infection despite bearing a LASV GP-compatible α-DG orthologue [134]. A single amino acid difference (N76S) between human and avian Lamp1 was pinpointed as the determinant reason for resistance in chickens.

The tetraspanin CD63 is the third and most recently discovered example of an intracellular viral receptor [280]. An important regulator of adhesion processes and membrane protein trafficking, it too was discovered by the Brummelkamp lab using a genome-wide haploid genetic screen to probe for cellular factors involved in LUJV entry. CD63, which had been previously implicated in HIV envelope protein-mediated fusion [309], was shown to specifically promote LUJV entry in much the same way as Lamp1 specifically promotes LASV entry. Like LASV GP, LUJV GP-mediated syncytia formation between cells expressing mutant CD63 expressed at the PM under acidic conditions, but could not mediate fusion between cells expressing WT (internal) CD63. Neutral pH binding (at pH 7.4) to the primary surface receptor for LUJV, NRP2, was effectively demonstrated by pull-down experiments; however, they were not able to show an interaction between LUJV GP1 with CD63 at pH 5.5. As the authors suggest, this could be due to a transient or low affinity interaction. Evidence of CD63's important role for LUJV entry is striking, however a pH-dependent receptor switch for LUJV can only be inferred at this point.

1.D. What is Known and Not Known about Arenavirus Fusion

Entry is an intensively studied aspect of the arenaviral life cycle. A detailed knowledge of entry pathways and host-virus interactions is critical for developing better therapeutics, many of which target the early steps in infection. Considerable progress has been made in identifying pro-viral host factors using the advanced screening techniques from the Brummelkamp lab and others. A number of important mechanistic insights have also been gained from recent crystal and cryo-EM structures of viral GPs, which have been solved under different pH conditions [212, 217, 218, 221, 224] and while bound to receptors [212, 225, 226], antibodies [202, 222, 223, 310], and drugs [311, 312]. Aided by these interdisciplinary efforts, we now have a better appreciation of the complexity of viral entry steps and how they contribute to overall pathogenicity.

One of the great puzzles of arenavirus entry in recent years arose from the intensive fusion studies of the Bartosch and Meulen labs that began roughly a decade ago [144, 216]. Both labs were working on finding the pH optima for arenavirus GP-mediated fusion using variations on the standard cell-cell fusion (CCF) assay (described in the earlier section on endosomal receptors). All of the viral GPs reported in the first paper (by the Meulen lab) fused under remarkably acidic conditions: pH ~5 for JUNV GP and IAV hemagglutinin (HA) (subgroup H7), and pH ~4 for LASV (Josiah) and LCMV (WE) GPs [216]. Fusion activity for all viral GPs at pH $\geq$ 5.5 was negligible, save for IAV HA, which abruptly dropped off at pH 5.8. The Bartosch lab then extended these findings by comparing fusion

pH with infectivity after inactivation by low pH exposure[11]. LASV GP fusion activity peaked at pH ~3 and had about half maximal activity at pH 4 (and very little activity at pH ≥ 5.0). Despite exhibiting peak fusogenicity at pH 3.0, LASV pseudoparticles exposed to this low pH were no longer infectious[12], whereas exposure to pH 4 before infection did not affect their infectivity at all. Approximately the same fusion and infectivity patterns were observed for LCMV. An interesting point made by the study authors was that, as low pH exposure will eventually damage or destroy virus particles, the pH of GP-mediated fusion activity can (and perhaps should) be evaluated alongside overall infectivity after low pH exposure.

A third arenavirus CCF paper worth discussion was published in 2014 [313], the same year as the Brummelkamp lab's seminal Lamp1 paper. Here, Tani et al. evaluated pH-dependent CCF alongside infectivity experiments (using pH-adjusted and re-neutralized pseudoviruses for the infections, as the Bartosch lab had done). Both sets of Tani's experiments included the GPs of LASV, JUNV, LUJV, and CHPV, which is of particular interest since direct comparisons of fusion activity for Old and New World arenavirus GPs are lacking. Holding LASV GP as a fixed feature for comparison between Tani's and Bartosch's studies, the fusion profile for LASV GP again shows peak CCF activity at pH 4, modest reduction at pH 3 (probably due to the further disintegration of

---

[11] These assays involve exposing pseudoviruses to pH-adjusted buffers for a short time, then reneutralizing the pH. The viruses are then used in infections to determine the approximate pH at which they begin to lose their infectivity.

[12] Transmission electron microscopy was also used by the Bartosch lab (Reference 144) to examine the morphologic appearances of the pseudoviruses (which had a VSV core) at various pHs. At pH 4, particles had pronounced shape alterations, but, at pH 3, the particle membranes had burst and content spillage was clearly visible.

cellular membranes given the relatively long exposure time[13]), and a ~10-fold decrease at pH 5 (a pH that, in our hands, is fairly well tolerated by cells, even for longer exposures; see Chapter 3). LASV pseudovirus infectivity begins to drop after pre-exposure to pH 5, is greatly diminished by pH 4, and is abolished by pH 3. These results again suggest that LASV infectivity begins to dwindle (as a result of inactivation) at a higher pH than when GP reaches its maximal fusion potential. Besides being impressively consistent with Bartosch's results, Tani's findings indicate that LASV pseudoviruses exhibit markedly higher resistance to pre-exposure to low pH relative to pseudotyped New World arenaviruses. This relatively high level of resistance to low pH inactivation by LASV GP pseudoviruses (with significant inactivation only pH < 5) has been observed by other labs as well [253].

As a final note on the Tani paper, which until 2017 was the only published study with LUJV fusion data, the authors successfully demonstrated pH-dependent CCF for the GPs of all arenaviruses *except* that of LUJV, the subject of their paper (which did not fuse at any pH tested). This frustrating "non-result" was cited by the Brummelkamp lab in their LUJV-CD63 paper as a motivator for the haploid screen for pro-LUJV cellular factors [280]. As they had had great success with their LASV CCF experiments by overexpressing Lamp1 at the PM, they pursued an analogous approach to find an additional triggering

[13] These three studies from the 1) Meulen lab, 2) Bartosch lab, and 3) Tani lab each had major differences in the design and execution of their CCF assays. **Cell lines** were: 1) Veros, 2) 293Ts, and 3) Huh7, respectively. **Reporters** were: 1) β-gal activity, 2) syncytia formation, and 3) both syncytia formation and luciferase activity. **Exposure times to low pH** in the pseudovirus pH inactivation experiments were: 1) N/A, 2) two minutes, and 3) five minutes. This brief list does not preclude other potentially consequential experimental differences.

factor for LUJV from within the endocytic pathway. Thus, with a presumptive intracellular receptor identified, the Brummelkamp group showed efficient ectopic LUJV GP-mediated fusion simply by ensuring that *both* of LUJV GP's fusion triggers, CD63 and low pH, were present.

The principle takeaway from these papers is that LASV GP has an exceptionally low – probably sub-physiological – pH optima for fusion without its fusion-triggering receptor. Prior to the discovery of the Lamp1 receptor, this finding was remarked upon quizzically in a number of publications, some even going so far as to suggest that lysosomal pH was lower than previously thought [177, 253, 258, 314]. However, Brummelkamp's paper helped to bridge the intuitive leap between pH hyposensitivity and endosomal receptor use.

1.E. Treatment Options for LASV and Other Hemorrhagic Fever Viruses

1.E.1. Current Treatment Guidelines

The WHO guidelines for treating LHF, which is grouped with other viral hemorrhagic fevers (VHFs), entail mostly palliative care, emphasizing maintaining circulatory volume, fluid and electrolyte balance, and blood pressure [315]. Mechanical ventilation, transfusion, renal dialysis, and anti-seizure therapy may be required. The first line pain medication is paracetamol, however ibuprofen, aspirin and other NSAIDs (and any other drug with anticoagulatory properties) are contraindicated due to their platelet effects. Sedatives such as haloperidol and diazepam are often given for anxiety. Severely ill

patients at risk for bacterial sepsis can be given oral or IV antibiotics such as ciprofloxacin, or ceftriaxone.

Ribavirin, often formulated in combination with pegylated interferon-α under the trade name Rebetol, is FDA approved for treatment of chronic HCV in adults, and is used as a nonspecific clinical therapeutic for respiratory syncytial virus (RSV) infections and VHFs caused by arenaviruses and CCHF. Ribavirin has also been shown to have antiviral activity against influenza, adenovirus, and La Crosse encephalitis virus (LACV) [316]. An analogue of guanosine, the prevailing model for ribavirin's mechanism of action (MOA) is that it halts viral replication. However, blocking viral cap-snatching, modulating the host immune response, and lethal mutagenesis have also been proposed as MOAs [139, 317]. Due to its limited efficacy in filovirus- and flavivirus-caused VHF, guidelines advise against treating these diseases with ribavirin. Side effects such as anemia, thrombocytosis, and birth defects are considerable, and tend to be more severe when given orally [318]. Given the side effects, its recommended use is only for post-exposure prophylaxis and for high-risk exposures to LASV and CCHF [315]. Ribavirin is most effective if started in patients during the initial six days after the onset of illness, but its efficacy rapidly diminishes if started later [104, 115, 319-326].

1.E.2. Treatment Strategies

Although LASV and EBOV belong to different families, their common use of a late endosomal receptor to gain entry into the cytoplasm is but one example of a broad list of similarities between these two late-penetrating viruses. These similarities are encouraging for efforts to identify broad-spectrum antivirals for these two, and perhaps more,

hemorrhagic fever viruses. Unfortunately, the prohibitive costs of drug design and development, particularly against relatively rare and geographically limited diseases, makes advancing even the most promising compounds difficult. Our lab and collaborators at the Integrated Research Facility (IRF) and USAMRIID have therefore focused on testing investigational or already-approved drugs (i.e. drugs that are safe, well-tolerated, and well-characterized) [327, 328]. From a starting list of 28 compounds screened at the IRF for anti-EBOV activity [329], we selected eight to investigate further based upon potential 1) targeting of one of the shared steps in the entry pathway with LASV and 2) the likelihood of synergistic effect when combined with another antiviral drug(s). We later selected arbidol as a ninth drug of interest. Although further details are provided in Chapter 4, these drugs are briefly described below and are summarized in **Figure 1.7** and in **Table 4.1**. Chemical structures are shown in **Appendix C**.

Apilimod has been shown to be a strong and specific inhibitor of PIKfyve, a kinase involved in regulating endosomal trafficking and maturation [327]. Since disruption of PIKfyve impairs trafficking of EBOV to late endosomes and lysosomes [330, 331], apilimod might be a promising therapeutic for many late penetrating viruses. Inhibitory concentrations of apilimod for blocking authentic EBOV replication and in a number of cell lines (including Huh-7, Veros, and macrophages) are in the low nanomolar range, tens to hundreds of times more potent than toremifene when tested in parallel [331]. Apilimod was evaluated in phase 2 clinical trials for treatment of rheumatoid arthritis [332] and Crohn's disease [333]; however, it did not improve clinical outcomes in either study. Thus, apilimod, while safe and well-tolerated, is currently unlicensed for any therapeutic purpose.

FIG 1.7. Druggable entry pathway features used by LASV and EBOV. Both viruses attach to receptors/attachment factors at the cell surface at neutral pH, but since Lassa can use both nonspecific attachment factors and its dedicated receptor, α-DG, it may be less susceptible to drugs targeting attachment and binding. Internalization through macropinocytosis (or "macropinocytosis-like" endocytosis) is similar in both viruses. Subsequently, both viruses may exhibit similar susceptibilities to drugs targeting later stages stages of trafficking in the pathway. Many pH-dependent viruses are susceptible to lysosomotropic agents during endosomal entry. Ebola GP's requirement for cathepsin-mediated activation offers additional druggable targets that almost certainly would not be effective against Lassa. Fusion inhibitors are a broad and complex class of drugs, and some, such as arbidol, may have roughly equivalent potency against LASV and EBOV. Lastly, endosomal receptor-specific drugs (e.g., targeting NPC1) are predicted to exhibit at least superior efficacy against one virus over the other, as we have observed for the CADs (which disrupt NPC1 binding). The asterisk (*) next to amiodarone, tetrandrine, and verapamil signifies that there is some debate over whether these drugs block trafficking or fusion.

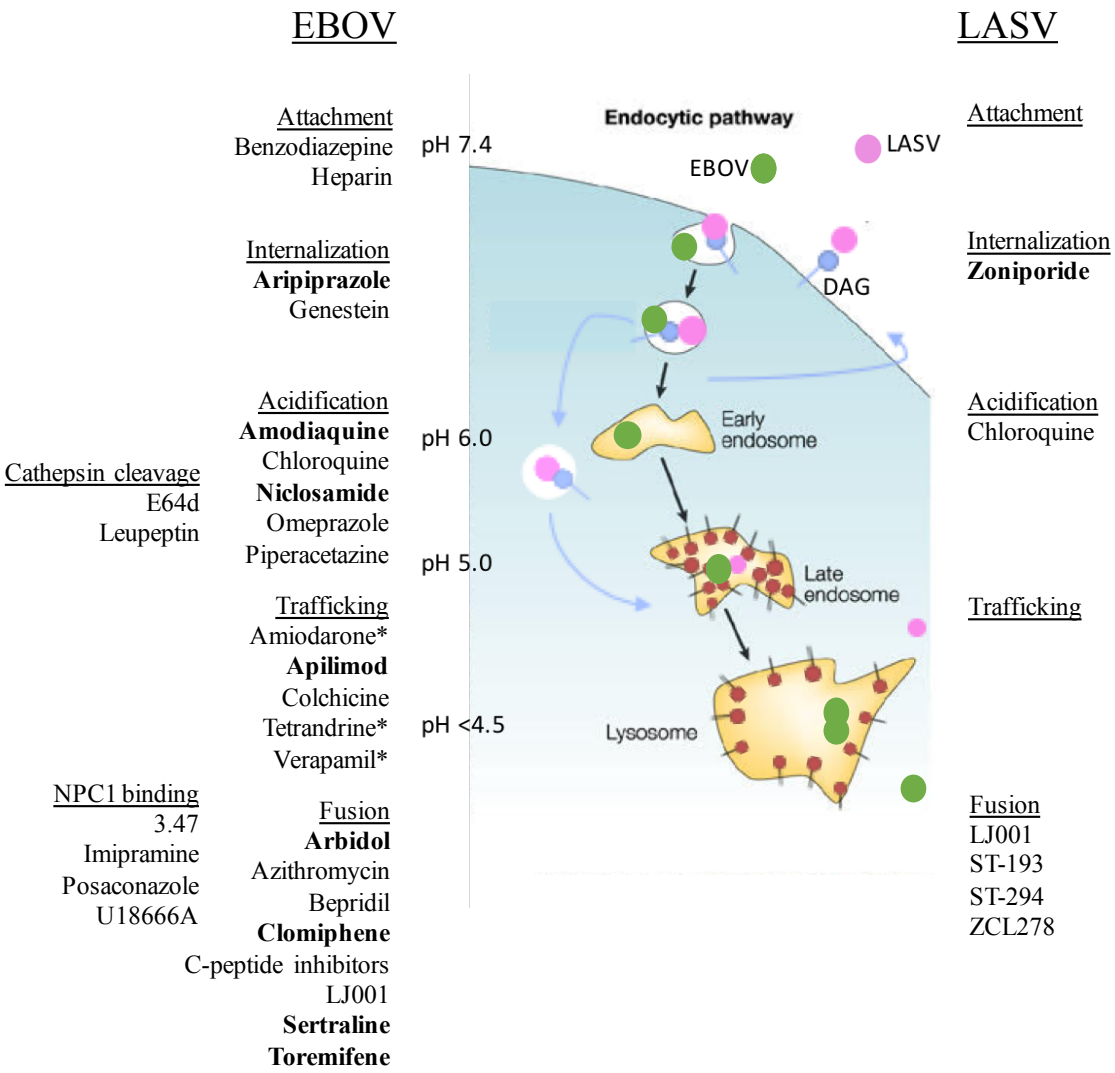
EBOV
LASV
Endocytic pathway
LASV
EBOV
DAG
Early endosome
Late endosome
Lysosome
pH 7.4
pH 6.0
pH 5.0
pH <4.5
Attachment
Benzodiazepine
Heparin
Internalization
Aripiprazole
Genestein
Acidification
Amodiaquine
Chloroquine
Niclosamide
Omeprazole
Piperacetazine
Trafficking
Amiodarone*
Apilimod
Colchicine
Tetrandrine*
Verapamil*
Fusion
Arbidol
Azithromycin
Bepridil
Clomiphene
C-peptide inhibitors
LJ001
Sertraline
Toremifene
Cathepsin cleavage
E64d
Leupeptin
NPC1 binding
3.47
Imipramine
Posaconazole
U18666A
Attachment
Internalization
Zoniporide
Acidification
Chloroquine
Trafficking
Fusion
LJ001
ST-193
ST-294
ZCL278

Niclosamide, an FDA-approved anthelmintic since 1960, inhibits endosomal acidification and has been shown to exhibit antiviral activity against EBOV, SARS, rhinovirus, influenza virus, rotavirus, and chikungunya virus (CHIKV) [334-337]. As a salicylanilide, niclosamide acidifies the cytoplasm by siphoning protons from the lysosome [338, 339]. Its IC_{50} against EBOV virus-like particle (VLP) entry is ~3 μM. Amodiaquine, an antimalarial aminoquinoline structurally similar to chloroquine, has broadly antipathogenic effects[14]. The probable MOA for blocking EBOV entry (IC_{50} ~4.4 μM) is that it disrupts endosomal acidification and consequently host proteolysis of GP. Although cathepsin-mediated effects would not be hypothesized to inhibit any known arenavirus, the drug has been shown to have an effective concentration (EC_{50}) of ~17 μM on authentic JUNV infection (which is in the range of its efficacy against CHIKV, but five to seven times less potent than its EC_{50} for EBOV) [334, 340].

Clomiphene and toremifene, both members of a functional drug class of selective estrogen receptor modulators (SERMs), are currently licensed and widely used in the US and Canada for the treatment of female infertility and metastatic breast cancer, respectively [334, 341]. Both drugs have been shown to improve survivability in a murine model of EBOV infection [342]. They appear to interfere with EBOV fusion in a manner unrelated to their estrogen receptor modulator function, possibly by disruption of the GP1-NPC1 interaction [328, 342], although computational analyses of the structure of SERMs have predicted that they may share a common target with chloroquine and other antimalarial

[14] Amodiaquine was used to treat one of the victims in the first (reported) LHF outbreak in Nigeria (1969). Thinking she had malaria, she self-administered amodiaquine eight days after caring for the index patient in Jos and died five days later (Reference 74)..

drugs [343]. Reported ranges IC_{50}s for EBOV are 0.8 – 2.4 μM [328, 334] for clomiphene and 0.03 – 0.16 μM for toremifene [328].

Sertraline, an antidepressant licensed under the tradename Zoloft, has been shown to inhibit EBOV (IC50 ~2.7 μM) and LCMV VLPs, albeit less potently for LCMV VLPs [328, 334]. Structurally, clomiphene, toremifene, and sertraline can be grouped together as cationic amphiphilic drugs (CADs). These compounds have distinct hydrophobic and hydrophilic groups with a tertiary amine group. They are thought to disrupt EBOV entry by interfering with a step involving NPC1, but without a direct effect on binding [344]. Like clomiphene and toremifene, sertraline is a functional inhibitor of acid sphingomyelinease (FIASMA), a subclass of weakly basic CADs that are anchored into the lysosomal membrane by a lipophilic moiety. As they accumulate in the lysosome, FIASMAs confer a positive charge to the luminal region that alters the electrostatic potential of the compartment [345]. This disrupts the ability of viral fusion proteins to effectively "grasp" and pull the target membrane toward the viral membrane [328, 346, 347].

Zoniporide is a potent inhibitor of the sodium hydrogen exchanger type 1 (NHE-1). Pursued as an anti-ischemic drug by Pfizer in 2002 [348], zoniporide was well tolerated in mid- to low-range doses during clinical trial testing; nevertheless, the drug showed a disappointing lack of efficacy [349-351]. After NHE was identified as a critical host factor for LCMV infection in an RNAi screen, however, zoniporide and several other NHE blockers were selected for further investigation into their potential antiviral activity [248]. When BHK-21 cells were treated with 50 – 100 μM of zoniporide, infectivity of rVSV-LCMV was reduced by over an order of magnitude [248].

Arbidol (Umifenovir) is a broad-spectrum antiviral licensed for clinical use in Russia and China for the treatment of IAV. In vitro testing of HepG2 cells has yielded arbidol EC_{50}s of 2.7 μM and 5.8 μM against infections with authentic EBOV and TACV, respectively [352]. Arbidol has an indole core that tends to associate with bulky aromatic amino acids by aromatic ring stacking [353, 354]. Its MOA(s) has been difficult to pinpoint due to the number potential targets (both host target acting and directly antiviral) that have been proposed (**Figure 1.8**). Despite the large number of possible entry and post-entry effects for arbidol, there is a preponderance of structural and functional evidence for fusion-specific effects on IAV HA. Crystal structures of IAV HA in complex with arbidol show that it binds in such a way as to stabilize HA in its prefusion conformation and prevent it from fusing with the endosomal membrane [312].

Consistent with this stabilizing effect, hemolysis fusion studies show that the pH for HA-mediated fusion (strain X:31, an IAV subtype 3 strain used in our studies) is shifted 0.3 pH units lower in the presence of 40 μM arbidol. The effect is even greater (almost an entire pH unit) for other strains of IAV [355, 356]. Finally, thermal shift assays (TSAs), which assess the effect of a ligand on protein stability, have shown that the melting temperature of X:31 HA is raised 1.5°C in the presence of 40 μM arbidol. Since IAV HA is a class I fusion protein like EBOV and LASV GP, it is reasonable to hypothesize that arbidol might similarly inhibit LASV and EBOV at an entry step. However, arbidol also has a propensity for intercalating into membranes (which has a stiffening effect), and this is thought to be its primary MOA against HCV [353, 357, 358].

FIG 1.8. Proposed antiviral activities for arbidol. The cartoon presents a generalized model of the major steps in viral infection and arbidol's possible MOA(s) against each step (**A**). Note that the diversity of targets may contribute to the broad-spectrum antiviral potential of arbidol. Arbidol has been shown to inhibit IAV HA fusion by stabilizing interactions with the fusogenic subunit of HA and preventing the conformational changes that occur during fusion activation (**B**). Here, the top image shows a side view of HA, with the receptor binding subunit in dark gray and the fusogenic subunit in light gray. Arbidol (yellow) lies 15-Å above the FP (shown in red). The images in **A** and **B** were obtained from open source materials published by Blaising et al. [359] and by Kadam et al. [312], respectively.

A

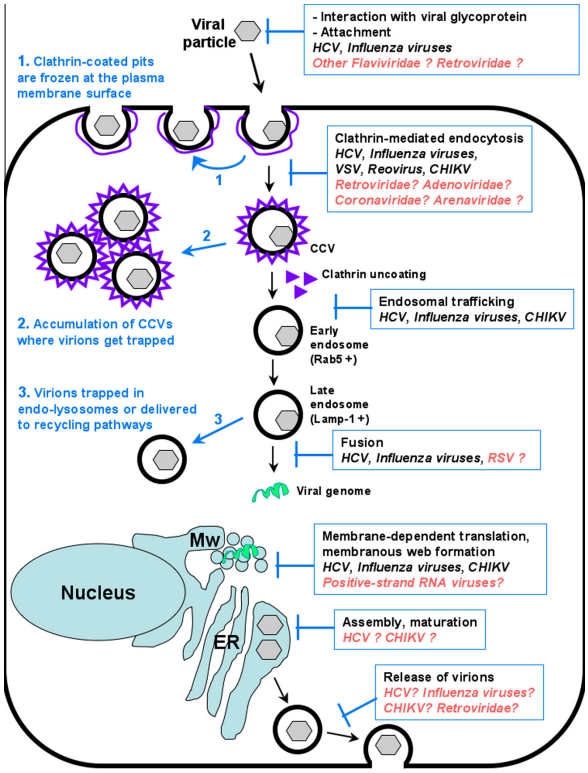
Viral particle
- Interaction with viral glycoprotein
- Attachment
HCV, Influenza viruses
Other Flaviviridae ? Retroviridae ?
1. Clathrin-coated pits are frozen at the plasma membrane surface
Clathrin-mediated endocytosis
HCV, Influenza viruses, VSV, Reovirus, CHIKV
Retroviridae? Adenoviridae? Coronaviridae? Arenaviridae ?
1
2
CCV
Clathrin uncoating
Endosomal trafficking
HCV, Influenza viruses, CHIKV
2. Accumulation of CCVs where virions get trapped
Early endosome (Rab5 +)
3. Virions trapped in endo-lysosomes or delivered to recycling pathways
3
Late endosome (Lamp-1 +)
Fusion
HCV, Influenza viruses, RSV ?
Viral genome
Mw
Membrane-dependent translation, membranous web formation
HCV, Influenza viruses, CHIKV
Positive-strand RNA viruses?
Nucleus
ER
Assembly, maturation
HCV ? CHIKV ?
Release of virions
HCV? Influenza viruses?
CHIKV? Retroviridae?

B

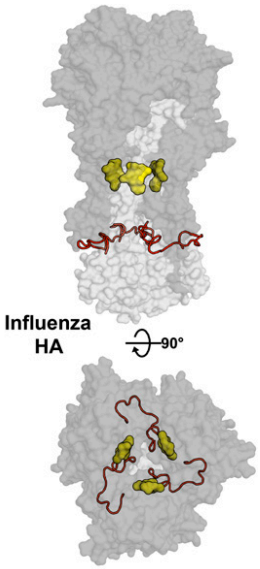
Influenza HA
90°

Additional studies are needed to better understand the MOAs for these drugs, particularly as we move toward considerations for strategic pairings in later synergy studies. As better minigenome and reverse genetics systems are developed [167, 360-364], the rate of discovery and characterization of new anti-arenaviral compounds is likely to increase. Exciting and completely novel compounds against LASV, such as amphipathic DNA polymers [365], siRNA-based therapies, and other small molecule inhibitors [366-370], continue to be tested.

1.F. Research Goals and Significance

1.F.1. Characterization of the Role of an Intracellular Receptor during LASV Entry

The report that LASV infection requires Lamp1 for entry raised a number of questions regarding Lamp1's specific role in the infectious process. Since Lamp1 is a resident membrane protein of late endosomes, the prevailing assumption was that its function must be related to promoting viral fusion with the endosomal membrane. My first goal was therefore to ask whether LASV requires Lamp1 for fusion, and then, if so, to further characterize its role in fusion. The broader significance of this work would be to shed light on the function of other recently discovered endosomal viral receptors as well as to provide additional therapeutic targets in LASV infection.

1.F.2. Investigation of the Mechanism of Action for Arbidol and Other Low Molecular Weight Inhibitors of LASV

Complementary to our mechanistic line of inquiry was the search for low molecular weight drugs that would inhibit both LASV and EBOV GP-mediated infections. These two viruses, as well as other clinically relevant members of the arena- and filovirus families, exploit similar pathways in their infectious cycles, can affect geographically overlapping regions, and cause a similar spectrum of symptoms. Thus, for this project goal, we chose to study drugs based on how their predicted MOA might be effective against common entry features of these two viruses. Given the unpredictable and devastating outbreak potential of hemorrhagic fever viruses, an ideal treatment strategy is to re-purpose already approved drugs (particularly those that inhibit viral infection at a pre-replication stage) that have been shown to be safe and well-tolerated in large numbers of people.

Using pseudovirus entry assays, my second project goal was to test the hypothesis that a compound(s) pre-screened for blocking EBOV entry would also block LASV virus entry with similar potency. I chose arbidol for more in depth studies because of the broad spectrum of viruses susceptible to it and its strong clinical record as an effective antiviral intervention.

Chapter 2

Materials and Methods

Cells. HEK 293T/17 (human embryonic kidney fibroblasts; ATCC CRL-11268 via University of Virginia Tissue Culture Facility), BHK21 (baby hamster kidney fibroblasts; ATCC CCL-10; a kind gift from James Casanova at the University of Virginia), and COS-7 (African Green monkey fibroblasts; ATCC CRL-1651; a kind gift from Dr. Douglas DeSimone at the University of Virginia) cells were maintained at 37^{o}C with 5% CO_2 in growth medium: high glucose Dulbecco's Modified Eagle Medium (DMEM) supplemented with 1% L-glutamine, 1% sodium pyruvate, 1% antibiotic/antimycotic, and 10% supplemented calf serum (SCS: Hyclone, GE Healthcare Bio-Sciences) or 10% fetal bovine serum (FBS).

shRNA knockdown of Lamp1. Validated shRNA against human Lamp1 (5' CCG GTG CTG CTG CCT TCT CAG TGA ACT ACT CGA GTA GTT CAC TGA GAA GGC AGC ATT TTT 3') in pLKO.1-puro vector was purchased from Sigma Aldrich (clone #TRCN0000029268). To produce lentiviruses, parental 293T cells (7 x 10^5 cells per 6cm^2 tissue culture dish) were transfected with 1μg pLKO.1 shRNA plasmid, 900 ng psPAX2 packaging plasmid, and 100 ng pDM2.G envelope plasmid using FuGENE 6 transfection reagent. The following morning, media was harvested and centrifuged at 1000 x *g* for 5 min to remove cellular debris, and the clarified, lentivirus-containing media was filtered through 0.45 μm filters. 293T cells (~40% confluent) were transduced with the lentivirus using 6 μg/mL polybrene. At 96 h postinfection, cells were split and transduced cells were selected with 3 μg/mL of puromycin. The extent of Lamp1 knockdown was determined by Western blot analysis of whole cell lysates and visualized using the Odyssey infrared imaging system (Licor). Protein quantification was performed using ImageJ software.

CRISPR/Cas9-mediated knockout of Lamp1. Lamp1 knockout (KO) cell lines were generated by CRISPR/Cas9-mediated genome editing. A guide RNA (gRNA) targeting the first exon of Lamp1 was selected using ThermoFisher's GeneArt CRISPR Design Tool. Primers for both strands covering the cleavage site (F, 5' caccGAA CGG GAC CGC GTG CAT AA 3'; R, 5' aaacTTA TGC ACG CGG TCC CGT TC 3' [lowercase letters indicate the complementary BbsI overhangs]) were annealed to each other to make a double-stranded oligo that was then cloned into the BbsI site of the pX330-U6-Chimeric_BB-CBh-hSpCas9 vector, which has both a gRNA scaffold site and Cas9 (the plasmid [Addgene plasmid #42230] was a kind gift from Mazhar Adli at the University of Virginia and Feng Zhang) [371, 372]. After sequencing to confirm correct insertion of the gRNA, pX330-U6 and an enhanced green fluorescent protein expression plasmid (to assess transfection efficiency) were co-transfected into 293T cells using Lipofectamine 2000. Lamp1 expression in transfected and untransfected populations was crudely compared by Western blot analysis. Cells with the gRNA treatment resulting in the lowest Lamp1 expression were stained with Lamp1 antibody (H4A3 from Developmental Studies Hybridoma Bank) and AlexaFluor 488 and subjected to negative selection for no/low surface Lamp1 expression via FACS. After expansion of singly sorted cells, clonal cell lines were permeabilized with 0.05% saponin, stained with Lamp1 antibody, and screened for null Lamp1 expression by in-cell Western (ICW) assay on a 96-well format as previously described [373]. From the Lamp1$^-$ clonal cell lines identified by ICW, eight clones were selected for further confirmation by traditional Western blot. To confirm gene disruption near the PAM site, a fragment of genomic DNA from parental (WT) cells and two of the clonal Lamp1 KO lines was amplified (F: 5' ACC CCA GCC TGG CGA CAG TGA GAC

TCC 3’; R: 5’ ATG GCA CAT GAC AGC GCA GGT TAC TGA CA 3’), cloned into a TOPO vector, and the region of interest was then sequenced to confirm gene disruption (5’ CCG TCT TCC CTG GAA TTG ACA GGC CTC AT 3’).

Generation of plasma membrane Lamp1. To transiently overexpress Lamp1 at the plasma membrane (pmLamp1), Agilent’s QuikChange II protocol was followed to delete the codon for the alanine residue at position 384 in the Lamp1 gene (pRK5-LAMP1-FLAG [Addgene plasmid # 71868] was a gift from David Sabatini) [374, 375]. The sequence of the forward primer was 5’ GTC GGC AGG AAG AGG AGT CACGGCTA CCA GAC TAT CTA GGC GGC CGC GAT C 3’, and that of the reverse primer was 5’ GAT CGC GGC CGC CTA GAT AGT CTG GTAGCCGTGA CTC CTC TTC CTG CCG AC 3’. The underlined residues represent the flanking residues around the deleted codon for alanine.

Viruses. To produce MLV pseudovirus particles (with either luciferase, Gag-βlaM, or both reporters), 293T cells in 10-cm^2 dishes were grown in DMEM containing 10% SCS to 80% confluence and then transfected with 6 μg of total DNA with the following plasmids at a 2:1:1:1 ratio of pTG-luc (a kind gift from both Jean Dubuisson at the Centre National de la Recherche Scientifique in Lille via Gary Whittaker at Cornell University), pCMV gag-pol (from Jean Millet at Cornell University and Jean Dubuisson), Gag-βlaM (produced by James Simmons), and viral glycoprotein (LASV Josiah strain GPC in pCMV from Gregory Melikyan at Emory University; LCMV Armstrong strain GPC in pCMV from Jack Nunberg at University of Montana and Juan de la Torre at Scripps Institute). At 48 h posttransfection (hpt), virus-containing media was harvested and clarified by low-speed

centrifugation and filtered through 0.45-μM-pore filters. Pseudoviruses were stored on ice and their titers were determined to achieve desired functional ranges by either luciferase infection assay or βlaM entry assay. After titration, pseudovirus stocks were stored at -80°C.

To produce VSV-luciferase pseudoviruses, 5 x 10^5 BHK21 cells were seeded (40 10-cm^2 dishes) in DMEM containing 10% SCS. Cells were transfected with 12 μg of plasmid expressing LASV GPC, LCMV GPC, or no GPC, using polyethylenimine (PEI). The following day, cells were infected for 1 h at 37°C with VSV-G helper virus expressing *Renilla* luciferase (diluted in serum-free media). After infection, cells were thoroughly washed with cold phosphate-buffered saline (PBS) and incubated O/N in complete DMEM. Supernatants containing pseudoviruses were collected and concentrated using Viva-Spin 20 (300-kDa molecular weight cutoff) and then pelleted through a 20% sucrose-HM (20 mM HEPES, 20 mM MES [morpholineethanesulfonic acid], 130 mM NaCl, pH 7.4) cushion. The pellet was resuspended in sterile 10% sucrose-HM.

To produce VSV-G luciferase helper virus**,** 5 x 10^5 BHK21 cells were seeded (5 10-cm^2 dishes) in DMEM containing 10% SCS. Cells were transfected with 12 μg of plasmid expressing VSV-G using PEI. The following day cells were infected for 1 h at 37°C with VSV-luciferase plaques in serum-free DMEM. After infection, cells were thoroughly washed with cold PBS and incubated O/N in complete DMEM at 37°C. Supernatants containing helper viruses were collected and stored at -80°C.

Pseudovirus infection assay. 293T cells (WT, Lamp1 KD, or Lamp1 KO) in DMEM containing 10% SCS were seeded onto fibronectin-coated white 96-well plates (3 x 10^4

cells/well). The following morning, cells were infected with an input of pseudovirus titered to achieve a target signal range and incubated at 37°C. At 48 h postinfection (hpi), cells infected with luciferase pseudoviruses were washed with PBS and lysed with Britelite reagent (Perkin Elmer), which also contains firefly luciferase substrate, and incubated for 10 min at room temperature while shaking before measuring luminescent output on a Promega GloMax luminometer. For assays using GFP pseudovirus infections, at 48 hpi, cells were washed, fixed, and analyzed for fluorescence by flow cytometry. For assays involving inhibition of infection with NH_4Cl, cells were pre-treated with drug diluted in Opti-MEM (OMEM) 1 h before infection with pseudovirus, as described elsewhere [245, 376].

Dose response curves. An effective dose range for each drug tested was based upon the highest drug concentration needed to elicit a near total reduction (95 – 99%) in infection signal. Two-fold dilutions of drug into OMEM were made from the highest concentration, and the 8-point series ended with a mock vehicle treatment (equivalent to the amount of solvent used in the highest concentration dose). BSC cells were pretreated with drug for 1 h and then infected with an amount of pseudoviruses determined to achieve a signal of 75,000 – 150,000 RLU. Cells were incubated in the presence of drug for 16 – 24 h, and then lysed with Britelite reagent following manufacturer's instructions. Luciferase signals were then measured and normalized to the highest signals in mock-treated wells. Non-linear regression analysis was applied to fit dose response curves (log [agonist] versus. response [variable slope]). Error bars reflect the standard deviation from triplicate wells. Interpolated IC_{50}s were determined from the curves and statistical analysis on all data and

were performed using GraphPad Prism 7 (GraphPad Software). Compounds were tested three separate times and a final IC_{50} for each drug was based upon the average of these three experiments.

Live virus yield reduction assay. Vero76 cells were seeded onto 6-well plates and utilized at full confluency. Cells were pretreated with indicated concentrations of arbidol, NH_4Cl, or ethanol vehicle for 1 hr at 37°C/5%CO_2. Cells were then infected with LASV (Josiah strain) at a multiplicity of infection (MOI) of 0.01 for 1 additional hr. Unadsorbed virus was removed with two consecutive washes followed by incubation for 24 h at 37°C, 5% CO_2. Drugs treatments were maintained during all steps, including washes and O/N incubation. Supernatants were harvested the following day and 10-fold serial dilutions made. These dilutions were used to infect ~90% confluent monolayers of Vero76 cells in 6-well plates for 1 h at 37°C, 5% CO_2 with rocking every 15 minutes. A primary overlay consisting of a 1:1 mixture of 1.6% SeaKemp agarose and 2X EBME supplemented with 20% FBS and 8% GlutaMAX (Gibco) was then added on top of the serial infection wells and allowed to solidify. Cells were incubated for 4 days at 37°C, 5%CO_2, followed by addition of a secondary overlay consisting of a 1:1 mixture identical to the above but with the addition of 8% Neutral Red (NR; Gibco) for a final NR concentration of 4%. Cells were incubated O/N prior to visual scoring of plaques. Plaque counts were then adjusted according to dilution and averaged.

Biosafety. All manipulations involving live LASV virus were performed in a biosafety level 4 containment suite at USAMRIID with personnel wearing positive-pressure

protective suits fitted with HEPA filters and umbilical fed air. USAMRIID is registered with the Centers for Disease Control Select Agent Program for the possession and use of biological select agents and toxins and has implemented a biological surety program in accordance with U.S. Army regulation AR 50-1 "Biological Surety."

Entry assay. To assess GPC-mediated entry, 293T cells grown in DMEM containing 10% SCS were seeded onto fibronectin-coated transparent 96-well plates. After 18 to 24 h, a titer-determined input of βlaM pseudoviruses was diluted in OMEM and bound to cells by spinfection at 250 x *g* for 1 h at 4°C. Cells were incubated at 37°C for 3 h before adding βlaM substrate (CCF2-AM; Invitrogen) and allowing an additional 1 h incubation at 37°C. Cells were then washed with PBS and allowed to incubate O/N at room temperature in loading buffer (phenol red-free DMEM, 5 mM probenecid, 2 mM L-glutamine, 25 mM HEPES, 200 nM bafilomycin, 10% FBS). The following day, cells were washed with PBS, fixed in 4% paraformaldehyde (PFAM), and analyzed for virus entry by either flow cytometry using a BD FACSCalibur or on a BioTek Cytation3 plate reader.

Cell-cell fusion assay. Effector populations of 293T cells, i.e. cells expressing LASV or LCMV GP, were seeded onto 6-well plates (3.75×10^5 cells/well). Receptor cell populations, i.e. cells representing Lamp1 phenotypes (pmLamp, WT, Lamp1 KD or KO cells), were seeded onto fibronectin-coated white 96-well plates (3×10^4 cells/well). The following morning, effector cells were transfected with 1 μg/well of either LASV or LCMV GPC plasmids, and an equivalent amount of DSP_{1-7} plasmid (a kind gift from Naoyuki Kondo) [377]; receptor cells were transfected with 33 ng/well of pRK-pmLamp1 vector

(when overexpressing Lamp1 at the PM) and equivalent amount of DSP_{8-11} plasmid. Lipofectamine 2000 was used for all transfections. At 24 hpt, effector cell media was replaced with fresh DMEM containing 60 μM EnduRen luciferase substrate (Promega). After incubating for 2 h at 37°C, effector cells were rinsed with PBS, detached with 0.05% trypsin-EDTA, and overlaid onto receptor cells (1.5 x 10^5 cells/well). The mixed cell populations were allowed to settle for 3 h at 37°C before pH pulsing the cells with HMS buffer (100 mM NaCl, 15 mM HEPES, 15 mM succinate, 15 mM MES, 2 mg/mL glucose) adjusted to the appropriate pH for 5 min at 37°C. The pH was then reneutralized with 20 mM HEPES in DMEM and cells were returned to 37°C for 1 h before recording luminescence on a Promega GloMax luminometer.

For dose response cell-cell fusion experiments, the indicated concentration of arbidol or vehicle was added to effector cells (expressing either LASV GP or IAV HA) after the 2 h incubation period with the EnduRen substrate. Effector cells were allowed to incubate in the presence of drug at 37°C for 1 h before proceeding with the overlay step. The presence of drug was maintained throughout the experiment.

Forced fusion at the plasma membrane. COS-7 cells were seeded on a 6-well plate to reach 60% confluence the day of transfection. Cells were transfected using Lipofectamine 2000 with 0.6 μg of pmLamp1 DNA and 1 μg of firefly luciferase DNA according the manufacturer's instructions. COS-7 cells (transfected with either pmLamp1 and firefly luciferase or firefly luciferase only) were seeded at a density of 15,000 cells/well on a fibronectin-coated white 96-well plate. The next day, cells were cooled on ice for 15 min. LASV VSV-luciferase (*Renilla*) pseudoviruses, the titer of which had been determined to

reach a target signal under control conditions, were added to cells in sextuplicate in serum-free DMEM at pH 6.5 and bound to the cells by centrifugation (250 x *g*, 1 h, 4°C). Cells were returned to ice and washed once with cold PBS. To promote fusion at the PM, a pH pulse was applied for 5 min at 37°C in prewarmed HMS buffer at different pH values (7.0, 6.0, 5.5 and 5.0). Cells were returned to ice, and complete DMEM containing 40 mM NH_4Cl (to block virus entry) was added. 16 h later, luciferase activities were measured using the Dual-Glo Luciferase Assay System (Promega) according to the manufacturer's instructions. Viral fusion with the PM was assessed by using a ratio of *Renilla* luciferase activity (an indicator for virus replication) over firefly luciferase activity (to account for the number of cells).

For dose response virus-cell fusion experiments, COS-7 cells were pre-treated for 1 h with the indicated concentration of arbidol or vehicle before binding LASV VSV pseudoviruses. Presence of drug was maintained throughout the assay.

GP1 dissociation assay. Lamp1 KO 293T cells seeded in a 6-well plate (6.5 x 10^5 cells/well) were transfected with C-terminal Flag-tagged LASV GPC (pCC421-LASV GPC vector was a kind gift from Jason Botten at the University of Vermont) using PEI. At 48 hpt, cells were rinsed 1X with cold PBS before adding NETI lysis buffer (150 mM NaCl, 1 mM EDTA, 50 mM Tris-HCl, 20 mM succinate, 0.5% IGEPAL). After 20 min of incubation on ice, lysates were collected and centrifuged at 4^oC for 15 min at 21,000 x g. Cleared lysates were then added to anti-Flag M2 magnetic beads (Sigma, #M8823) at a 2.5:1 ratio of lysate:bead resin and allowed to incubate at 4^oC under slow rotation for 1 h. Beads were washed twice with cold lysis buffer, then divided equally into separate aliquots

according to the number of pH points assayed. Beads were pulsed with NETI lysis buffer with 0.5% Triton X-100 adjusted to the appropriate pH for 1 min (or the indicated time) at 37°C. After the pH pulse, samples were reneutralized with 1 M Tris-HCl, pH 8.5 before collecting the supernatants for later analysis, washing the beads 2X with cold NETI lysis buffer, and eluting protein from the beads with 0.1 M glycine, pH 3.5.

Chapter 3

Lamp1 Increases the Efficiency of Lassa Virus Infection by Promoting Fusion in Less Acidic Endosomal Compartments

Adapted from Hulseberg, C. E., Fénéant L. Szymańska K.M., and White J.M.

MBio (2018)

Abstract

Lassa virus (LASV) is an arenavirus whose entry into host cells is mediated by a glycoprotein (GP) complex comprised of a receptor binding subunit, GP1, a fusogenic transmembrane subunit, GP2, and a stable signal peptide. After receptor-mediated internalization, arenaviruses converge in the endocytic pathway where they are thought to undergo low pH-triggered, GP-mediated fusion with a late endosome membrane. A unique feature of LASV entry is a pH-dependent switch from a primary cell surface receptor (alpha-dystroglycan) to an endosomal receptor, lysosomal-associated membrane protein, Lamp1. Despite evidence that the interaction between LASV GP1 and Lamp1 is critical, the function of Lamp1 in promoting LASV infection remains poorly characterized. Here we used WT and Lamp1 knockout (KO) cells to show that Lamp1 increases the efficiency of, but is not absolutely required for, LASV entry and infection. We then used cell-cell and pseudovirus-cell surface fusion assays to demonstrate that LASV GPC-mediated fusion occurs at a significantly higher pH when Lamp1 is present compared to when Lamp1 is missing. Correspondingly, we found that LASV entry occurs through less acidic endosomes in WT ($Lamp1^{+}$) versus KO ($Lamp1^{-}$) cells. We propose that, by elevating the pH threshold for fusion, Lamp1 allows LASV particles to exit the endocytic pathway before they encounter an increasingly acidic and harsh proteolytic environment, which could inactivate a significant percentage of incoming viruses. In this manner Lamp1 increases the overall efficiency of LASV entry and infection.

Introduction

Lassa virus (LASV) is the most clinically important member of the *Arenaviridae*, a diverse family of enveloped, negative-sense RNA viruses, which currently includes seven recognized hemorrhagic fever viruses [2]. Infections in humans typically involve inhalation of the excreta of rodents, which are the natural reservoirs of the viruses, or ingestion of contaminated food or water [138]. Arenaviruses are classified into two groups according to their phylogenetic relatedness and the geographic range of their respective rodent carriers: New World arenaviruses are limited to the Americas, and Old World arenaviruses, which include LASV, are generally confined to Africa. Lymphocytic choriomeningitis virus (LCMV), an Old World arenavirus with worldwide distribution, is of particular note because it has long served as a prototypical arenavirus and is among the best-studied of all viruses.

As with other Old World arenaviruses, LASV particles use trimeric glycoprotein spikes on their surface to engage the alpha subunit of dystroglycan (α-DG), its primary cell surface receptor [278]. Upon binding to α-DG, LASV particles are internalized into compartments in the endocytic pathway. The acidified environment within maturing endosomes eventually triggers fusion between the viral and endosomal membranes allowing the viral genome to be released through the resulting fusion pore into the cytoplasm. This membrane fusion event is mediated by the viral glycoprotein (GP) complex, which is comprised of a receptor binding subunit, GP1, a fusogenic transmembrane subunit, GP2, and a stable signal peptide. As the pH of the endocytic compartment decreases, GP1 dissociates from the complex, triggering major

reorganizational changes in GP2 and uncovering the hydrophobic fusion loop that drives membrane fusion [214].

An interesting feature of LASV is that it employs a second, intracellular receptor. En route in the endocytic pathway, the GP1 subunit undergoes a pH-dependent switch from the α-DG surface receptor to its endosomal receptor, Lamp1 [135, 221]. This pairing of LASV GP1 with Lamp1 is only the second example of a virus using an intracellular receptor, the first being the use of Niemann-Pick C1 (NPC1) by the GP1 of Ebola and other filoviruses [301, 378]. While these interactions are now well documented, the precise manner(s) in which Lamp1 and NPC1 promote viral entry remains unknown.

In this study, we explored the role of Lamp1 in LASV fusion and entry. We first found that a low level of Lamp1 supports robust entry and that entry can even occur, albeit attenuated, in cells lacking Lamp1. We next showed that Lamp1 upwardly shifts the pH dependence of LASV GPC-mediated fusion from its unusually low optimum of pH $\leq$ 4 [144, 216] to the higher, more physiologic range found within the endocytic pathway. Consistently, we found that entry of LASV GP pseudoviruses occurs in less acidic endosomes in cells containing versus cells lacking Lamp1. Taken together we propose that Lamp1 increases the overall efficiency of LASV entry and infection by promoting fusion in a more hospitable, less acidic endosomal compartment.

FIG 3.1. Knockdown of Lamp1 does not suppress LASV pseudovirus infection. The effect of Lamp1 deficiency on LASV (**A**) and LCMV (**B**) pseudovirus (denoted by **ψ**) infection over a range of pseudoviral inputs (indicated by black triangle on abscissa) was evaluated based on expression of the luciferase reporter. Lamp1-knockdown (KD) cells express 17.1% ± 7.8% WT levels of Lamp1 (n=7) (inset in panel **A**). Each data point is the average of triplicate measurements from one representative experiment (performed five times with similar results). Error bars indicate standard deviation (SD). KD values did not significantly differ from WT values in any data point by unpaired, two-tailed *t* test.

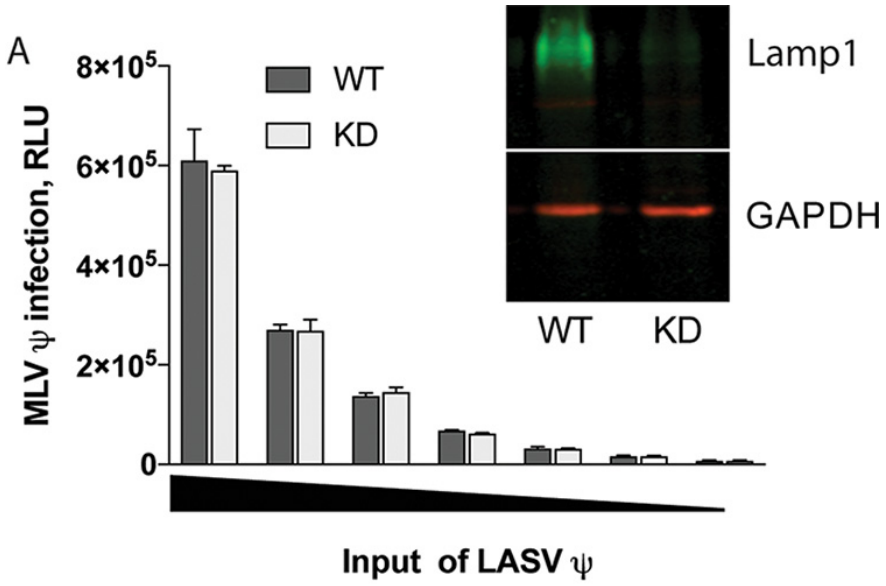
A
8×10^5
6×10^5
4×10^5
2×10^5
0
MLV ψ infection, RLU
WT
KD
Lamp1
GAPDH
WT
KD
Input of LASV ψ

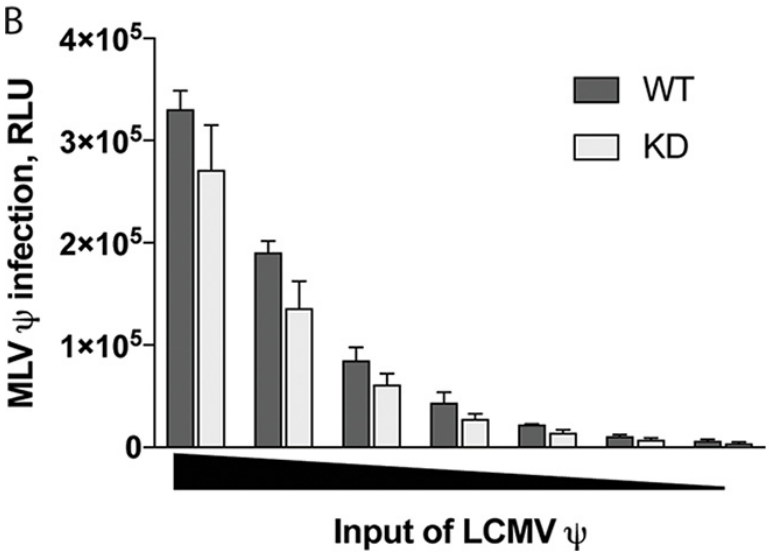
B
4×10^5
3×10^5
2×10^5
1×10^5
0
MLV ψ infection, RLU
WT
KD
Input of LCMV ψ

Results

A low level of Lamp1 supports robust LASV GP-mediated infection. Lamp1 was recently reported to serve as the intracellular receptor for LASV. To begin to explore the role of Lamp1, we first generated a stable line of 293T cells in which Lamp1 expression was strongly reduced using a lentivirus encoding an shRNA to knockdown Lamp1 expression. This knockdown reduced Lamp1 expression to ~15% relative to expression in WT cells (**Figure 3.1**). Nonetheless, Lamp1 KD cells and WT cells were equally susceptible to infection with MLV pseudoviruses bearing LASV GPC (and encoding luciferase) at all inputs of virus tested. Since LCMV GPC does not interact with Lamp1, LCMV infections were, as expected, unaffected by decreased Lamp1 expression (**Figure 3.1.B**). This finding (**Figure 3.1.A**) suggested that residual Lamp1 expression in Lamp1 KD cells is sufficient to support efficient LASV GPC-mediated infection.

The absence of Lamp1 reduces, but does not eliminate, LASV GP-mediated entry and infection. To test the effects of a complete loss of Lamp1 on LASV entry and infection, we generated Lamp1 KO cell lines using CRISPR Cas9 gene editing (**Figure 3.S.1**). An initial assessment of LASV MLV pseudovirus infection in eight clonal KO cell lines revealed that infection occurred but was reduced to ~20% the efficiency in WT cells (**Figure 3.2.A**). In contrast, and as expected, LCMV MLV pseudoviruses were as infectious in the KO cell lines as they were in the parental WT cells (**Figure 3.2.B**). Three of these KO cell lines, all of which demonstrated undetectable levels of Lamp1 via Western blot (**Figure 3.2.C**), were selected for further testing. We again found that these KO cell lines were susceptible to LASV MLV pseudovirus infection at ~15% - 30% the level seen

FIG 3.2. Knockout of Lamp1 reduces but does not abolish LASV GP-mediated infection. Eight Lamp1 KO clones (see Materials and Methods) were screened for infection with LASV (**A**) and LCMV (**B**) MLV pseudoviruses. Data represent average RLU ± SD, measured in triplicate, from one experiment, repeat two additional times with similar results. The level of LASV infection across these eight Lamp1 KO clones was 22% ± 5.3% of that seen in WT cells. (**C**) Representative blot (out of five similar blots) of lysates from three KO clones showing that Lamp1 was not detectable. (**D**) The above clonal KO lines were infected in quadruplicate with a moderate input (titered determined for a signal of ~100,000 relative light units [RLU] in WT cells) of either LASV or LCMV MLV luciferase pseudoviruses. Data were normalized to maximal signal from WT cells and statistical significance was calculated by comparing percent infection in KO cells against percent infection in WT cells using a two-way analysis of variance (ANOVA). Error bars represent SD, **, $P < 0.01$; ***, $P < 0.001$. (**E**) One representative clone (2G8) was assayed in triplicate for infection with high, medium, and low input levels of LASV GPC pseudoviruses. Pseudoviruses lacking glycoprotein ("No GP") were used to establish a background signal, indicated by a dashed line. Error bars represent SD. *, $P < 0.01$; **** $P < 0.0001$, and ns, not significant, based on multiple unpaired, two-tailed *t* tests. The experiment was repeated twice with similar results. (F) The same clonal KO lines tested in **D** were infected with LASV and LCMV VSV pseudoviruses encoding GFP, and the titer was determined for 40 to 70% infection in WT cells. Signal from the "No GP" control pseudoviruses was subtracted from all measurements. As in **D**, infection signal from triplicate samples was normalized to WT cells and statistical analysis applied to the efficiency of infection in KO cells compared to WT cells.

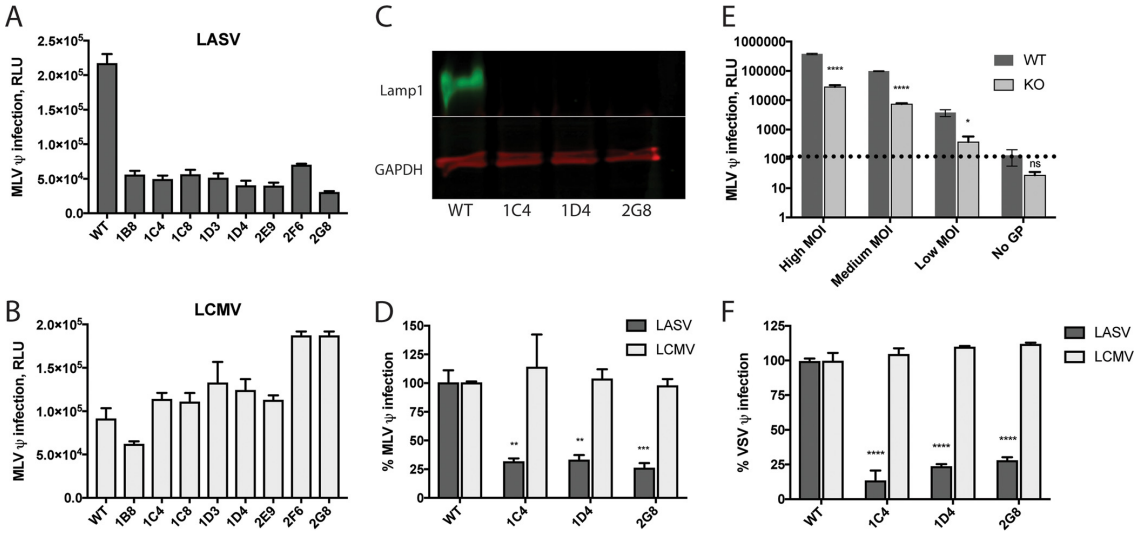
A
LASV
MLV ψ infection, RLU
2.5×10^5
2.0×10^5
1.5×10^5
1.0×10^5
5.0×10^4
0.0
WT
1B8
1C4
1C8
1D3
1D4
2E9
2F6
2G8
B
LCMV
MLV ψ infection, RLU
2.0×10^5
1.5×10^5
1.0×10^5
5.0×10^4
0.0
C
Lamp1
GAPDH
WT
1C4
1D4
2G8
D
% MLV ψ infection
150
125
100
75
50
25
0
LASV
LCMV
**
**
***
E
MLV ψ infection, RLU
1000000
100000
10000
1000
100
10
1
WT
KO
****
****
*
ns
High MOI
Medium MOI
Low MOI
No GP
F
% VSV ψ infection
125
100
75
50
25
0
LASV
LCMV
****
****
****

in WT cells (**Figure 3.2.D**). Notably, this low level of infection was seen across a wide range of pseudovirus inputs (**Figure 3.2.E**). To assess this finding with a different pseudovirus system, we performed the analysis again using VSV pseudoviruses bearing LASV or LCMV GP and encoding a GFP reporter (**Figure 3.2.F**). In agreement with the findings using MLV pseudoviruses, we found that LASV VSV pseudoviruses infect Lamp1 KO cells at ~15% - 30% the efficiency in WT cells, while LCMV VSV pseudoviruses infected KO cells as efficiently as WT cells.

The findings in **Figure 3.2** (using two different types of pseudoviruses whose only common feature is expression of LASV GPC) suggested that GP-mediated entry is reduced, but not abolished, in these Lamp1 KO cells. To test this proposal, we used a complementary approach and infected cells with pseudoviruses carrying an MLV-Gag-β-lactamase (βlaM) chimeric protein. Upon entering the cytoplasm, Gag-βlaM cleaves the CCF2-AM substrate (which is loaded into cells shortly after infection), and the resulting change in fluorescence of the product from green to blue provides a sensitive readout for viral entry [379-382]. We infected WT and Lamp1 KO cells with a range of MLV-Gag-βlaM pseudovirus inputs bearing either LASV or LCMV GP. As seen in **Figure 3.3**, entry mediated by LASV GP occurred in Lamp1 KO cells at ~25 - 35% the level seen in WT cells. In contrast, and as expected, entry of pseudoviruses bearing LCMV GP occurred at roughly the same level in WT and KO cells.

FIG 3.3. Knockout of Lamp1 reduces, but does not eliminate, LASV GP-mediated entry. Lamp1-dependent entry was assayed by infecting WT and KO cells in triplicate with high, medium, and low inputs of LASV (**A**) and LCMV (**B**) MLV-βlaM pseudoviruses. Fluorescent signals (indicating cleavage of βlaM upon entry into the cytoplasm) from infected KO cells were normalized to those from WT cells at each input. Background signal from uninfected control cells loaded with βlaM substrate was subtracted from all data points. A negative control infection using "No GP" pseudoviruses (not shown) generated a fluorescent signal roughly equivalent to the substrate-only background signal. Data show the average of normalized triplicate fluorescence measurements ± SD from a single representative experiment. The experiment was performed three times with similar results. **, $P < 0.01$; ****, $P < 0.0001$, based on unpaired, two-tailed *t* test.

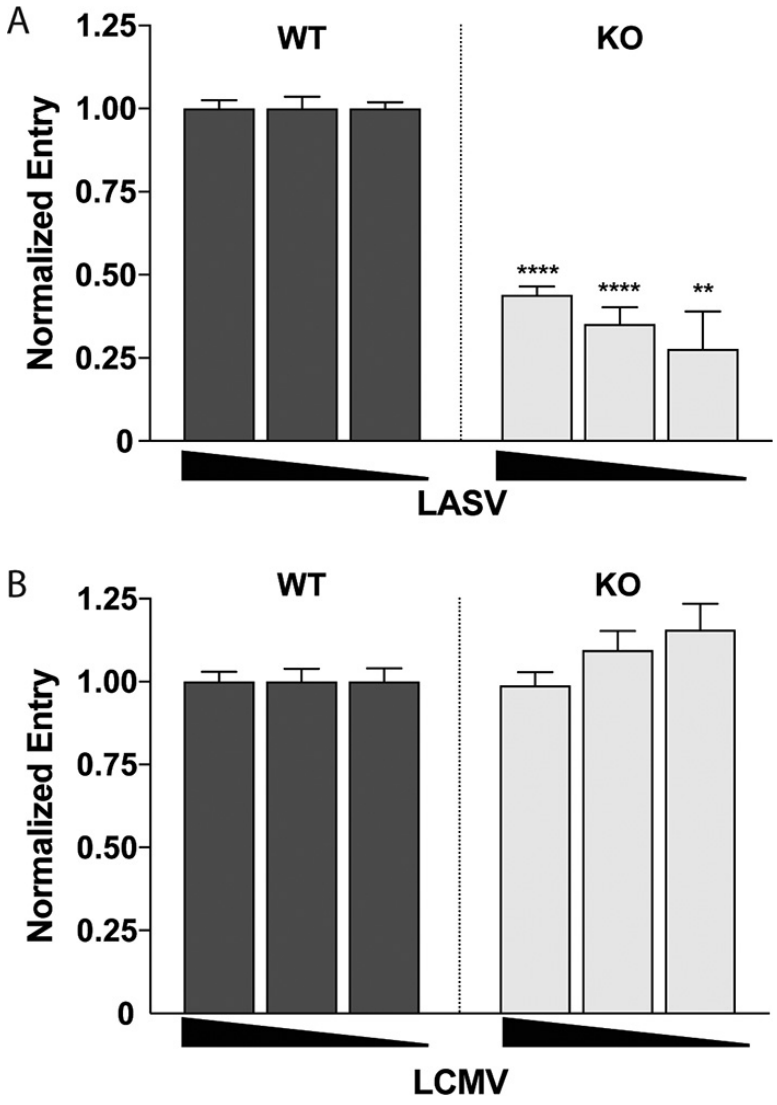
A
WT
KO
Normalized Entry
1.25
1.00
0.75
0.50
0.25
0
****
****
**
LASV
B
WT
KO
Normalized Entry
1.25
1.00
0.75
0.50
0.25
0
LCMV

The results presented in **Figures 3.1** to **3.3** suggest that, in our system, Lamp1 increases the efficiency of, but is not absolutely required for, LASV GP-mediated entry and infection. In Lamp1 KO 293T cells, entry and infection by both MLV and VSV pseudovirus particles expressing LASV GPC occurs at ~20% - 30% the level seen in WT cells. We note that the requirement for Lamp1 appears more stringent using authentic LASV in different cells [135]. The fusion enhancing effect of Lamp1 is also specific, as it is not seen for LCMV GP-mediated entry or infection. Moreover, results of our KD analysis indicate that a low level of Lamp1 (~15% of WT) in 293T cells suffices for efficient LASV GPC-mediated entry and infection.

Lamp1 increases the extent of, and raises the pH threshold for, LASV GP-mediated fusion. Using a visual syncytial assay, Jae et al. reported no LASV GP-mediated fusion at pH 5.5 in Lamp1-deficient 293T cells (generated by TALEN-mediated gene disruption); robust syncytia formation at the same pH was, however, observed in cells overexpressing a mutant Lamp1 directed to the cell surface [135]. Earlier observations have documented an unusually low pH requirement for both LASV and LCMV GP-mediated syncytia formation, with optimal activity at pH $\leq$ 4 [144, 216, 313]. Lamp1 is progressively enriched in maturing endosomes and has been reported to be most abundant in late endosomes, where the pH range is ~4.5 to 5.5 [383]. Coupling these three prior observations with our finding that LASV GP-mediated entry and infection can occur (albeit at reduced efficiency) in Lamp1 KO cells, we postulated that by binding to LASV GP, Lamp1 promotes fusion at a higher (less acidic) pH. We describe three lines of experimentation to test this hypothesis (**Figures 3.4** to **3.7**).

FIG 3.4. Lamp1 increases the extent and raises the pH threshold of LASV GP-mediated fusion. In panels **A** and **C**, luminescence shows the extent of cell-cell fusion with WT (dark boxes) or pmLamp1 (light boxes) cells for LASV (**A**) and LCMV **(C**). Data represent RLU ± SD from the average of triplicate measurements. Dashed lines in panels **A** and **C** indicate background signal. In **B** and **D**, the data were normalized to fusion at pH 4.5 and replotted to show the corresponding pH dependence of cell-cell fusion for LASV (**B**) and LCMV (**D**). Dashed lines in **B** and **D** indicate 50% fusion efficiency. The LASV experiment was performed two additional times with similar results. Error bars represent the average ± SD of normalized values.

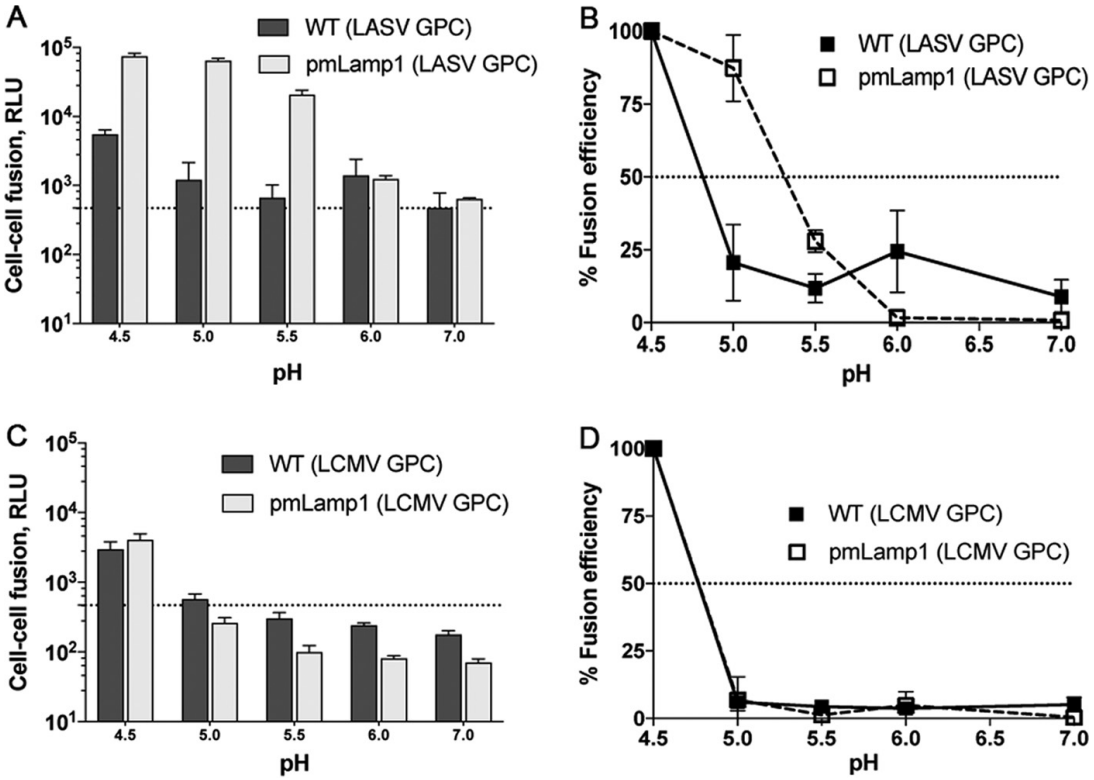
A
WT (LASV GPC)
pmLamp1 (LASV GPC)
Cell-cell fusion, RLU
pH
B
WT (LASV GPC)
pmLamp1 (LASV GPC)
% Fusion efficiency
pH
C
WT (LCMV GPC)
pmLamp1 (LCMV GPC)
Cell-cell fusion, RLU
pH
D
WT (LCMV GPC)
pmLamp1 (LCMV GPC)
% Fusion efficiency
pH

In the first set of experiments we employed a highly sensitive split-luciferase cell-cell fusion (CCF) assay to rigorously assess the extent and pH dependence of LASV GP-mediated CCF in the presence and absence of Lamp1 at the cell surface over a range of pH values. In this experiment (diagrammed schematically in **Figure 3.S.2** in the supplemental material), one set of 293T cells expressed LASV or LCMV GPC, and one-half of a split luciferase/GFP construct. This set was then cocultured with target 293T cells expressing the other half of the split luciferase/GFP construct and different levels of cell surface Lamp1: WT, Lamp1 KD, Lamp1 KO, or cells transiently overexpressing plasma membrane-directed Lamp1 (pmLamp1). The cocultures were then briefly exposed to buffers of defined pH, re-neutralized, and assayed for luciferase activity after one hour. The different levels of Lamp1 on the surface of the target cells, determined by flow cytometry, is shown in **Figure 3.S.2**. Note that pmLamp1 cells express at least 20-fold more Lamp1 at the cell surface than WT or KD cells, both of which have little to no detectable surface Lamp1.

We first compared the fusogenicity of LASV GP-expressing cells by coculturing them with either pmLamp1 or WT cells and then briefly pulsing with pH-adjusted buffer to trigger fusion. The difference in LASV GP-mediated fusion efficiency with target cells was evident at pH < 6, where fusion with pmLamp1 cells was 1-2 log units higher than with WT cells (measured in 0.5 pH unit increments). When fusion at all pH values was normalized to activity at pH 4.5, a prominent, upward pH shift in fusogenicity was seen with pmLamp1 cells (**Figure 3.4.B**). For example, fusion with WT cells at pH 5 was ~20% that seen at pH 4.5, while fusion with pmLamp1 cells at the same pH was similar to that seen at pH 4.5. Even at pH 5.5 there was appreciable fusion (~40% of that seen at pH 4.5)

with pmLamp1 cells, whereas only background levels of fusion were seen with WT cells. Notably, LASV GP-mediated fusion with Lamp1-deficient KD and KO cells was not significantly different relative to WT cells (**Figure 3.S.3**), as expected given the virtually undetectable levels of Lamp1 at the surfaces of KD and KO cells (**Figure 3.S.2**). To test the specificity of the Lamp1-dependent change in fusion pH, we assayed LCMV GPC-mediated fusion with WT and pmLamp1 cells. As expected, Lamp1 neither increased the extent nor altered the pH threshold of LCMV GP-mediated fusion (**Figure 3.4.C** and **3.4.D**).

As a complementary approach, we tested whether overexpression of pmLamp1 affects the fusion pH of intact, cell-bound pseudoviruses using a system that bypasses the normal endocytic pathway and forces virus fusion at the PM [384, 385]. LASV GPC VSV pseudoviruses bearing a luciferase reporter were bound to WT or pmLamp1-expressing COS7 cells in the cold for 1 h. Cells were then briefly exposed to a range of pH-adjusted buffers to trigger fusion before re-neutralizing the media. Immediately following re-neutralization, cells were treated with the lysosomotropic agent NH_4Cl to inhibit acidification of endosomes and therefore block natural entry through the endocytic pathway. After 24 h, GPC-mediated LASV pseudovirus fusion (virus-cell fusion, or VCF) with the PM was assessed by luciferase output. As seen in **Figure 3.5**, in the absence of pmLamp1, a low level of fusion was observed at pH 5.0 and pH 5.5. (Forced fusion at the PM could not be reliably assessed at pH 4.5 due to severe cell loss.) In sharp contrast, strong fusion signals were observed at pH 5.0 and pH 5.5 with pmLamp1 cells. Thus, the more alkaline pH threshold for LASV GPC-mediated CCF (**Figure 3.4**) as well as VCF

FIG 3.5. The extent and pH dependence of LASV pseudovirus (ψ) fusion with the cell surface in the presence and absence of pmLamp1. LASV VSV pseudoviruses were bound to precooled, untransfected WT or pmLamp1-expressing COS-7 cells. The cells were pulsed at the indicated pH for 5 min at 37°C, reneutralized, and then treated with 40 mM NH_4Cl to raise endosomal pH. After 24 h, cells were lysed and assessed for viral fusion with the plasma membrane using the ratio of *Renilla* luciferase activity (virus replication) over firefly luciferase activity (number of cells). Data are from a single experiment and represent average RLU ± SD of sextuplicate measurements. Statistical significance of fusion with WT versus pmLamp1 cells was demonstrated at pH 5.0 and 5.5 using multiple unpaired *t* tests (**, $P < 0.01$; ****, $P < 0.0001$). A Grubbs' test permitted removal of an outlier ($Z = 1.7715$) from a measurement of fusion with pmLamp1 at pH 7. The experiment was repeated a second time with virtually identical results.

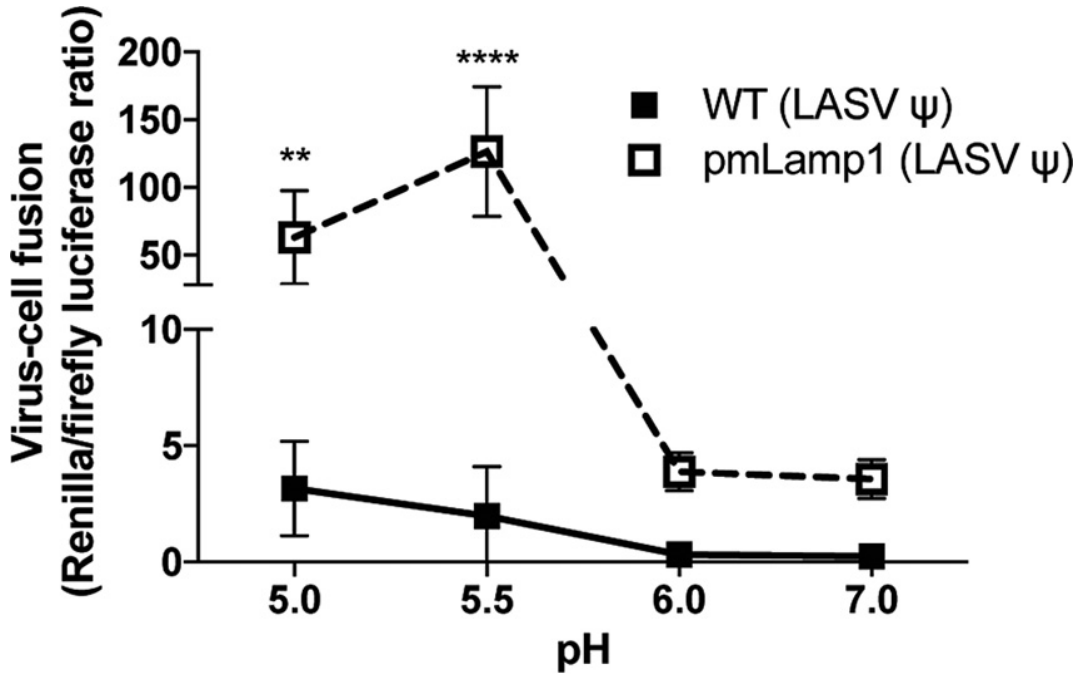
Virus-cell fusion
(Renilla/firefly luciferase ratio)
200
150
100
50
10
5
0
**
****
WT (LASV ψ)
pmLamp1 (LASV ψ)
5.0
5.5
6.0
7.0
pH

(**Figure 3.5**) strongly suggests that Lamp1 facilitates fusion of LASV particles in less acidic endosomes than when Lamp1 is lacking.

Lamp1 promotes LASV GP-mediated entry in less acidic endosomes. Lamp1 promotes both CCF (**Figure 3.4**) and VCF (**Figure 3.5**) at pH 5.0 to 5.5, while significant fusion in the absence of Lamp1 is only supported at pH ≤ 4.5. Thus, we postulated that in WT cells, LASV GP-mediated entry occurs in endosomes that are less acidic than the endosomes from which LASV GP directs fusion when Lamp1 is absent. If this were the case, then LASV should more adeptly infect WT cells than Lamp1 KO cells when the pH is raised with an inhibitor of endosomal acidification. In other words, LASV infection in Lamp1 KO cells should be more sensitive to the effects of NH_4Cl than infection in WT ($Lamp1^+$) cells. To test this hypothesis, we progressively raised the endosomal pH with increasing concentrations of NH_4Cl to compare the effect on LASV GP-mediated pseudovirus infection in WT versus Lamp1 KO cells[15] [376]. Since infection in Lamp1 KO cells is ~20% that seen in WT cells, we used two inputs (low and high) of titered LASV MLV pseudoviruses to achieve a roughly equivalent infection signal in WT (low input) and Lamp1 KO (high input) cells. As seen in **Figure 3.6.A**, infection in Lamp1 KO cells was, indeed, more sensitive to the neutralizing effects of NH_4Cl. Accordingly, a higher

[15] This approach was inspired by recent work on IAV fusion by Gerlach et al. (Reference 376). Sensitivity to NH_4Cl was used to compare HA-dependent fusion pH in different strains of influenza.

FIG 3.6. LASV, but not LCMV, GP-mediated infection is more sensitive to NH_4Cl in cells lacking Lamp1. Lamp1 WT and KO cells were pretreated with NH_4Cl at the indicated concentrations. WT or KO (purple or red lines in **A**, respectively) cells were then infected with (**A**) LASV MLV pseudoviruses at high input (titer determined for ~150,000-RLU signal in mock-treated WT cells [closed symbols]) or low input (titer determined for ~50,000-RLU signal [open symbols]), or (**B**) LASV or LCMV (blue and green lines in **B**, respectively) MLV pseudoviruses at a single input (titer determined for ~100,000-RLU signal in mock-treated WT cells). At 24 hpi, cells were lysed and analyzed for firefly luciferase activity. Infection signal was normalized to mock-treated cells. At 1 and 2 mM NH_4Cl concentrations (**A**), KO infection was compared to WT infection at either high or low MOI using an unpaired, two-tailed *t* test. In **B**, a one-way ANOVA was used to compare LCMV-infected cells (both WT and KO) and LASV-infected KO cells, to LASV-infected WT cells at 2 mM NH_4Cl treatment. **, $P < 0.01$; ***, $P < 0.001$; and ****, $P < 0.0001$. Data are from a single experiment that was performed two additional times with similar results.

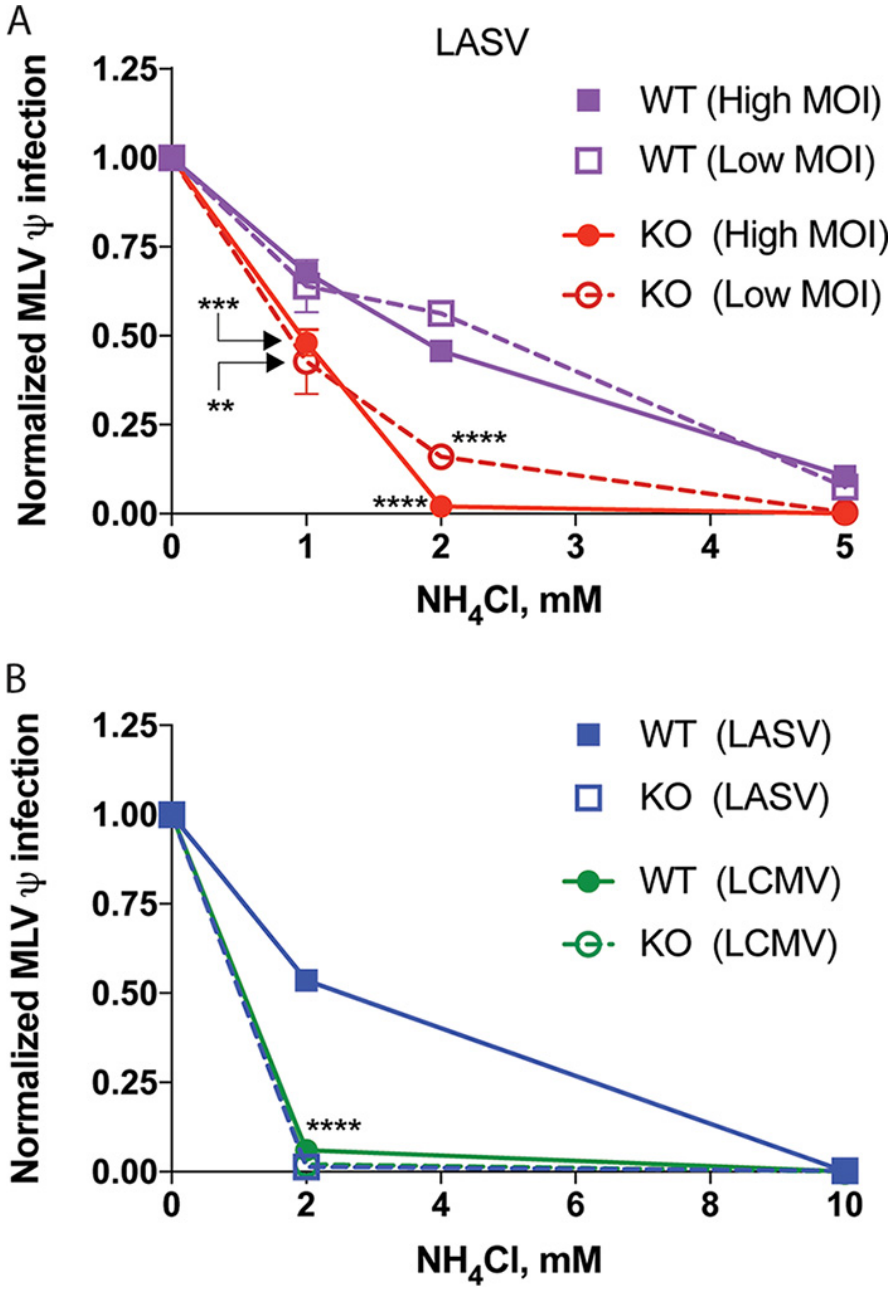
A
LASV
Normalized MLV ψ infection
1.25
1.00
0.75
0.50
0.25
0.00
0
1
2
3
4
5
NH4Cl, mM
WT (High MOI)
WT (Low MOI)
KO (High MOI)
KO (Low MOI)
***
**
****
****
B
Normalized MLV ψ infection
1.25
1.00
0.75
0.50
0.25
0.00
0
2
4
6
8
10
NH4Cl, mM
WT (LASV)
KO (LASV)
WT (LCMV)
KO (LCMV)
****

concentration of NH_4Cl was needed to block LASV GP-mediated infection in WT ($Lamp1^+$) cells. (This effect was seen at both the low and high inputs of LASV pseudoviruses.) As expected, since LCMV does not require Lamp1 (**Figures 3.2.B**, **3.2.D**, and **3.2.F** and **Figures 3.5.C** and **3.5.D**), we did not see any difference in the NH_4Cl sensitivity of LCMV infection in WT versus Lamp1 KO cells (**Figure 3.6.B**).

To more thoroughly evaluate the Lamp1-dependent change in sensitivity to NH_4Cl (raising endosomal pH), we generated 8-point dose response curves and determined inhibitory concentrations for both LASV and LCMV (**Figure 3.7** and **Table 3.1**). Consistent with our earlier experiment (**Figure 3.6**), a greater difference in inhibitory concentrations between WT and KO cells was seen for LASV when compared to LCMV GP-mediated infections. In Table 1 we present inhibitory concentration values for the effects of NH_4Cl on LASV and LCMV GPC-mediated infection in WT and KO cells. The differentials for these inhibitory concentrations (**Table 3.1**) are graphically compared in **Figure 3.7.C**, which clearly shows a significant change in sensitivity of LASV, but not LCMV, to NH_4Cl in Lamp1 KO versus WT cells.

Collectively, the results in **Figures 3.4** to **3.7** suggest that LASV GP-mediated fusion and entry occur in less acidic endosomes when Lamp1 is present than when Lamp1 is absent, whereas LCMV fusion and entry occur in endosomes with the same approximate pH in cells containing or lacking endogenous Lamp1.

FIG 3.7. Dose responses of LASV and LCMV GP-mediated infection to NH_4Cl in cells ± Lamp1. WT (solid lines, filled circles) and KO (dashed lines, empty boxes) cells were pre-treated with NH_4Cl at the indicated concentrations. Cells were then infected in triplicate with (**A**) LASV or (**B**) LCMV MLV pseudoviruses (titered for ~75,000-100,000 RLU signal in mock-treated WT cells). At 24 hpi, cells were lysed and analyzed for firefly luciferase activity. Infection signal was normalized to mock-treated cells, converted to inhibition values, and fitted to a sigmoidal, dose-response curve. 50% and 90% inhibitory concentrations are indicated by red and black dashed lines, respectively. Data shown in **A** and **B** are from a single experiment which was performed two additional times with similar results. In **C**, the average differences between inhibitory NH_4Cl concentrations for LASV and LCMV in WT and KO cells from the three experiments are shown ($\Delta mM = IC_{WT} - IC_{KO}$). See TABLE 1 for details. * indicates $p < 0.05$, ** indicates $p < 0.01$, and *** indicates $p < 0.001$.

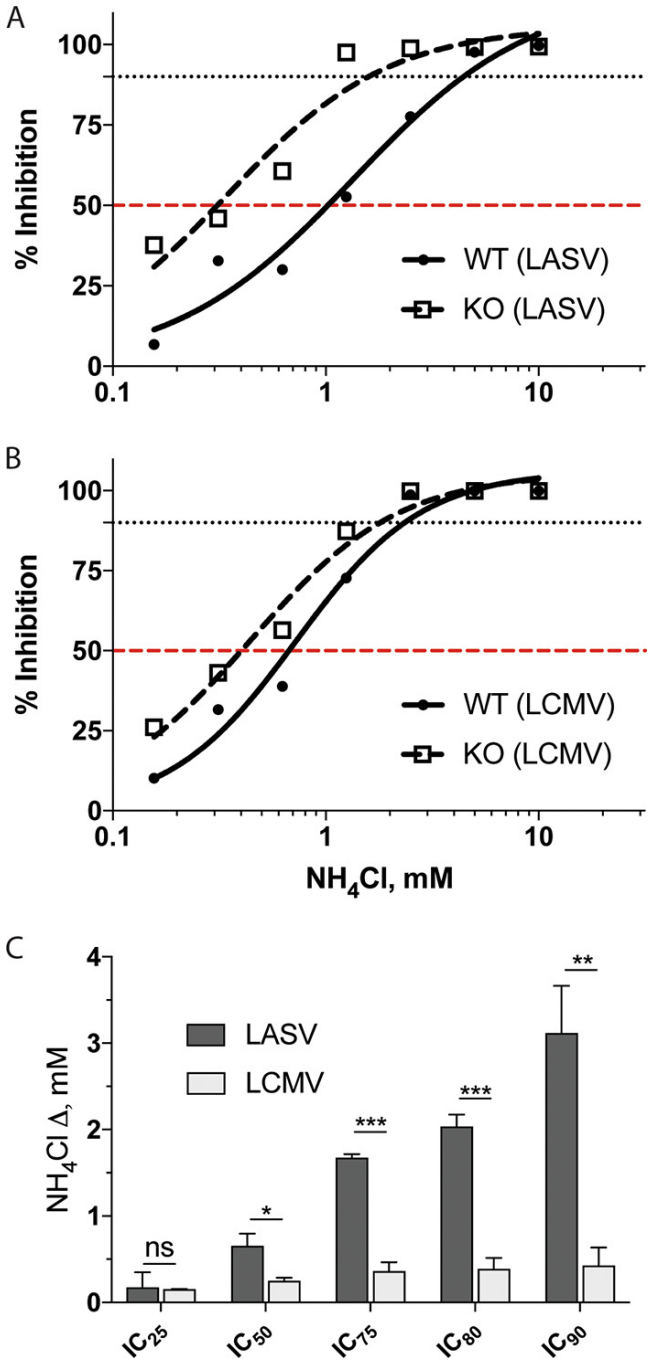
A
100
75
50
25
0
% Inhibition
WT (LASV)
KO (LASV)
0.1
1
10
B
100
75
50
25
0
% Inhibition
WT (LCMV)
KO (LCMV)
0.1
1
10
NH4Cl, mM
C
4
3
2
1
0
NH4Cl Δ, mM
LASV
LCMV
ns
*
***
***
**
IC25
IC50
IC75
IC80
IC90

TABLE 3.1. Concentrations of NH_4Cl needed to inhibit LASV and LCMV GP-mediated infection in WT or KO cells.

IC	Result (mM) for[a]:					
	LASV			LCMV		
	IC_{WT}	IC_{KO}	$\Delta = IC_{WT} - IC_{KO}$	IC_{WT}	IC_{KO}	$\Delta = IC_{WT} - IC_{KO}$
IC_{25}	0.48 ± 0.08	0.30 ± 0.21	0.18 ± 0.14	0.32 ± 0.01	0.17 ± 0.01	0.15 ± 0.00
IC_{50}	1.17 ± 0.15	0.51 ± 0.26	0.65 ± 0.12	0.64 ± 0.04	0.39 ± 0.02	0.25 ± 0.03
IC_{75}	2.57 ± 0.31	0.89 ± 0.28	1.68 ± 0.03	1.24 ± 0.12	0.87 ± 0.04	0.36 ± 0.08
IC_{80}	3.07 ± 0.39	1.03 ± 0.28	2.04 ± 0.11	1.45 ± 0.15	1.06 ± 0.05	0.39 ± 0.10
IC_{90}	4.65 ± 0.70	1.53 ± 0.28	3.12 ± 0.45	2.16 ± 0.26	1.73 ± 0.09	0.43 ± 0.17

[a]Data are the averages ± SD from three experiments. The differences between the WT and KO values for both LASV and LCMV are shown graphically in Fig. 7C.

Discussion

In the present study, we provide evidence that Lamp1 plays a significant, but not absolutely essential, role in LASV entry, and we further provide evidence for how Lamp1 promotes LASV entry. Our findings can be summarized as follows: (i) A robust, ~85%, decrease in Lamp1 expression does not dampen the efficiency of LASV pseudovirus infection of 293T cells over a range of input multiplicities. (ii) Knockout of Lamp1 expression in 293T cells diminishes, but does not abolish, entry and infection (shown using three different sets of LASV pseudoviruses bearing different reporters [luciferase, GFP, and βlaM] as well as different viral cores [VSV and MLV]). (iii) LASV GP-mediated fusion, evidenced in both CCF and VCF assays, is markedly more active at a higher pH when Lamp1 is present. This suggested that LASV entry occurs in less acidic endosomes when they contain Lamp1. (iv) Indeed, LASV pseudovirus infection is more efficient in WT ($Lamp1^{+}$) cells treated with a given amount of an inhibitor of endosomal acidification than in KO ($Lamp1^{-}$) cells. We propose that by promoting fusion and entry in less acidic endosomes, Lamp1 increases the overall efficiency of LASV entry and infection (**Figure 3.8**).

FIG 3.8. Model of LASV entry into cells ± Lamp1. After initial attachment to α–DG at the cell surface, LASV particles are internalized into compartments within the endocytic pathway. The proposed pathway for Lamp1$^-$ (KO) cells (left) indicates LASV GP-mediated fusion and entry from highly acidic endosomes. In Lamp1$^+$ (WT) cells, the receptor switch to Lamp1 elevates the pH threshold for GP-mediated fusion, ensuring efficient entry from a less acidic endosome. We further propose that entry in Lamp1$^+$cells is more efficient because the particles avoid inactivation by extremely low pH and/or proteases within less hospitable, Lamp1$^-$ endosomes.

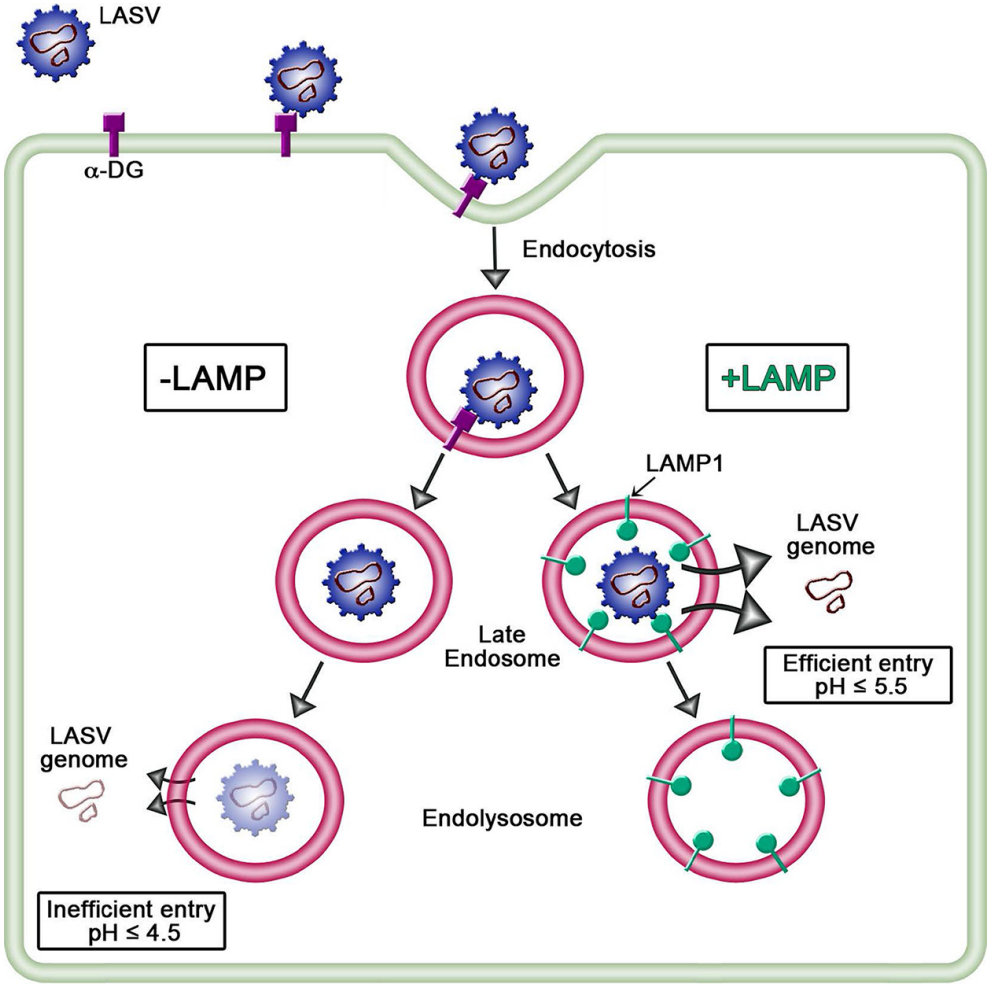
LASV
α-DG
Endocytosis
-LAMP
+LAMP
LAMP1
LASV genome
Late Endosome
Efficient entry pH ≤ 5.5
LASV genome
Endolysosome
Inefficient entry pH ≤ 4.5

It was initially curious to us that the strong reduction in Lamp1 in the shRNA-mediated KD cells failed to affect even a modest decrease in LASV infection efficiency. However, given the ubiquitous expression and high abundance of Lamp1, which accounts for ~0.1% of total cellular protein and has been estimated to reach ~2 million Lamp1 molecules per cell [386, 387], it is likely that the remaining Lamp1 in these KD cells is a surfeit to support LASV GP-mediated pseudovirus infection, even at the highest inputs of pseudovirus tested. Furthermore, although Lamp1 reaches peak enrichment within acidic late endosomes/lysosomes, LASV GP-Lamp1 binding is biochemically feasible at pH ≤ 6.5 [135]. Thus, the receptor switch from α-DG to Lamp1 [135] might be handily supported within earlier endosomes, despite relatively light carriage of Lamp1 in these maturing compartments [388, 389].

In our system, lack of Lamp1 did not confer the full resistance to LASV infection expected from loss of an absolutely required receptor. One possibility to explain this would be compensatory interactions with another endosomal protein(s). A leading candidate, Lamp2, is not likely to play such a role: it did not emerge in the screen for pro-LASV factors, did not rescue infection in Lamp1 KO cells, and does not appear to physically interact with LASV GP [135]. However, the tetraspanin CD63 was recently identified as promoting fusion and infection by LUJV [280]. It would therefore be interesting to know whether CD63 could (partially) support LASV entry in cells lacking Lamp1. Another possibility is that the level of resistance of LASV infection in Lamp1 KO cells varies among cell types. We note, however, that studies with WT and Lamp1$^{-/-}$ mice also intimated an important, albeit non-essential role for Lamp1: at six days post infection Lassa titers remained high in WT tissues but fell below the detection limit in Lamp1$^{-/-}$ tissues;

however, at three days post infection, comparable levels of virus were found in serum and LASV was also detected in spleen and serum in Lamp1$^{-/-}$ mice. This suggests that the absence of Lamp1 (in Lamp1$^{-/-}$ mice) may have hindered or slowed the infection enough to provide a window of opportunity for the immune system to clear the virus by six days. In the context of a physiologic Lassa infection in a homozygous Lamp1-deficient, but otherwise susceptible and immunocompetent host, perhaps a reduced number of Lassa particles escaping from late, highly acidified endocytic compartments allows for the establishment, but not sustainment, of infection.

Before the importance of Lamp1 in LASV entry was realized [135], several groups concluded (from CCF-based evidence) that LASV GP-mediated fusion occurs under remarkably acidic (pH $\leq$ 4.5) conditions, perhaps even within lysosomes [144, 216]. Our work (**Figures 3.4** and **3.5**) and that of Jae et al indicate, however, that robust LASV GP-mediated fusion can occur at pH 5.5 if Lamp1 is present. Moreover, we provide evidence (**Figures 3.6** and **3.7**) that LASV GPC-mediated entry occurs in less acidic endosomes in Lamp1^{+} versus Lamp1^{-} negative endosomes, as modeled in **Figure 3.8**. A corollary is that in the absence of Lamp1, LASV must traffic to more acidic, and potentially more proteolytic, endosomes, which may inactivate significant numbers of LASV particles before they are able to fuse. We further propose that by binding to LASV GPC, Lamp1 promotes a critical fusion-inducing conformational change at a higher pH than when Lamp1 is absent. Future experiments are needed to test this hypothesis and, if correct, to elucidate the specific change involved, whether dissociation of GP1 from GP2 or refolding of GP2 to pre-hairpin or hairpin conformations [231].

The question arises as to whether other Old World arenaviruses employ intracellular (endosomal) receptors. A second example is likely LUJV. As mentioned above, CD63 enhances fusion and entry by LUJV. However, unlike for LASV GPC and Lamp1, a binding interaction has not yet been observed between LUJV GPC and CD63 [280]. What about LCMV, the prototypical Old World arenavirus? LCMV GPC-mediated infection, entry, and fusion were not affected by the absence of Lamp1 (**Figures 3.1** to **3.4**, **3.6**, and **3.7**) [135], and loss of CD63 did not impair LCMV GPC-mediated infection [280]. Moreover, consistent with the observed pH dependence of LCMV fusion being remarkably low (optimal at pH $\leq$ 4.5) regardless of the presence or absence of Lamp1, we found that LCMV infection (in WT cells) is considerably more sensitive to NH_4Cl than LASV infection; it is, in fact, quite similar to the sensitivity of LASV infection in cells lacking Lamp1 in endosomes (**Figure 3.6.B**). While it certainly remains possible that LCMV employs a pro-viral endosomal fusion factor, the aforementioned collective observations suggest that this may not be the case. If so, it is possible that LCMV GPC is better able to tolerate the harsher conditions within more acidic endosomes than LASV (and LUJV), and therefore undergo low pH-dependent fusion activation unassisted by endosomal receptors. Future experiments will be needed to test this hypothesis and to fully assess which arenaviruses do and which, if any, do not employ assisted fusion in endosomes.

FIG 3.S.1. Overview of workflow for generating and validating Lamp1 KO 293T cells. Four gRNAs targeting early Lamp1 exons were cloned into the pX330-U6 vector (dual Cas9-gRNA scaffold). 293T cells were then separately transfected with each of the gRNAs (and one population transfected with all four gRNAs) and lysed one week later for comparison of total Lamp1 levels via Western blot. The cell population transfected with gRNA #1 (indicated by black caret) was stained with Lamp1 antibody and AF-488 and then subjected to negative selection by FACS. After allowing for expansion of singly sorted cells, clonal cell lines were seeded onto 96 well plates, permeabilized, and screened for Lamp1 expression via In-Cell Western. Cells from Lamp1$^-$ clones were lysed and further confirmed for null Lamp1 expression by Western blot. Two of these clones and parental cells were then subjected to genomic sequencing around the PAM site. Note, the mixed sequence for the 2G8 clone suggests that the alleles were modified differently, however both alleles are disrupted relative to WT sequence.

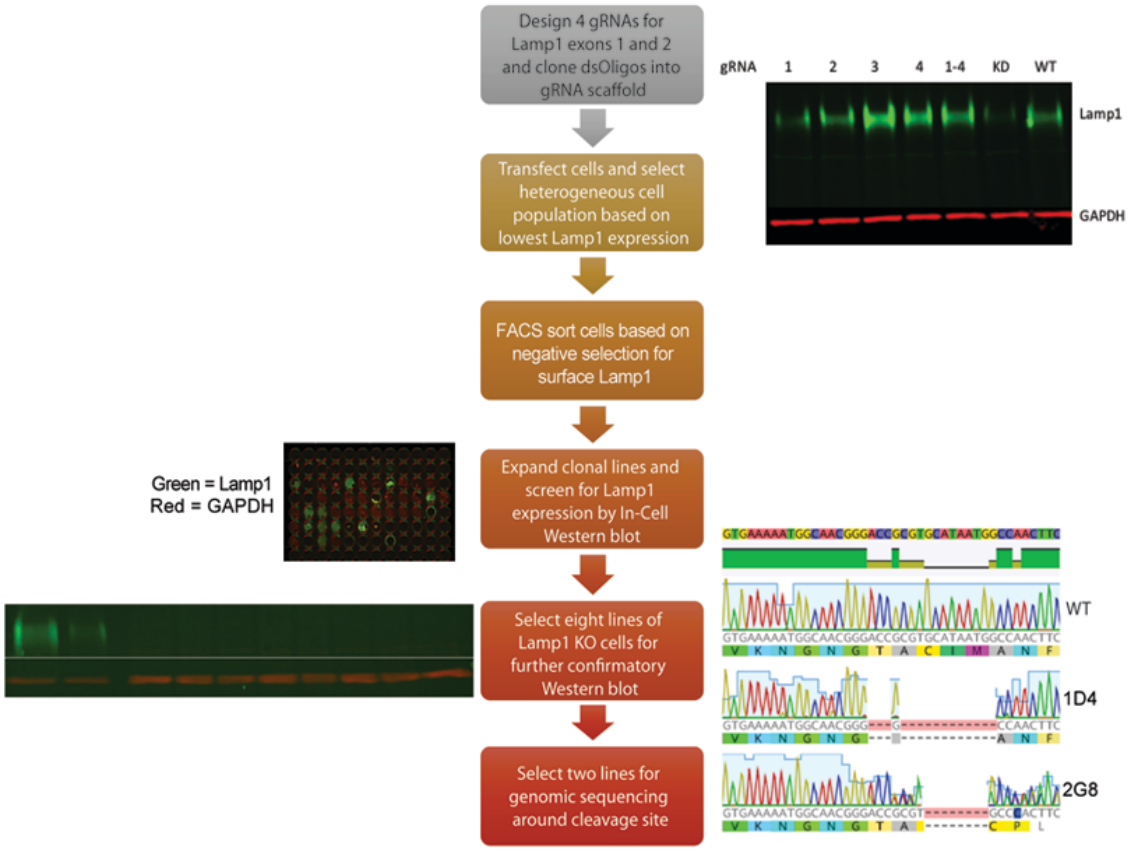
Design 4 gRNAs for Lamp1 exons 1 and 2 and clone dsOligos into gRNA scaffold
Transfect cells and select heterogeneous cell population based on lowest Lamp1 expression
FACS sort cells based on negative selection for surface Lamp1
Expand clonal lines and screen for Lamp1 expression by In-Cell Western blot
Select eight lines of Lamp1 KO cells for further confirmatory Western blot
Select two lines for genomic sequencing around cleavage site
gRNA 1 2 3 4 1-4 KD WT
Lamp1
GAPDH
Green = Lamp1
Red = GAPDH
WT
1D4
2G8

FIG 3.S.2. Cell-cell fusion assay schematic. (**A**) Effector cells (left) are transfected to express either LASV or LMCV GP and one-half of a dual split protein ("DSP" represents luciferase and GFP). Target cells (right) are transfected to express either DSP2 alone, or DSP2 plus pmLamp1. After providing a luciferase substrate to effector cells, effector cells are lifted and overlaid onto the target cells, and the cocultured cells are then pulsed with pH-adjusted buffer to trigger GP-mediated CCF. Following reneutralization and a further 1 h incubation, the luminescence from the reconstituted luciferase reporter is recorded as an indicator of fusion. (**B**) The percentage of target cells with detectable Lamp1 at the surface was determined by flow cytometry. See Materials and Methods for detailed information.

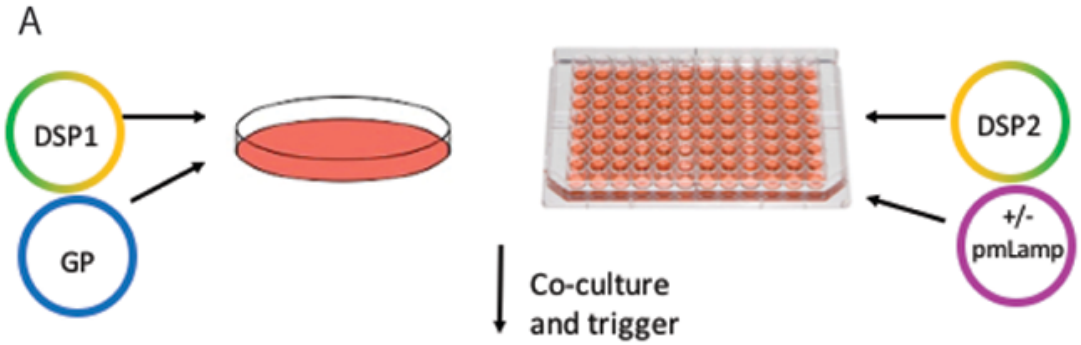

DSP1 and 2 = luminescence (luciferase) and fluorescence (GFP)

B

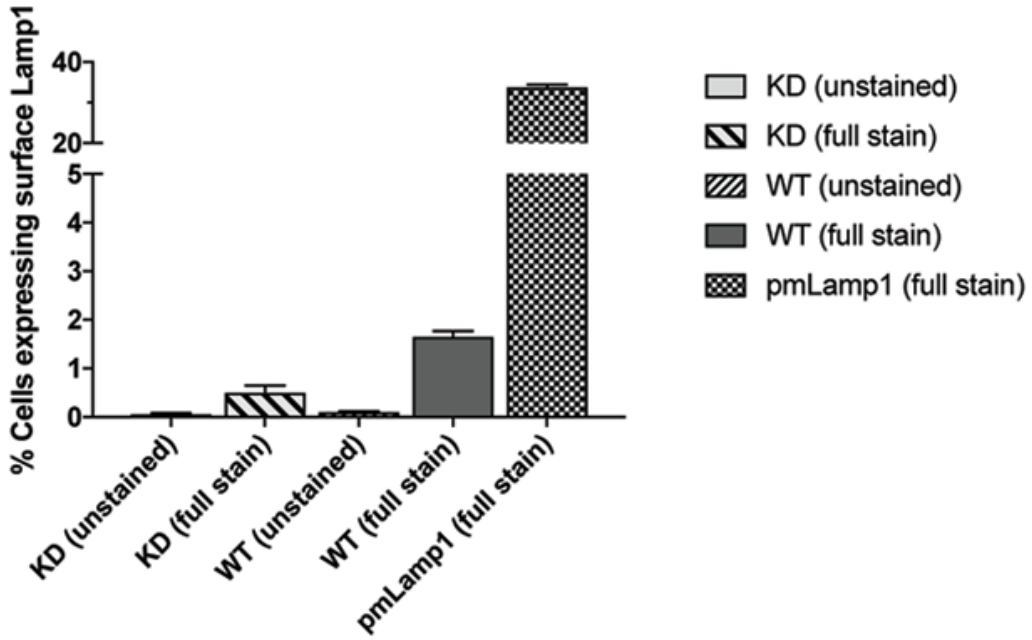

FIG 3.S.3. Levels of LASV GP-mediated cell-cell fusion with WT cells or cells expressing limited (KD) or no (KO) Lamp1 is not significantly different. In **A** and **C**, triplicate measurements of luminescence show the extent of LASV GP-mediated fusion with WT cells compared to either KD (**A**) or KO (**C**) cells. In **B** and **D**, the corresponding normalized pH dependence of fusion with either KD (**B**) or KO (**D**) cells is shown. Statistical significance of fusion efficiency with WT or Lamp1 KD or KO cells at pH 5.0 and 5.5 was assessed using an unpaired, two-tailed *t* test.

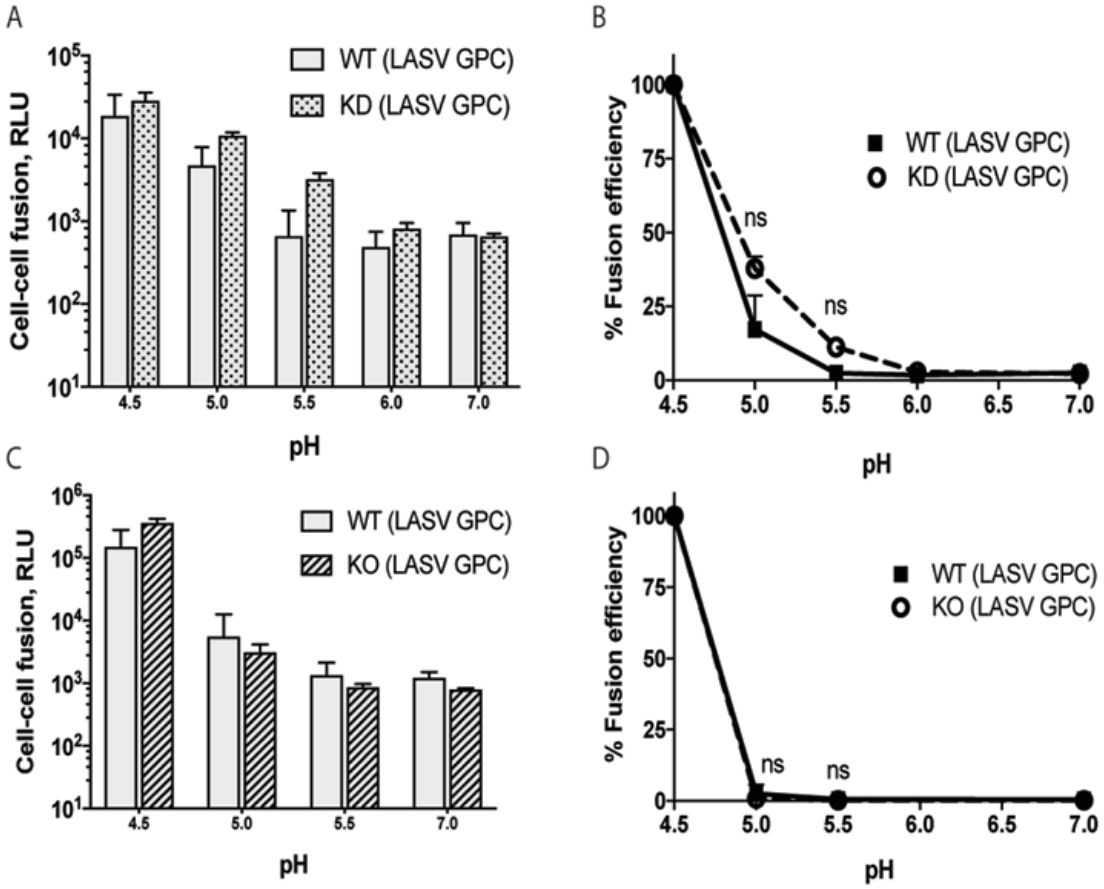
A
Cell-cell fusion, RLU
WT (LASV GPC)
KD (LASV GPC)
pH
B
% Fusion efficiency
WT (LASV GPC)
KD (LASV GPC)
ns
ns
pH
C
Cell-cell fusion, RLU
WT (LASV GPC)
KO (LASV GPC)
pH
D
% Fusion efficiency
WT (LASV GPC)
KO (LASV GPC)
ns
ns
pH

Chapter 4

Arbidol and Other Low Molecular Weight Drugs with Potential to Inhibit both Lassa and Ebola Viruses

(Manuscript in Preparation)

Christine Hulseberg, Lucie Fénéant, Katarzyna Szymańska, Natalie Kessler, Elizabeth Nelson, Charles Shoemaker, Connie Schmaljohn, Stephen Polyak, and Judith M. White

Abstract

Antiviral therapies that impede virus entry are attractive because they act on the very first phase of the infectious cycle. In addition, since they may be used in combination with agent(s) that target later steps, there is potential for drug synergies, thereby lowering the doses needed and hence likely reducing cytotoxicity and emergence of viral resistance. Furthermore, drugs that target pathways common to multiple viruses could be developed into broad spectrum antivirals, which are particularly desirable when laboratory-based viral identification is limited or impractical, e.g. in an outbreak setting. Here we directly compared the potency of drugs known to be active against Ebola virus (EBOV) with their potency against Lassa virus (LASV). These are two unrelated but highly pathogenic hemorrhagic fever viruses that use endosomal receptors and low pH to trigger fusion, and that have surfaced in outbreaks in Africa in 2018. Six drugs (amodiaquine, apilimod, arbidol, aripiprazole, niclosamide, and zoniporide) showed roughly equivalent inhibition of entry of LASV and EBOV glycoprotein-bearing pseudoviruses; an additional three drugs (clomiphene, sertraline and toremifene) were more potent against EBOV. We chose to focus on arbidol, which is licensed abroad as an anti-influenza drug and exhibits activity against a diverse array of clinically relevant viruses. We first showed that arbidol inhibits infection by authentic LASV. We next found that arbidol inhibits LASV glycoprotein (GP)-mediated fusion, using both CCF and VCF assays. Lastly we provide evidence that arbidol stabilizes LASV GP, reminiscent of its activity on influenza hemagglutinin. These findings suggest that arbidol inhibits LASV, at least in part, by blocking changes in LASV GP required for fusion. We discuss our findings in terms of the potential to develop a drug cocktail that could inhibit both LASV and EBOV.

Introduction

Lassa virus (LASV) is an enveloped ambisense RNA virus belonging to the Arenaviridae family. As the most clinically significant member of this large family, LASV is a major pathogen in West Africa, where it infects an estimated 300,000 people each year [138, 390, 391], LASV has also been responsible for a number of imported cases of Lassa hemorrhagic fever (LHF) in Europe and North America in recent years [107, 108, 110, 111]. The 2018 outbreak of LHF in Nigeria was particularly severe, with over 430 confirmed positive cases and a case fatality rate (CFR) of ~25% [392, 393]. Classic symptoms of acute LHF include malaise, headache, fever, vomiting, respiratory distress, facial edema, and hemorrhaging of mucosal surfaces [54, 93, 116]. Even in fatal cases, however, patients may not present with redolent hemorrhagic fever symptoms, complicating diagnosis [394].

The only antiviral treatment option for LHF is the guanosine analogue, ribavirin [315]. There are a substantial number of contraindications and adverse effects associated with ribavirin, and its efficacy in clinical trial settings remains controversial and under-evaluated (to date, the only clinical evaluation of ribavirin was conducted in 1986 [323]). Furthermore, while ribavirin is effective against other hemorrhagic fever arenaviruses and the bunyavirus Crimean-Congo hemorrhagic fever virus (CCHF) [395, 396], it has limited efficacy against the hemorrhagic fever filoviruses and flaviviruses [318, 322]. Thus, current guidelines recommend ribavirin only after high-risk exposures to LASV [318, 320]. Given the partial geographic overlap between EBOV and LASV in West Africa and similar clinical presentation in early infection stages, it would be highly advantageous to have antiviral therapeutics that are effective against both viruses.

Many promising new compounds against LASV have been identified in high-throughput screens, but the limited geographical endemicity of LASV, its inefficient person-to-person transmission, and low re-infection rates make the prospect of collecting adequate clinical trial data on new drugs impractical. Thus, a more practical approach to expeditiously grow the arsenal of drugs against these highly pathogenic viruses is to screen already approved drugs for their antiviral activities. When this strategy was employed to identify FDA approved compounds with inhibitory effects on EBOV, a surprisingly large number of drugs with repurposing potential were identified [328, 342, 343, 397-402]. Many of these drugs are thought to act upon the entry stages of EBOV infection.

Potent viral entry inhibitors are particularly valuable as therapeutics since blocking infection early in the infectious cycle reduces cellular and tissue damage associated with the production of viral progeny. LASV has several key entry features in common with EBOV: 1) it is internalized into the endocytic pathway by a macropinocytotic-like process after initial contact with surface receptors/attachment factors, 2) low pH is needed to trigger fusion, and 3) an endosomal receptor promotes endosomal escape (Lamp1 for LASV and NPC1 for EBOV) [269, 272, 301, 378]. Hence, we selected nine low molecular weight drugs for further testing that have been previously shown to inhibit EBOV entry. Six of these drugs have FDA approval (aripiprazole, amodiaquine, clomiphene, niclosamide, sertraline, and toremifene), one is licensed abroad (arbidol), and two have been evaluated in clinical trials (apilimod and zoniporide).

One of the compounds we tested, the anti-influenza drug arbidol, is the only drug specifically developed and used as an antiviral therapy. It has been shown to have inhibitory effects on an expansive and diverse range of viruses, e.g. DNA and RNA viruses,

capsid and enveloped viruses, etc. [352-354, 358, 359, 403-407]. Studies aimed at determining arbidol's mechanism of action (MOA) (comprehensively reviewed by Blaising et al. [359]) implicate a number of possible antiviral effects for the drug, including several stages of entry and, indeed, virtually every major step during the infectious life cycle (**Figure 1.8**). However, arbidol's principle inhibitory effect on influenza virus (IAV), for which it has been a licensed treatment in China and Russia for many years, appears to be during the later stages of entry, near when IAV fuses with endosomal membranes. While arbidol can bind directly to influenza HA and inhibit its ability to transition to an activated conformation [312, 355], it is not yet clear whether this is its sole or primary mechanism of anti-influenza activity, or if arbidol also impairs fusion by intercalating into the viral or target membrane (thereby altering the membrane character and rendering it less yielding for viral fusion [358]). Given that IAV HA is a class I viral fusion protein, as are the GPs of LASV and EBOV, we hypothesize that arbidol disrupts the entry steps of LASV and EBOV using either (or both) of these mechanisms. Therefore, we selected arbidol for additional testing in both experiments with authentic LASV and in mechanistic studies aimed at evaluating its MOA.

Results

Small molecule inhibitors of LASV and EBOV entry. Enveloped, late-penetrating viruses rely on their GPs to mediate the entire entry process, from attachment to the cell surface to fusion within endosomal membranes. To compare the potency of drugs as entry inhibitors of LASV and EBOV infection, we used murine leukemia viruses (MLV) carrying a luciferase reporter and pseudotyped with either LASV or EBOV GP. Dosing

ranges were determined by establishing the highest concentration of each drug needed to elicit a near-total inhibition of infection (~95-99% reduction of luciferase signal). The remaining doses in each series were 2-fold serially decreased from the highest concentration. A mock, vehicle-only treatment was included as an anchor point in each series to assess the extent of inhibition in treated cells. Since the multiplicity of infection (MOI) in live virus dose response experiments has been shown to significantly affect inhibitory concentrations (IC_{50}) of drug [408], we ensured a consistent input of pseudovirus across all drug assays by using previously titer-determined amounts of pseudovirus corresponding to a range of 75,000 – 150,000 RLU in mock-treated samples.

Table 4.1 shows a summary of the results of the dose response assays, reporting the IC_{50} values for each of the nine drugs tested against LASV and EBOV. The IC_{50} values for EBOV infections are in generally good agreement with effective ranges from other published reports [328, 342, 352, 402]. As seen in Table 1, the drugs can be binned into two groups according to whether the ratio of the IC_{50}s (LASV:EBOV) was greater or less than four. Clomiphene, toremifene, and sertraline were the only drugs that were >4-fold more potent against EBOV than LASV. The remaining drugs (amodiaquine, apilimod, aripiprazole, niclosamide, and zoniporide) showed approximately equivalent (if not stronger) efficacy against LASV and EBOV GP-mediated infection.

Table 4.1. Low molecular weight drugs of interest as potential LASV and EBOV entry inhibitors. The compounds were selected primarily on the basis of whether they met the following criteria: 1) inhibition of EBOV entry, 2) demonstrated viability as a pharmacological agent (preferably having already gained FDA approval), and 3) had a proposed MOA that could reasonably be expected to block both LASV and EBOV entry. Structures for these compounds are included in **Appendix A**. References with information on clinical trial data or antiviral testing for each drug are included on the left column. The average IC_{50}s for each drug (±SD) are shown. The far right column presents relative potency as a ratio of IC_{50}s for LASV:EBOV (L:E).

Drug	FDA approval	Proposed MOA	Class	LASV IC_{50} (µM)	EBOV IC_{50} (µM)	Ratio (L:E)
Aripiprazole [328, 409]	Yes	Internalization	Antipsychotic	1.1	3.8	0.3 †
Zoniporide [248, 348, 349, 351, 410, 411]	No (Pre §)	Internalization	Antiarrhythmic	87.8±44.0	100.1±64.7	0.9
Amodiaquine [334, 340, 401, 402, 412]	Yes	Acidification	Antimalarial	3.0	5.3	0.6 ‡
Niclosamide [334-337, 402, 413]	Yes	Acidification	Anthelmintic	0.13±0.07	0.24±0.12	0.5
Apilimod [327, 331, 414]	No (P2)	Trafficking	Antirheumatic	0.04±0.01	0.03±0.01	1.3
Arbidol [312, 326, 352, 353, 358, 359, 397, 403, 415-417]	No (P4 ¶)	Fusion (+)	Antiviral	1.7±0.6	2.7±0.4	0.6
Clomiphene [328, 334, 342, 344, 398, 402, 418]	Yes	Fusion	SERM	7.5±2.2	1.8±1.3	4.2
Sertraline [328, 334]	Yes	Fusion	Antidepressant	3.6±0.8	0.5±0.2	7.2
Toremifene [312, 328, 331, 334, 342, 401, 402, 408, 419]	Yes	Fusion	SERM	3.2±1.4	0.4±0.2	8.0

† n = 2 experiments. The average IC_{50}s from three separate experiments are shown for all drugs, with the exceptions of aripiprazole (which has been tested once) and amodiaquine (which has been tested twice). Experiments are in progress to complete these series.

‡ n = 1 experiment

§ Preclinical trials indicated neurological impairment in dogs and mice, possibly due to prolonged extracellular acidification (see References 337, 339, and 397). Zoniporide is intended for short-term management of surgical complications in myocardial ischemic injury.

¶ Recent progress reports for the only registered clinical trial for arbidol (NCT01651663) are not available on https://clinicaltrials.gov/ct2/show/NCT01651663 (study completion was scheduled for 2015).

Arbidol is modestly more potent against LASV GP-mediated infection than infection mediated by either EBOV GP or IAV HA (**Figure 4.1**). The average IC_{50} against EBOV is 2.7 ± 0.4 μM in BSC cells. This is the same concentration as the EC_{50} reported by Pécheur et al. from authentic virus infections in HepG2 cells using EBOV Zaire Kikwit at an MOI of 0.5 [352]. Pécheur at al. also reported an EC_{50} of 5.8 μM (in Vero cells) against the New World arenavirus, Tacaribe virus (TACV); to the best of our knowledge, the latter study is the only published evaluation of arbidol's efficacy on an arenavirus.

As the top concentration of arbidol we tested (40 μM) resulted in less than 50% cytotoxicity in BSC cells,[16] we could not interpolate a half maximal cytotoxic concentration (CC_{50}) (**Figure 4.1.C**). Before proceeding to dose response studies with authentic virus, we visually observed Vero cells for cytotoxic effects upon prolonged exposure (~120 h) to four concentrations of arbidol, ranging from 10 - 80 μM. Vero cells appeared healthy even in the presence of 80 μM of arbidol until the fifth day (**Appendix B.2**).

[16] Arbidol is soluble in either 10% ethanol or DMSO, but 50 μM arbidol prepared in ethanol is less damaging to BSC cells (~25% cytotoxicity) than the same concentration prepared in DMSO (~47% cytotoxicity; **Appendix B.1**). In the literature, CC_{50}s for arbidol vary between 20 and 200 μM, depending on cell type, duration of exposure, initial cell health, and solvent (Reference 259).

FIG 4.1. Arbidol dose response for LASV and EBOV GP-mediated pseudovirus infection. Representative comparative arbidol dose response curves for LASV and EBOV (**A**) and LASV and X:31 IAV (**B**). Cells were pretreated with arbidol for 1 h before infection with MLV luciferase pseudoviruses (previously titered to achieve a target signal range of 75,000 – 150,000 RLU in mock-treated cells). Luciferase signals were measured 24 h later and normalized to the maximal infection signal from mock-treated cells. The horizontal red dashed line indicates 50% inhibition. The experiment was performed two additional times with similar results. Cytotoxic effects in BSC cells using this range of arbidol were not severe enough to establish a CC_{50} (**C**). All doses were tested in triplicate wells. Error bars represent standard deviations.

A

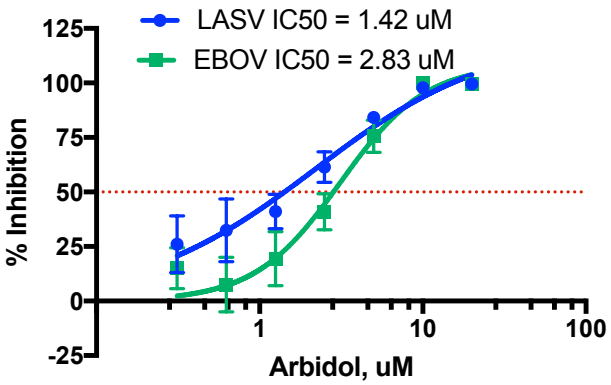
LASV IC50 = 1.42 uM
EBOV IC50 = 2.83 uM
% Inhibition
125
100
75
50
25
0
-25
1
10
100
Arbidol, uM

B

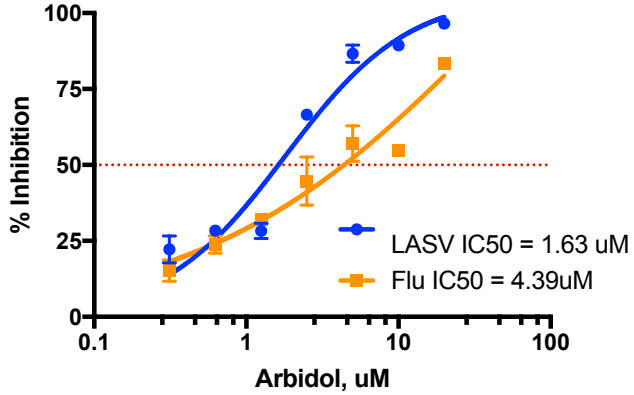
% Inhibition
100
75
50
25
0
0.1
1
10
100
Arbidol, uM
LASV IC50 = 1.63 uM
Flu IC50 = 4.39uM

C

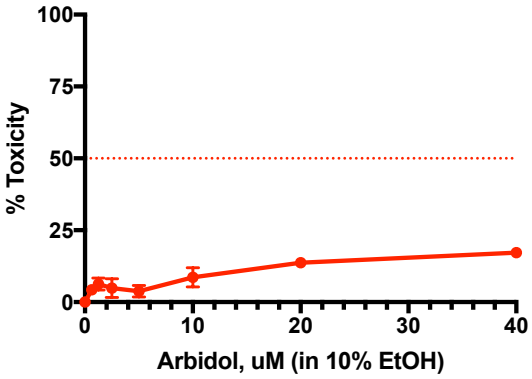
% Toxicity
100
75
50
25
0
0
10
20
30
40
Arbidol, uM (in 10% EtOH)

Arbidol blocks authentic LASV infection. To evaluate the efficacy of arbidol on authentic LASV (Josiah) infection, we performed live virus reduction assays under BSL4 conditions. The presence of Arbidol was maintained throughout the experiment (see Methods). In the first of two experiments (both shown in **Figure 4.2**), the IC_{50} was ~ 10 μM, and, in the second experiment, the IC_{50} was ~20 μM.

Arbidol blocks LASV GP-mediated fusion. We next asked if arbidol impairs LASV GP-mediated fusion, as it does for other viruses [312, 353, 354, 356, 358]. Given that optimal LASV fusion requires the endosomal protein Lamp1, we used cells expressing Lamp1 at the plasma membrane (pmLamp) as fusion targets. Cell-cell fusion (CCF) was then induced between cocultured effector cells (expressing LASV GP at their surface) and target cells (expressing Lamp1 at their surface) by briefly exposing the cells to low pH.

For **Figure 4.3,** effector cells expressing LASV GP or IAV HA were pretreated for one hour with the indicated concentration of arbidol, cocultured with pmLamp1-expressing target cells, and then triggered to fuse by brief exposure to pH 5 (all while maintaining the cells in the presence of arbidol). The efficiency of CCF was then assessed by measuring the activity of a luciferase reporter that is functionally restored upon cytoplasmic mixing of fused cells [377].

FIG 4.2. Arbidol inhibits authentic LASV infection. Vero76 cells were pretreated with arbidol at the indicated concentrations (or vehicle or NH_4Cl) for 1 h before infection with LASV (Josiah strain) virus at an MOI of 0.01. Following a 1 h binding period at 4°C, unadsorbed virus was removed and cells were incubated for 24 h in the presence of drug. Culture supernatants were harvested, serially diluted 10-fold in fresh medium, and then titered on Vero76 cells by a 96 h plaque assay. The experiment was performed twice (the experiments are shown separately in **A** and **B**). Error bars indicate the standard deviation of infectious titers (which, after correcting for dilution, were averaged from two different dilutions of virus per tested dose).

A

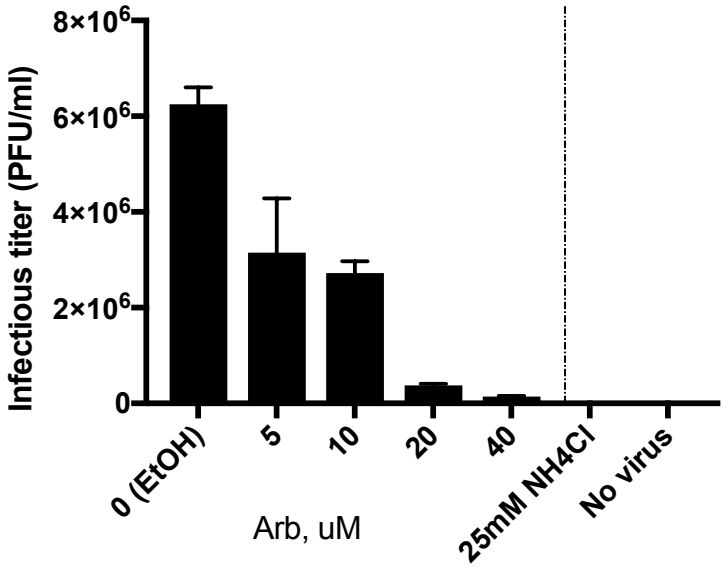
8×10^6
6×10^6
4×10^6
2×10^6
0
Infectious titer (PFU/ml)
0 (EtOH)
5
10
20
40
25mM NH4Cl
No virus
Arb, uM

B

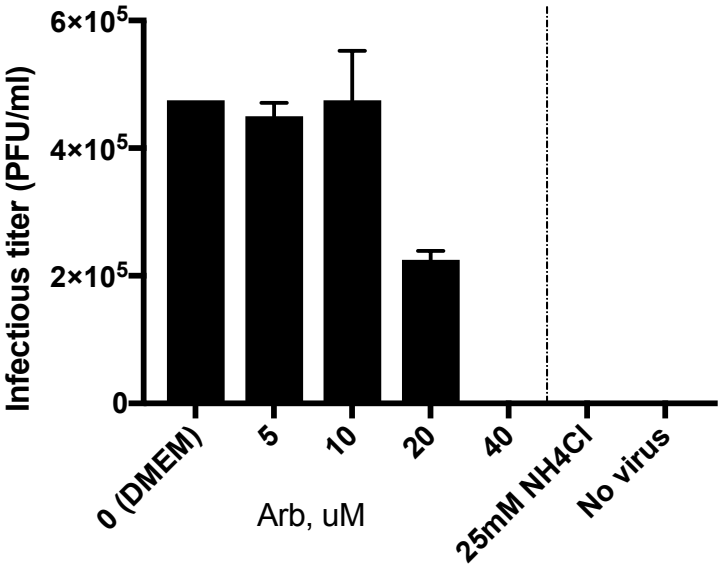
6×10^5
4×10^5
2×10^5
0
Infectious titer (PFU/ml)
0 (DMEM)
5
10
20
40
25mM NH4Cl
No virus
Arb, uM

As seen in **Figure 4.3**, both LASV GP- and IAV HA-mediated CCF were inhibited by arbidol in a dose dependent manner. The average fusion inhibitory concentration (FIC_{50}) of arbidol from three CCF experiments suggests that LASV GP-mediated fusion (FIC_{50} ~25 μM) (**Figure 4.3.A**) is modestly more sensitive to arbidol than IAV HA-mediated fusion (FIC_{50} > 40 μM) (**Figure 4.3.B**).

We next employed a complementary virus-cell fusion (VCF) assay that assesses fusion of LASV GP-VSV pseudoviruses with cells expressing Lamp1 at their surface, as previously described [420]. **Figure 4.3.C** shows that the LASV FIC_{50} (~ 14 μM) and the overall dose responses to arbidol in the VCF assay are in good agreement with the results from the LASV GP CCF assay shown in **Figure 4.3.A**.

FIG 4.3. Arbidol suppresses viral GP-mediated fusion but does not measurably shift the pH of fusion. After allowing 2 h for luciferase substrate loading, effector 293T cells expressing either LASV GP (**A**) or IAV HA (**B**) at the PM were pretreated with the indicated concentrations of arbidol for 1 additional h before coculturing with target 293T cells (under continued presence of drug). After 3 h, the cultures were pulsed with pH 5 buffer for 5 min at 37ºC. Luminescent signal, measured in triplicate samples, indicates the extent of CCF at pH 5. Error bars indicate standard deviation after normalizing signals from treated wells to those from mock treatments. In **C** and **D**, fusion is forced at the PM of COS-7 cells by LASV VSV pseudoviruses (bearing a *Renilla* luciferase reporter) after preventing entry through the natural (endosomal) entry pathway with 40 mM NH_4Cl. Cells were briefly pulsed with buffers at either pH 5 (**C**) or a range of pH values (**D**) and then reneutralized. After 12 – 18 h incubation at 37ºC, luciferase activity was measured for both the *Renilla* reporter (as an indicator of infection at the PM) as well as firefly luciferase (transiently expressed in the COS-7 cells as a means of standardizing transfected cell numbers). The ratio of *Renilla* and firefly luciferase reporters (RLUC/FLUC) was then normalized to fusion activity in mock-treated cells as a function of arbidol dose response (**C**) or the RLUC/FLUC ratios were directly plotted as a function of pH dependence (**D**). Panels **A**, **B**, and **D** show representative experiments, each performed two additional times with similar results. Panel **C** shows the average of three experiments. In **D**, *** indicates $p < 0.001$, and **** indicates $p < 0.0001$.

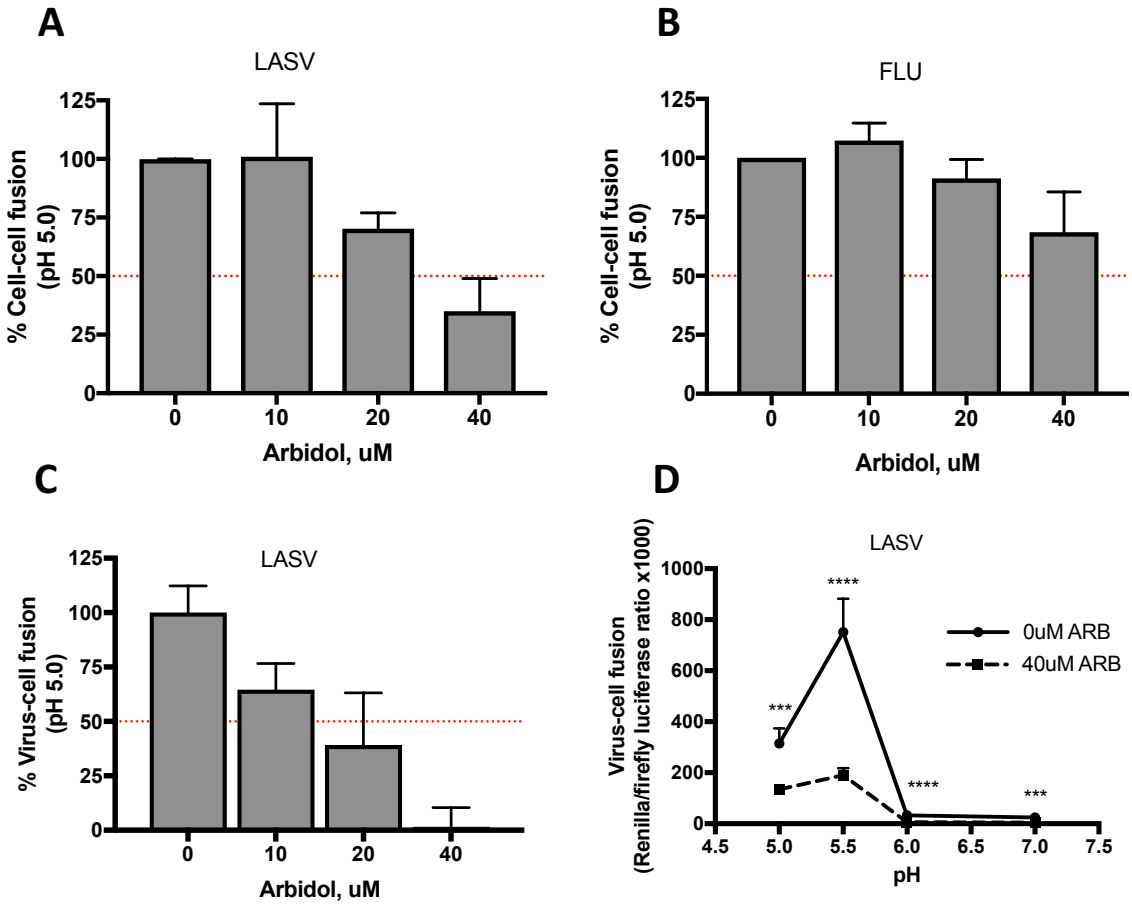
A
LASV
% Cell-cell fusion (pH 5.0)
125
100
75
50
25
0
0
10
20
40
Arbidol, uM
B
FLU
% Cell-cell fusion (pH 5.0)
125
100
75
50
25
0
0
10
20
40
Arbidol, uM
C
LASV
% Virus-cell fusion (pH 5.0)
125
100
75
50
25
0
0
10
20
40
Arbidol, uM
D
LASV
Virus-cell fusion (Renilla/firefly luciferase ratio x1000)
1000
800
600
400
200
0
4.5
5.0
5.5
6.0
6.5
7.0
7.5
pH
0uM ARB
40uM ARB
***
****
****
***

Effects of arbidol effects on LASV GP1 dissociation. Since two independent assays showed that arbidol can impair the fusion activity of LASV GP, we next asked whether it impairs a key conformational change in GP1 required for fusion activation. Upon exposure to a low pH trigger, LASV GP undergoes a series of structural rearrangements, one of the earliest being dissociation of the receptor binding GP1 subunit from the GP2 subunit on the surface of the virus particle (which is needed to allow the fusion loop in GP2 to access the target membrane) [216, 261]. Preliminary experiments using LASV GP captured onto beads showed that dissociation of the 44 kDa GP1 subunit is sub-optimal at temperatures < 37°C (**Appendix B.3.A-B**) and occurs half maximally at pH ~6.4 at 37°C (**Appendix B.3.C-D**).

Having optimized these experimental parameters and constructed the baseline pH-dependent dissociation curve for LASV GP1 in **Appendix B.3.D**, we next treated LASV GP immobilized onto beads with either 0, 10, or 40 μM arbidol to determine if the kinetics of GP1 dissociation were altered by the drug **(Figure 4.4.A**). When LASV GP was triggered at pH 6.5 in the presence of either 10 or 40 μM of arbidol, half maximal release of GP1 into the supernatant (indicated by the horizontal red dashed line) was delayed relative to untreated GP **(Figure 4.4.B**).

FIG 4.4. Arbidol impairs LASV GP1 dissociation. LASV GP (bearing a GP2 C-terminal Flag tag) was captured onto magnetic beads coated with anti-Flag M2 antibody at 4°C. After removing unbound LASV GP, the beads were incubated for 1 h (4°C) with the indicated concentration of arbidol (0, 10, or 40 μM) before brief exposure to pH 6.5 buffer for the indicated time (0, 1, 2.5, or 5 min) at 37°C. After collecting the supernatants, the pH was reneutralized, the beads were washed twice, and bound proteins were eluted from the beads. Both supernatant and bead-eluted protein fractions were subjected to Western blot analysis (**A**). After quantifying pixel intensity of the 44 kDa GP1 bands, the percent of GP1 dissociation was determined by dividing the detected in the supernatant by the total GP1 (supernatant plus pellet) detected on the blot (**B**).

A

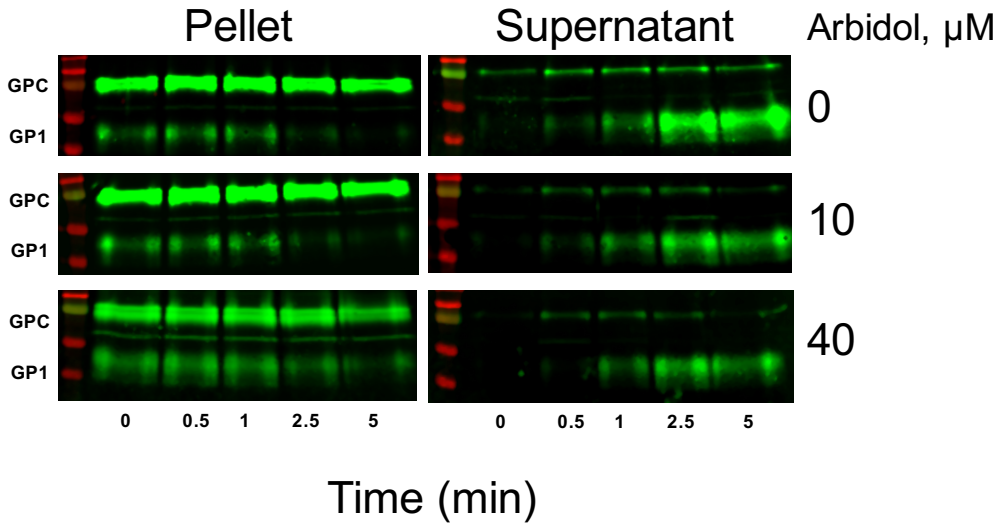
Pellet
Supernatant
Arbidol, μM
GPC
GP1
0
10
40
0 0.5 1 2.5 5
0 0.5 1 2.5 5
Time (min)

B

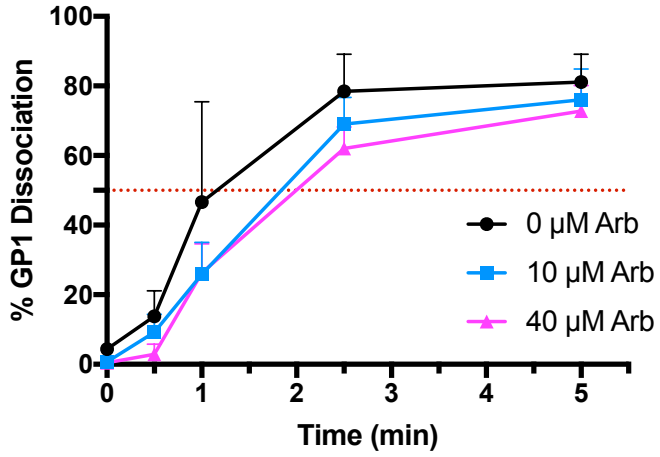
% GP1 Dissociation
100
80
60
40
20
0
0 1 2 3 4 5
Time (min)
0 μM Arb
10 μM Arb
40 μM Arb

Discussion

There were two primary goals of this study: 1) to identify drugs with equal potency against both LASV and EBOV entry by conducting parallel testing with pseudoviruses, and 2) having arbidol as having approximately equal potency against LASV and EBOV, LASV entry. Towards the first goal, we took note of the many common features used by LASV and EBOV during entry to select nine low molecular weight drugs with demonstrated inhibitory effects on EBOV entry, which we predicted would display similar inhibitory effects on LASV [269]. Low molecular weight drugs tend to have both lower production costs and favorable pharmacokinetic profiles (often including availability) than biological therapeutics. Preference was also given to compounds with FDA approval (and in advanced clinical testing) since this would reduce the high costs and prolonged clinical trial periods associated with evaluating novel drugs.

We identified three drugs, clomiphene, toremifene, and sertraline (all previously shown to impair EBOV entry [328, 334, 398]), to be greater than 4-fold more potent against EBOV. Shoemaker et al. proposed that these three drugs, which belong to the structural class of cationic amphiphilic drugs (CADs) (**Appendix A**), affect EBOV entry by altering the membranes of late endosomes/lysosomes. These membrane effects cause an accumulation of cholesterol in the late endosome that closely resembles the phenotype of NPC1 knockout cells [344]. Although CADs were not reported to interfere directly with the binding of EBOV GP to its endosomal receptor, NPC1, they did inhibit EBOV entry in an NPC1-dependent pathway. Given that NPC1 is implicated in the MOAs for clomiphene and toremifene, it is perhaps not surprising that these two drugs are more effective inhibitors of EBOV entry.

In addition to its NPC1-dependent effects, toremifene also binds directly to EBOV GP[17], causing destabilizing effects that are reflected by the decreased melt temperatures of EBOV GP-toremifene complexes [409, 421]. Sertraline also binds directly to EBOV GP, although the relatively low affinity interaction (K_D ~ 0.95 mM [409]) compared its IC_{50} range against EBOV (0.5 μM by us, and 3 μM by others [328]), indicate sertraline's inhibitory effects on EBOV are likely due to targeting of host factors. It is not immediately evident why this would not also impact LASV fusion, but it is possible that the disruption occurs at a point downstream of LASV's endosomal escape.

Six of the nine drugs showed equivalent entry inhibition for LASV: amodiaquine, apilimod, aripiprazole, arbidol, niclosamide, and zoniporide (**Table 3.1**). Two of these drugs, aripiprazole and zoniporide, are thought to be disrupt EBOV internalization. Since aripiprazole (whose binding potential has been specifically evaluated for EBOV GP [409]) does not have affinity for EBOV GP, it is reasonable to propose a broader, host-targeting antiviral MOA for it. Zoniporide inhibits macropinocytosis of LCMV by targeting NHE-1 (IC_{50} ~50 – 60 μM) [248]. Amodiaquine and niclosamide, an antimalarial and an anthelmintic, respectively, both suppress the acidification of endosomes, which confer broadly antiviral properties to both of these drugs [331, 334, 401]. The PIKfyve inhibitor apilimod disrupts EBOV trafficking to the late endosome with concentrations in the low nanomolar range [331]. Although not FDA approved, it was well tolerated in phase 2

[17] Clomiphene is structurally similar to toremifene so it may also bind directly to EBOV GP; to my knowledge, however, this has not been tested. Most direct comparisons of the ability of these two compounds to inhibit EBOV entry (including ours in **Table 3.1**) indicate that toremifene is a much more potent inhibitor of EBOV so it would be interesting to evaluate whether the reduced potency of clomiphene is proportional to its limited binding affinity for EBOV GP.

clinical trials where it was evaluated as a treatment for arthritis and Crohn's Disease [332, 333].

Having proposed mechanisms by which each of these six small molecule drugs may block both LASV and EBOV in similar manners, combinatorial testing has begun to determine whether they can be used synergistically. Besides the extremely practical information gained from these direct comparisons of IC_{50}s for LASV and EBOV, this study also provides mechanistic insights into similarities and differences of these two viruses.

To pursue our second goal of characterizing the MOA of arbidol for LASV infections, we first demonstrate that the drug is roughly equally potent against both LASV and EBOV GP-mediated infection (**Figure 4.1.A**). Since arbidol is licensed (abroad) for the treatment of IAV infections, we also show that arbidol is at least as effective, if not slightly more, an inhibitor of LASV-GP mediated entry than it is an inhibitor of IAV HA-mediated entry using the same experimental platform (**Figure 4.1.B**).

To explore arbidol's potential to interfere with LASV fusion, we use two complementary assays to probe effects of increasing concentrations of arbidol on fusion at cell surface. Both LASV GP- and IAV HA-mediated CCF is inhibited in a dose-dependent manner (**Figure 4.2.A-B**). Consistent with the pseudovirus infection-based assays (**Figure 4.1**), the FIC_{50} is lower for LASV GP than IAV HA. Despite showing similar (if not lower) FIC_{50}s for LASV GP with the VCF assay, arbidol did not appear to cause a detectable shift in LASV GP's fusion pH profile. Arbidol binds to IAV HA with fairly high affinity[18] [312].

[18] Arbidol binding constants for IAV HAs are highly strain-dependent; for subgroup H3 strains such as X:31 (which we use), Brancato et al. have reported a Kd of ~5.6 μM (and about 8-fold higher in H2 subgroups) (Reference 356).

Subtle downward shifts in fusion pH optima of just -0.3 pH units have been reported for X:31 strains (HA subtype 3) in the presence of 40 μM arbidol [356]; even modest changes in fusion pH can have profound implications for overall viral infectivity [376], as I discuss further in Chapter 5.

Finally, we present preliminary evidence suggesting that arbidol may impede a pH-dependent conformational change in activated LASV GP that precedes membrane fusion. We reproducibly show that, in the presence of arbidol, the rate of GP1 dissociation from immobilized LASV GP is delayed relative to untreated controls (**Figure 4.4.B**). Currently we are testing whether the half maximal pH of GP1 dissociation of ~6.4 (**Appendix B.3.D**) is shifted by arbidol in a dose dependent manner.

Based on the above considerations and preliminary findings, it would therefore be worthwhile to more finely interrogate the pH dependence of LASV fusion in the presence of arbidol and to determine, by structural means, whether arbidol binds to LASV GP and, by biochemical means, whether arbidol affects the stability of LASV GP [312, 356].

Chapter 5

Summary and Future Directions

The body of my doctoral work was driven by two major goals: 1) to determine the role of Lamp1 in LASV fusion and entry (Chapter 3) and 2) to identify drugs with the potential to inhibit both LASV and EBOV entry (Chapter 4). Here, I will briefly summarize the results of these two studies and discuss directions for future experimentation for each.

5.A. Summary of the role of Lamp1 in LASV fusion

In Chapter 3 we provide evidence that the interaction between LASV GP1 and Lamp1 permits LASV to escape from endosomes at a higher pH, a discovery that has profound implications for the overall fitness of the virus and its ability to survive in the ecological niche of a human host. While a severe (>80%) reduction in cellular levels of Lamp1 via shRNA-mediated knockdown does not have a suppressive effect on LASV MLV pseudovirus infection relative to WT parental cells (**Figure 3.1**), infections in a complete Lamp1 knockout cell line (using CRISPR-Cas9) are reduced to just 15 - 30% that of parental ($Lamp1^{+}$) cells (**Figure 3.2**). Given the importance of Lamp1 in LASV infection, we made extensive efforts to validate the Lamp1 knockout cells[19]. Without the ability to

[19] Guide RNAs were targeted to the first exon of Lamp1 near a region that encodes for an Asp residue that, once glycosylated, is critical for binding to LASV GP1. After negatively selecting cells stained with Lamp1 antibody by FACS, the clonal populations (after expansion) were screened en masse by a high throughput in-cell Western blot. Of the dozens of clonal cell lines screened, all clearly showed binary staining patterns (green or red for presence or absence of Lamp1, respectively) (**Figure 3.S.1**). This indicated that the populations were indeed at least clonal (either homozygous WT or homozygous knockout). Traditional Western blotting further confirmed the Lamp1-null phenotype before any cell-based experiments were conducted. Three KO clonal lines, 1C4, 1D4 and 2G8, were picked for many of these experiments and 2G8 was used exclusively for experiments where only one knockout line was needed. The 1D4 and 2G8 clones were later sent to Genewiz for confirmation of editing around the predicted cleavage site in exon 1. Both cell lines were homozygous mutants, and 1D4 had frameshift mutations on both alleles. However, roughly 50% of the reads returned on the 2G8 line reflected a 15-nucleotide deletion. Given that

test the knockout lines with authentic virus in a BSL4 facility, we drew upon other pseudovirus infection systems (**Figures 3.2.F** and **3.3.A**) and reporters (**Figure 3.3.A**) to show that LASV infection is consistently diminished, but not abolished, in the absence of Lamp1.

The parental and Lamp1 knockout cell lines were used for a series of fusion experiments aimed at recapitulating LASV GP-mediated fusion at the cell surface, where pH can be tightly controlled. By mutating its lysosomal targeting signal, Lamp1 can be highly overexpressed at the PM (pmLamp); thus, two distinct endosomal receptor phenotypes ($Lamp1^+$ and $Lamp1^-$) can be used to study fusion at the cell surface[20] [422]. Not only is LASV GP more fusogenic with pmLamp1-expressing cells (**Figure 3.4.A**), but its pH threshold for fusion is also shifted upwards considerably, to pH ~5.5 (**Figure 3.4.B**). In contrast, LCMV GP is indifferent to the presence of Lamp1 (**Figure 3.4.C**), and its

---

the mutation was in a site that is critical for GP1 interaction, it is possible, if not likely, that the five-residue deletion would at least compromise the binding affinity for LASV GP1 (or result in haploinsufficiency). Since we only had one Lamp1 mAb available (and the epitope for this particular Lamp1 mAb, H4A3, had not been mapped) we could not determine by additional blotting whether the failure to detect Lamp1 in that line was due to it a) not being expressed at all, b) being expressed, but to such a low extent that it was beyond the detection limit of Western blotting, or c) the H4A3 epitope was unrecognizable, but functional Lamp1 was still expressed. Therefore, to confirm a key result obtained from using the 2G8 knockout cells, the NH_4Cl sensitivity experiment (**Figure 3.6**) was repeated with the 1D4 knockout cells. The experiment yielded almost identical results to the original experiment with 2G8 cells, confirming that the Lamp-phenotype supported our claims about its role in promoting escape from less acidic endosomes.

[20] Most of the limited amounts of Lamp1 on the surface of WT cells is transiently present near damaged sites of the PM, where Lamp1-rich lysosomes are exocytosed to the PM to patch the wounded areas (Reference 422). Accordingly, when compared by flow cytometry (**Figure 3.S.2.B**) and surface biotinylation, the levels of Lamp1 on the PM of WT, KO, and KD cells are only minutely different from one another. If any residual Lamp1 is present at the PM of these different cells, it is not enough to elicit measurable changes in LASV GP fusogenicity (**Figure 3.S.3**); thus, for the purposes of the CCF and VCF assays, KO, KD, and WT cells have essentially the same Lamp1-null PM phenotype.

maximal fusion pH of ≤ 4.5 remains the same ± Lamp1 (with almost no activity at pH > 4.5) (**Figure 3.4.D**). To complement the CCF assay, we used a standard fusion assay in the field in which induced fusion of pseudoviruses with the PM is forced by exposure to low pH while normal virus entry through endosomes is blockaded through application of a lysosomotropic agent. Here again, we found that expression of pmLamp1 infection at the cell surface supports a substantial increase in LASV GP fusion activity, and, most notably, that fusion occurs under more alkaline conditions (**Figure 3.5**).

While PM fusion assays are intrinsically more tractable and advantageous for controlling experimental variables, e.g., pH, the GP of LASV is designed to fuse with endosomal membranes, which have a different composition, radius of curvature, concavity, and exposure to ions and enzymes than cell surface membranes. Hence, the pH optima for fusion as measured in the CCF and VCF assays (**Figures 3.4** and **3.5**) may not reflect the actual pH of endosomal fusion for LASV GP. Nonetheless, by comparing the sensitivity of LASV infection to the lysosomotropic agent NH_4Cl in WT (Lamp1+) and Lamp1 KO cells, we observed a differential sensitivity consistent with a higher pH in the endosomes where LASV fusion occurs in WT cells (**Figure 3.6**). The increased tolerance to NH_4Cl conditions does not change when different inputs of pseudovirus (corresponding to 10-fold increases and decreases in infection signal) are added, suggesting that the result is not due to saturating effects of virus (**Figure 3.6.A**). When the sensitivities of GPs to elevated pH are examined in finer detail (using a broader range of NH_4Cl concentrations), the enhanced tolerance of LASV GP in WT cells is striking, particularly at the high end of the range, where a nearly 3-fold higher concentration of NH_4Cl is needed to suppress LASV infection in WT cells compared to cells lacking Lamp1 (**Table 3.1**).

The data in **Figures 3.6 – 3.7** and **Table 3.1** present what is perhaps the strongest evidence to corroborate our overall hypothesis: that the Lamp1 interaction ensures that LASV entry occurs in less acidic compartments. Since our model only proposes that reduced efficiency of LASV infection in the absence of Lamp is a consequence of inactivation/degradation of the majority of virus particles (because they fail to escape from the endocytic pathway beforehand), we are considering future experiments to assess LASV particle degradation to prove or disprove this idea.

In reconciling the previously reported "remarkably low" activation pH for LASV GP fusion at the cell surface (measured in the absence of Lamp1) [144, 216, 423], we return to the discussion I initiated late in Chapter 1. We can reasonably speculate that LASV switches to an endosomal receptor in order to hasten the activation of its GP at a higher pH, probably nearer to 5.5 (**Figures 3.4.B** and **3.5**). We were not the first group to demonstrate that LASV GP-mediated fusion at the PM is enhanced by Lamp1 [135], nor were we the first to speculate that Lamp1 promotes fusion at higher pH[21] [258, 424], but we were the first to provide multiple lines of experimental evidence supporting a model for the Lamp1-dependent upward shift in fusion pH [420]. It seems apparent in hindsight that the artificial nature of ectopic fusion assays might easily omit important host cell factors enriched in the natural viral entry pathway. However, recall that, unlike LUJV GP (which has scarcely any fusion activity at the PM [423]), the fusion activity of LASV GP and

[21] Acciani et al. (Reference 258) published a hypothesis-based proposal about the Lamp1 role as we were preparing to submit our manuscript (Chapter 3), and, in 2016, Cohen-Dvashi et al. (Reference 217) found Lamp1 expression at the cell surface resulted in increased syncytia area of LASV GP-fused cells.

indeed a number of other arenaviral GPs [144, 216, 423] under low pH is actually fairly robust at the PM, even without the presence of endosomal components.

The fact that virus can be recovered from the tissues of WT and Lamp1$^{-/-}$ mice three days after LASV infection [135] suggests that, while viremia is greatly reduced in these animals, LASV replication is still sufficiently robust (on an organismal level) so as to be detectable. Our model suggests that, without Lamp1, most incoming LASV particles will eventually be degraded or acid-inactivated, having failed to escape the later trajectory of this degradative and highly acidic arm of the pathway (**Figure 3.8**). Perhaps in a Lamp1-free cell, a greatly attenuated number of virus particles will somehow stochastically manage to escape to the cytoplasm, where they will replicate, assemble, bud, and infect new cells. Given the already delicate balance between virus and host in this Lamp1-free scenario, however, the disadvantaged virus will handily lose to the host immune defenses, which will clear the virus before high levels of viremia are established and the infection progresses to a fulminant disease state. Thus, the distinction between an endosomal receptor (or other cellular co-factor) being a requirement for a single round of infection in a cellular context versus it being a requirement for stable occupation within a host organismal niche is a subtle, but important, one to make.

So why do LASV and LUJV use intracellular receptors while other arenaviruses (presumably) do not? Does intracellular receptor usage contribute to pathogenicity in or transmissibility to humans? Do strains (or lineages) of LASV have differences in their fusion pH optima? Strains of IAV have differences in their maximal fusion pH that can be traceable to specific amino acids in their HA proteins; the resulting differences in fusion pH optima are highly correlative with the sensitivity of these various strains to host innate

defenses, particularly in IFN-stimulated cells. Furthermore, avian strains that fuse at more alkaline pH are associated with enhanced zoonosis [376]. We have shown that Lamp1 shifts the pH of LASV GP fusion upward to a more alkaline pH [420]. Would the absence of Lamp1 restore the induction of the IFN response during LASV infection? Immune suppression is a hallmark of severe LASV infection, so it would seem a reasonable (and testable) hypothesis that, as with certain IAV HAs, the relatively high fusion pH of LASV (in the presence Lamp1) would suppress IFN induction, and, by extension, lead to pathogenicity. Could the use of Lamp1 be an evolutionary adaption to overcome host restriction factors, thereby enhancing virulence?

If engagement of Lamp1 confers enhanced virulence to LASV infections, what is different about the highly pathogenic New World arenaviruses? Small-interfering RNA-based screens for cellular factors needed for JUNV entry have not yielded any hits that are reminiscent of intracellular receptors [425]. Is this due to a limitation in the design or execution of the screen, or does JUNV GP fusion really occur without the aid of an intracellular receptor? CCF-based data for JUNV indicate that its GP fuses maximally at a full pH unit higher (pH ~5) than LCMV and LASV GPs (which both fuse at pH ~4, for LASV GP in systems sans Lamp1) [216]. Could this difference be due to use of an as yet unidentified receptor for JUNV that would be expressed at the cell surface *as well as* in endosomes?

And what about LCMV, which is classified as an Old World arenavirus? Our cell-based data (**Figures 3.6** and **3.7**) indicate a genuine difference between how LCMV and LASV GP respond to elevated pH (imposed by a lysosomotropic agent) during the course of a natural infection through the endocytic pathway. This suggests that LCMV does not

use an endosomal receptor. If this is the case, and if LASV is indeed able to more aptly retain infectivity after low pH exposure than LCMV [144, 423], how do LCMV particles survive the harsh conditions in the late endosome/lysosome? What advantage(s) could be gained from escaping from the endocytic pathway at such a late point?

Moreover, what are the differences between LASV and LCMV GP1 that account for Lamp1's specific binding to LASV GP1? To date, the best answers to this question are from structure-based analyses by the Saphire lab [260] and from the surface plasmon resonance (SPR) studies and pulldown assays of mutant LASV GP1 proteins by the Diskin lab [426]. The residues implicated as Lamp1 binding determinants map to a connective loop between an α-helix (α3) and a β strand (β5) on LASV GP1 (**Figure 5.1**). Dr. Saphire suggests in her recent review article that the subtle conformational changes that spread the GP1 subunits apart upon exposure to low pH are also an important prerequisite for LASV GP1 binding to Lamp1 [260]. Superimposed LASV and LCMV GP1 structures confirm that LCMV GP1 lacks the open prefusion configuration adopted by LASV GP1. However, the GP1 of the nonpathogenic Old World Morogoro virus (MORV) (which is genetically closer to LASV than LCMV) *does* assume roughly the same open, "primed" prefusion configuration as LASV GP1 [426]. The reason MORV GP1 does not bind to Lamp1 is due to a compositional, rather than a conformational, difference from LASV GP1: the charge distribution of residues near the pH-sensing histidine triad of MORV GP1 confers an overall less positive charge on the region than in the same region of LASV GP1. Upon grafting the entire β-hairpin element from LASV GP1 onto MORV GP1, the Diskin lab found that this chimeric GP1 could then bind to Lamp1, albeit more weakly than LASV GP1 ($GP1_{LASV}$ K_D ~ 15 nM; $GP1_{Chimera}$ K_D ~ 450 nM) [426]. This supports the notion that

both compositional and configurational elements are involved in forming the Lamp1 binding site on LASV GP1.

LASV has a high mutation rate and is under constant pressure to adapt to host immune defenses and better survive in the ecological niches of its human and rodent hosts. Comprehensive screening efforts have teased out a handful of important cellular entry factors for LASV, but there are hundreds, if not thousands, of additional pro-viral hits below the statistical cut-off scores for inclusion in these analyses [135]. Would some of these entry hits fulfill redundant or ersatz roles in viral fusion if their primary host cell factors were defective (or were suppressed by host targeting interventions)?

We now know of three intracellular (endosomal) virus receptors: NPC1 (for EBOV), Lamp1 (for LASV), and CD63 (for LUJV). Do these receptors serve similar functions in viral entry? For EBOV GP, the conserved RBS is exposed after endosomal cathepsins cleave off its mucin domain and glycan cap (GPd) [237]. Binding of NPC1 could conceivably provide concealment for the RBS by preventing antibody recognition. However, neither LASV nor LUJV GP would require this protection since arenavirus entry does not require a cathepsin-mediated GP activation step. Low pH receptor switches may also "capture" viruses in sorting endosomes, directing them into the appropriate arm of the pathway and ensuring that they are not recycled back to the PM. This idea has not been formally ruled out, but it is not clear how engagement with endosomal receptors would guide them to late endosomes.

As a final comment on the likelihood that endosomal receptors serve analogous purposes, I again call attention to the fusion studies conducted by Tani et al. (discussed in Chapter 1) that directly compared LASV and LUJV GP fusion pH at the PM without

ectopic overexpression of their respective receptors [423]. Whereas LASV GP is fusogenic at very low pH without its receptor, LUJV GP is not fusion competent at any pH tested (down to pH 3.0) without CD63 [423]. Although this could be a result of the basal and transient presence of Lamp1 at the PM, our comparisons of CCF with WT versus Lamp1-KD or KO cells indicate that LASV GP fusion can occur (albeit inefficiently) in the total absence of Lamp1. Furthermore, our lab's efforts to study EBOV GP fusion at the PM have been met with considerable challenges: combinations of known or suspected EBOV GP fusion triggers (NPC1, low pH, elevated temperature, elevated calcium concentration, or pre-cathepsin-priming of GP) have failed to activate EBOV GP-mediated CCF (L. Fénéant, unpublished data). Thus, I think it is ultimately unlikely that NPC1, Lamp1, and CD63 have analogous functions in supporting viral entry, but it is a very active area of research with much to be learned from future experimentation.

FIG 5.1. Location of receptor binding sites on LASV GP1. The GP1 and GP2 subunits are white and black, respectively. The histidine triad (residues H92, H93, and H230) is represented by the green ball-and-stick moieties [221]. The locations of residues involved in binding α-DG (residues H131, N148, Y150, R190, I254) [202] and Lamp1 (residues L188, M192, A195, Y200, A202, D204, G206, S216) [426] are labeled in dark blue and orange red, respectively. The protein surface is based upon the prefusion LASV GP crystal structure determined by Hastie et al. (PDB 5VK2) [202]. Molecular graphics were performed using the UCSF Chimera package.

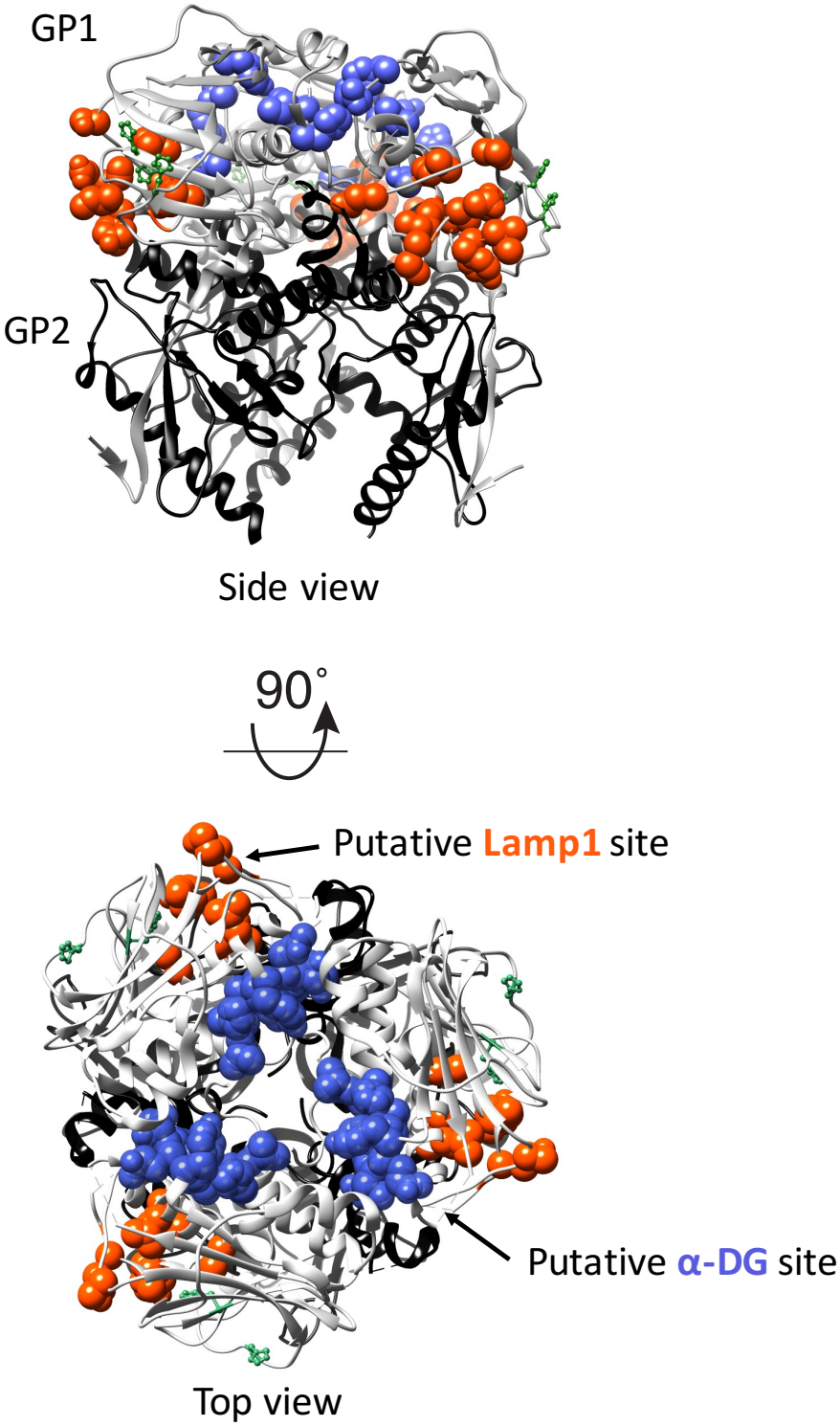
GP1
GP2
Side view
90°
Putative Lamp1 site
Putative α-DG site
Top view

5.B. Summary on the efficacy of arbidol and other low molecular weight drugs to inhibit entry of both LASV and EBOV

In response to the high mortality rates that resulted from 2014-2016 EBOV epidemic, multiple labs intensified efforts to identify FDA approved drugs (or drugs with a viable pharmacokinetic profile) that could be repurposed as therapeutics for EVD. Recognizing that LHF, like EVD, has no specific licensed treatments available, I compiled a list of potential EBOV inhibitors from the literature, divided them according to whether they were known or proposed to be entry or post-entry inhibitors, and then, to the best of my ability, presumptively assigned them to steps in the EBOV entry pathway against which they are presumed to have activity (based on their known structural and functional characteristics) (**Figure 1.8**). Using a straightforward entry-focused approach, I then tested each compound's inhibitory effects on LASV and EBOV GP-mediated pseudovirus infection in parallel. This allowed for the identification of six EBOV inhibitors that would (and three inhibitors that would not) provide equal protection against LASV at the entry stage **(Table 4.1)**.

Of the six drugs with approximately equivalent potency against both LASV and EBOV entry, arbidol was of particular interest due to its decades long history of clinical use for the treatment of influenza and other respiratory viruses [427-431], low degree of resistance [359], and broad-spectrum antiviral effects [352, 359]. Evaluating arbidol first strictly on the merits of its ability to inhibit GP-mediated infections of LASV, EBOV, and IAV, we show that it suppresses pseudovirus entry mediated by all three viral GPs in the low micromolar range (**Figure 4.1**). In live LASV infections, arbidol also exerts dose dependent suppression of infection, albeit at a higher concentration (**Figure 4.2**). A number

of factors may be responsible for the higher IC_{50} observed for blockade of authentic LASV infection. Different cells lines were used, but BSC cells (used for the pseudovirus infections) and Vero76 cells (used for the live virus infections) are both monkey kidney cell lines that typically behave in a similar manner. The MOI used for the live virus experiments (MOI = 0.01, a commonly used input for infections with this strain of LASV) could also have been higher than the input of pseudoviruses used; higher MOIs have been shown to increase drug EC_{50}s [408].

Arbidol suppresses LASV GP- and IAV HA-mediated fusion at the PM with IC_{50}s of ~10 μM and ~20 μM respectively **(Figure 4.3.A-B)**. Inhibition is even more apparent (~14 μM) when fusion of LASV GP VSV pseudovirus with the PM was measured (**Figure 4.3.C)**, although this fusion suppression was not accompanied by a detectable shift in the fusion pH threshold (**Figure 4.3.D**). As arbidol has been shown to block IAV fusion both by direct interactions with HA [312] and through interactions with the target membrane that disrupt fusion [353, 357, 358], it is difficult at this time to predict which mechanism most directly impacts LASV GP-mediated fusion. (Furthermore, the dual binding capacity for both lipids and proteins may contribute, in part, to much of the variability in IC_{50}s observed in different assays.) Since Lamp1 binding to LASV GP1 presents a unique additional target for arbidol, our final goal in this effort, which is currently underway, is to determine whether the drug disrupts the interaction, either by shifting the pH at which Lamp1 binds to GP1 or shifting the pH at which GP1 is released from GP2. Our early data indicate that arbidol can impede GP1 dissociation, at least in the absence of Lamp1.

Having demonstrated that, at a minimum, arbidol impairs LASV infection at the fusion step, we will add it to a list of compounds that will be evaluated in combination for

synergistic effects against LASV and EBOV. Aripiprazole, zoniporide, amodiaquine, and, niclosamide are all good candidates[22] for pairing with arbidol since we predict they act upon viral entry features upstream of fusion. As the internalization blocker aripiprazole was recently shown to synergize with piperacetazine (another acidification blocker) to block EBOV VLP infections [329], another two-drug combination of keen interest is aripiprazole with either of the acidification blockers we have tested (amodiaquine or niclosamide). Three-drug combinations (e.g., aripiprazole, amodiaquine, and arbidol) are also in the pipeline for testing of synergistic entry inhibitors, as are combinations of entry inhibitors with postentry inhibitors such as favipiravir, stampidine, zidampidine, omacetaxine, or ribavirin [326, 432-437].

In conclusion, the two projects presented in chapters 3 and 4 of this thesis converge on a common goal, where mechanistic studies inform translational ones and *vice versa*. Not only can our findings about Lamp1's role in LASV fusion be viewed through the lens of drug discovery and further characterization, but they also be extended to broaden our understanding of how other viruses enter cells and how they can be inhibited at the entry stage.

[22] Apilimod will likely not be included in further testing as an antiviral therapeutic; the disruptive effects this antirheumatic drug has on cytokine expression would be undesirable during a viral infection (Reference 329).

FIG 5.2. EBOV entry inhibitors with equal potency against LASV. Of the nine EBOV entry inhibitors we tested, three compounds (clomiphene, sertraline, and toremifene, shown in blue text) were more potent against EBOV entry, while the other six compounds (amodiaquine, apilimod, arbidol, aripiprazole, niclosamide, and zoniporide, shown in orange text) demonstrated roughly equivalent potency against both LASV and EBOV GP-mediated infection. The asterisk (*) near amiodarone, tetrandrine, and verapamil signifies that there is some debate over whether these drugs block trafficking or fusion.

Ebola

Attachment
Benzodiazepine
Heparin

Internalization
Aripiprazole
Genestein
Zoniporide

Acidification
Amodiaquine
Chloroquine
Niclosamide
Omeprazole
Piperacetazine

Trafficking
Amiodarone*
Apilimod
Colchicine
Tetrandrine*
Verapamil*

Fusion
Arbidol
Azithromycin
Bepridil
Clomiphene
C-peptide inhibitors
LJ001
Sertraline
Toremifene

Cathepsin cleavage
E64d
Leupeptin

NPC1 binding
3.47
Imipramine
Posaconazole
U18666A

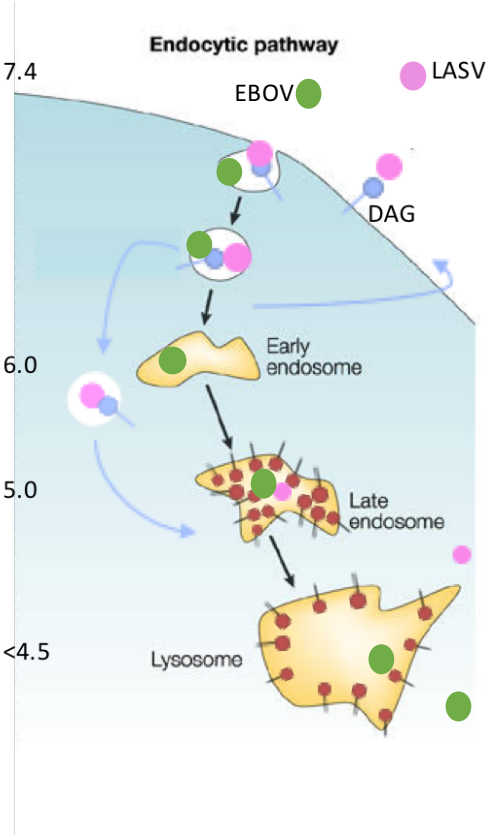

Lassa

Attachment

Internalization
Aripiprazole
Zoniporide

Acidification
Amodiaquine
Chloroquine
Niclosamide

Trafficking
Apilimod

Fusion
Arbidol
LJ001
ST-193
ST-294
ZCL278

Literature Cited

1. *International Committee on Taxonomy of Viruses [Internet]. [cited 2018 May 11].* http://www.ictvonline.org/.
2. Radoshitzky, S.R., et al., *Past, present, and future of arenavirus taxonomy.* Arch Virol, 2015. **160**(7): p. 1851-74.
3. Forni, D., et al., *Ancient Evolution of Mammarenaviruses: Adaptation via Changes in the L Protein and No Evidence for Host-Virus Codivergence.* Genome Biol Evol, 2018. **10**(3): p. 863-874.
4. Zong, M., I. Fofana, and H. Choe, *Human and host species transferrin receptor 1 use by North American arenaviruses.* J Virol, 2014. **88**(16): p. 9418-28.
5. Muckenfuss, R.S., *Clinical Observations and Laboratory Investigations on the 1933 Epidemic of Encephalitis in St. Louis.* Bull N Y Acad Med, 1934. **10**(7): p. 444-53.
6. Armstrong, C. and L.K. Sweet, *Lymphocytic choriomeningitis. Report of two cases, with recovery of the virus from gray mice (Mus musculus) trapped in the two infected households.* Public Health Reports, 1939. **54**(17): p. pp 673-684.
7. Rivers, T.M. and T.F. Scott, *Meningitis in Man Caused by a Filterable Virus : Ii. Identification of the Etiological Agent.* J Exp Med, 1936. **63**(3): p. 415-32.
8. Scott, T.F. and T.M. Rivers, *Meningitis in Man Caused by a Filterable Virus : I. Two Cases and the Method of Obtaining a Virus from Their Spinal Fluids.* J Exp Med, 1936. **63**(3): p. 397-414.

9. Traub, E., *A Filterable Virus Recovered from White Mice.* Science, 1935. **81**(2099): p. 298-9.

10. Traub, E., *The Epidemiology of Lymphocytic Choriomeningitis in White Mice.* J Exp Med, 1936. **64**(2): p. 183-200.

11. Traub, E., *An Epidemic in a Mouse Colony Due to the Virus of Acute Lymphocytic Choriomeningitis.* J Exp Med, 1936. **63**(4): p. 533-46.

12. Smadel, J.E. and M.J. Wall, *Lymphocytic Choriomeningitis in the Syrian Hamster.* J Exp Med, 1942. **75**(6): p. 581-91.

13. Biggar, R.J., T.J. Schmidt, and J.P. Woodall, *Lymphocytic choriomeningitis in laboratory personnel exposed to hamsters inadvertently infected with LCM virus.* J Am Vet Med Assoc, 1977. **171**(9): p. 829-32.

14. Buchmeier, M.J., et al., *The virology and immunobiology of lymphocytic choriomeningitis virus infection.* Adv Immunol, 1980. **30**: p. 275-331.

15. Hinman, A.R., et al., *Outbreak of lymphocytic choriomeningitis virus infections in medical center personnel.* Am J Epidemiol, 1975. **101**(2): p. 103-10.

16. Skinner, H.H. and E.H. Knight, *Monitoring mouse stocks for lymphocytic chloriomeningitis virus--a human pathogen.* Lab Anim, 1971. **5**(1): p. 73-87.

17. Mahy, B.W., et al., *Virus zoonoses and their potential for contamination of cell cultures.* Dev Biol Stand, 1991. **75**: p. 183-9.

18. Dykewicz, C.A., et al., *Lymphocytic choriomeningitis outbreak associated with nude mice in a research institute.* JAMA, 1992. **267**(10): p. 1349-53.

19. Aebischer, O., et al., *Lymphocytic choriomeningitis virus infection induced by percutaneous exposure.* Occup Med (Lond), 2016. **66**(2): p. 171-3.

20. Cummins, D., *Arenaviral haemorrhagic fevers.* Blood Rev, 1991. **5**(3): p. 129-37.

21. Lapošová, K., S. Pastoreková, and J. Tomášková, *Lymphocytic choriomeningitis virus: invisible but not innocent.* Acta Virol, 2013. **57**(2): p. 160-70.

22. Gregg, M.B., *Recent outbreaks of lymphocytic choriomeningitis in the United States of America.* Bull World Health Organ, 1975. **52**(4-6): p. 549-53.

23. Biggar, R.J., et al., *Lymphocytic choriomeningitis outbreak associated with pet hamsters. Fifty-seven cases from New York State.* JAMA, 1975. **232**(5): p. 494-500.

24. Knust, B., et al., *Lymphocytic choriomeningitis virus in employees and mice at multipremises feeder-rodent operation, United States, 2012.* Emerg Infect Dis, 2014. **20**(2): p. 240-7.

25. Fischer, S.A., et al., *Transmission of lymphocytic choriomeningitis virus by organ transplantation.* N Engl J Med, 2006. **354**(21): p. 2235-49.

26. Macneil, A., et al., *Solid organ transplant-associated lymphocytic choriomeningitis, United States, 2011.* Emerg Infect Dis, 2012. **18**(8): p. 1256-62.

27. Arribalzaga, R.A., *[New epidemic disease due to unidentified germ: nephrotoxic, leukopenic and enanthematous hyperthermia].* Dia Med, 1955. **27**(40): p. 1204-10.

28. Parodi, A.S., et al., *[Concerning the epidemic outbreak in Junin].* Dia Med, 1958. **30**(62): p. 2300-1.

29. Charrel, R.N. and X. de Lamballerie, *Arenaviruses other than Lassa virus.* Antiviral Res, 2003. **57**(1-2): p. 89-100.

30. Marr, J.S. and J.B. Kiracofe, *Was the huey cocoliztli a haemorrhagic fever?* Med Hist, 2000. **44**(3): p. 341-62.

31. Acuna-Soto, R., L.C. Romero, and J.H. Maguire, *Large epidemics of hemorrhagic fevers in Mexico 1545-1815.* Am J Trop Med Hyg, 2000. **62**(6): p. 733-9.

32. Kunz, S., *The role of the vascular endothelium in arenavirus haemorrhagic fevers.* Thromb Haemost, 2009. **102**(6): p. 1024-9.

33. Ölschläger, S. and L. Flatz, *Vaccination strategies against highly pathogenic arenaviruses: the next steps toward clinical trials.* PLoS Pathog, 2013. **9**(4): p. e1003212.

34. Enria, D.A., A.M. Briggiler, and Z. Sanchez, *Treatment of Argentine hemorrhagic fever.* Antiviral Res, 2008. **78**(1): p. 132-9.

35. Mackenzie, R.B., *Epidemiology of Machupo virus infection. I. Pattern of human infection, San Joaquin, Bolivia, 1962-1964.* Am J Trop Med Hyg, 1965. **14**(5): p. 808-13.

36. Centers for Disease, C. and Prevention, *Bolivian hemorrhagic fever--El Beni Department, Bolivia, 1994.* MMWR Morb Mortal Wkly Rep, 1994. **43**(50): p. 943-6.

37. Peters, C.J., *Emerging infections: lessons from the viral hemorrhagic fevers.* Trans Am Clin Climatol Assoc, 2006. **117**: p. 189-96; discussion 196-7.

38. Johnson, K.M., et al., *Virus Isolations from Human Cases of Hemorrhagic Fever in Bolivia.* Proc Soc Exp Biol Med, 1965. **118**: p. 113-8.

39. Johnson, K.M., et al., *Chronic infection of rodents by Machupo virus.* Science, 1965. **150**(3703): p. 1618-9.

40. Peters, C.J., et al., *Hemorrhagic fever in Cochabamba, Bolivia, 1971.* Am J Epidemiol, 1974. **99**(6): p. 425-33.

41. Kilgore, P.E., et al., *Treatment of Bolivian hemorrhagic fever with intravenous ribavirin.* Clin Infect Dis, 1997. **24**(4): p. 718-22.

42. Aguilar, P.V., et al., *Reemergence of Bolivian hemorrhagic fever, 2007-2008.* Emerg Infect Dis, 2009. **15**(9): p. 1526-8.

43. Patterson, M., A. Grant, and S. Paessler, *Epidemiology and pathogenesis of Bolivian hemorrhagic fever.* Curr Opin Virol, 2014. **5**: p. 82-90.

44. Salas, R., et al., *Venezuelan haemorrhagic fever.* Lancet, 1991. **338**(8774): p. 1033-6.

45. Tesh, R.B., et al., *Description of Guanarito virus (Arenaviridae: Arenavirus), the etiologic agent of Venezuelan hemorrhagic fever.* Am J Trop Med Hyg, 1994. **50**(4): p. 452-9.

46. de Manzione, N., et al., *Venezuelan hemorrhagic fever: clinical and epidemiological studies of 165 cases.* Clin Infect Dis, 1998. **26**(2): p. 308-13.

47. ProMED-mail., *Venezuelan Hemorrhagic Fever - Venezuela. ProMED-email; 20170609.5095816*.

48. Coimbra, T.L.M., et al., *New arenavirus isolated in Brazil.* Lancet, 1994. **343**(8894): p. 391-2.

49. Vasconcelos, P.F., et al., *[Laboratory-acquired human infection with SP H 114202 virus (Arenavirus: Arenaviridae family): clinical and laboratory aspects]*. Rev Inst Med Trop Sao Paulo, 1993. **35**(6): p. 521-5.

50. Centers for Disease, C. and Prevention, *Arenavirus infection--Connecticut, 1994.* MMWR Morb Mortal Wkly Rep, 1994. **43**(34): p. 635-6.

51. Barry, M., et al., *Brief report: treatment of a laboratory-acquired Sabia virus infection.* N Engl J Med, 1995. **333**(5): p. 294-6.

52. Ellwanger, J.H. and J.A. Chies, *Keeping track of hidden dangers - The short history of the Sabiá virus.* Rev Soc Bras Med Trop, 2017. **50**(1): p. 3-8.

53. Delgado, S., et al., *Chapare virus, a newly discovered arenavirus isolated from a fatal hemorrhagic fever case in Bolivia.* PLoS Pathog, 2008. **4**(4): p. e1000047.

54. Grande-Perez, A., et al., *Arenavirus Quasispecies and Their Biological Implications.* Curr Top Microbiol Immunol, 2016. **392**: p. 231-76.

55. ProMED-mail. *Lujo Virus, A Novel Arenavirus - South Africa ex Zambia. ProMED-email; 20090601.2042*.

56. Paweska, J.T., et al., *Nosocomial outbreak of novel arenavirus infection, southern Africa.* Emerg Infect Dis, 2009. **15**(10): p. 1598-602.

57. Sewlall, N.H., et al., *Clinical features and patient management of Lujo hemorrhagic fever.* PLoS Negl Trop Dis, 2014. **8**(11): p. e3233.

58. Andersen, K.G., et al., *Clinical Sequencing Uncovers Origins and Evolution of Lassa Virus.* Cell, 2015. **162**(4): p. 738-50.

59. Manning, J.T., N. Forrester, and S. Paessler, *Lassa virus isolates from Mali and the Ivory Coast represent an emerging fifth lineage.* Front Microbiol, 2015. **6**: p. 1037.

60. Sabeti, P.C., et al., *Genome-wide detection and characterization of positive selection in human populations.* Nature, 2007. **449**(7164): p. 913-8.

61. International HapMap, C., et al., *A second generation human haplotype map of over 3.1 million SNPs.* Nature, 2007. **449**(7164): p. 851-61.

62. Andersen, K.G., et al., *Genome-wide scans provide evidence for positive selection of genes implicated in Lassa fever.* Philos Trans R Soc Lond B Biol Sci, 2012. **367**(1590): p. 868-77.

63. Rotimi, C.N., et al., *The genomic landscape of African populations in health and disease.* Hum Mol Genet, 2017. **26**(R2): p. R225-R236.

64. Gibb, R., et al., *Understanding the cryptic nature of Lassa fever in West Africa.* Pathog Glob Health, 2017. **111**(6): p. 276-288.

65. Hallam, H.J., et al., *Baseline mapping of Lassa fever virology, epidemiology and vaccine research and development.* NPJ Vaccines, 2018. **3**: p. 11.

66. Haas, W.H., et al., *Imported Lassa fever in Germany: surveillance and management of contact persons.* Clin Infect Dis, 2003. **36**(10): p. 1254-8.

67. Lalis, A., et al., *The impact of human conflict on the genetics of Mastomys natalensis and Lassa virus in West Africa.* PLoS One, 2012. **7**(5): p. e37068.

68. LeGac, P., *Recherches sur le typhus des savanes de l'Oubangui-Chari. La maladie des Boughbous.* Bull Soc Path exot, 1946. **39**: p. 97-103.

69. Monath, T.P., *Lassa fever: review of epidemiology and epizootiology.* Bull World Health Organ, 1975. **52**(4-6): p. 577-92.

70. Rose, J.R., *A new clinical entity?* Lancet, 1956. **2**: p. 197.

71. Rose, J.R., *An outbreak of encephalomyelitis in Sierra Leone.* Lancet, 1957. **273**(7002): p. 914-6.

72. Henderson, B.E., et al., *Lassa fever. Virological and serological studies.* Trans R Soc Trop Med Hyg, 1972. **66**(3): p. 409-16.

73. Bond, N., et al., *A historical look at the first reported cases of Lassa fever: IgG antibodies 40 years after acute infection.* Am J Trop Med Hyg, 2013. **88**(2): p. 241-4.

74. Frame, J.D., et al., *Lassa fever, a new virus disease of man from West Africa. I. Clinical description and pathological findings.* Am J Trop Med Hyg, 1970. **19**(4): p. 670-6.

75. Fuller, J.G., *Fever! The hunt for a new killer virus*. 1974, New York,: Reader's Digest Press; distributed by Dutton. 297 p.

76. Buckley, S.M., J. Casals, and W.G. Downs, *Isolation and antigenic characterization of Lassa virus.* Nature, 1970. **227**(5254): p. 174.

77. Leifer, E., D.J. Gocke, and H. Bourne, *Lassa fever, a new virus disease of man from West Africa. II. Report of a laboratory-acquired infection treated with plasma from a person recently recovered from the disease.* Am J Trop Med Hyg, 1970. **19**(4): p. 677-9.

78. Kuehne, R.W., *Biological containment facility for studying infectious disease.* Appl Microbiol, 1973. **26**(3): p. 239-43.

79. Borio, L., et al., *Hemorrhagic fever viruses as biological weapons: medical and public health management.* JAMA, 2002. **287**(18): p. 2391-405.

80. Troup, J.M., et al., *An outbreak of Lassa fever on the Jos plateau, Nigeria, in January-February 1970. A preliminary report.* Am J Trop Med Hyg, 1970. **19**(4): p. 695-6.

81. Carey, D.E., et al., *Lassa fever. Epidemiological aspects of the 1970 epidemic, Jos, Nigeria.* Trans R Soc Trop Med Hyg, 1972. **66**(3): p. 402-8.

82. Bausch, D.G., S.S. Sesay, and B. Oshin, *On the front lines of Lassa fever.* Emerg Infect Dis, 2004. **10**(10): p. 1889-90.

83. Mertens, P.E., et al., *Clinical presentation of Lassa fever cases during the hospital epidemic at Zorzor, Liberia, March-April 1972.* Am J Trop Med Hyg, 1973. **22**(6): p. 780-4.

84. Edington, G.M. and H.A. White, *The pathology of Lassa fever.* Trans R Soc Trop Med Hyg, 1972. **66**(3): p. 381-9.

85. Fraser, D.W., et al., *Lassa fever in the Eastern Province of Sierra Leone, 1970-1972. I. Epidemiologic studies.* Am J Trop Med Hyg, 1974. **23**(6): p. 1131-9.

86. Monath, T.P., et al., *Lassa fever in the Eastern Province of Sierra Leone, 1970-1972. II. Clinical observations and virological studies on selected hospital cases.* Am J Trop Med Hyg, 1974. **23**(6): p. 1140-9.

87. McCormick, J.B., et al., *A prospective study of the epidemiology and ecology of Lassa fever.* J Infect Dis, 1987. **155**(3): p. 437-44.

88. Kerneis, S., et al., *Prevalence and risk factors of Lassa seropositivity in inhabitants of the forest region of Guinea: a cross-sectional study.* PLoS Negl Trop Dis, 2009. **3**(11): p. e548.

89. Shaffer, J.G., et al., *Lassa fever in post-conflict sierra leone.* PLoS Negl Trop Dis, 2014. **8**(3): p. e2748.

90. Khan, S.H., et al., *New opportunities for field research on the pathogenesis and treatment of Lassa fever.* Antiviral Res, 2008. **78**(1): p. 103-15.

91. Goba, A., et al., *An Outbreak of Ebola Virus Disease in the Lassa Fever Zone.* J Infect Dis, 2016. **214**(suppl 3): p. S110-S121.

92. Bausch, D.G., *The year that Ebola virus took over west Africa: missed opportunities for prevention.* Am J Trop Med Hyg, 2015. **92**(2): p. 229-32.

93. Yun, N.E. and D.H. Walker, *Pathogenesis of Lassa fever.* Viruses, 2012. **4**(10): p. 2031-48.

94. Mylne, A.Q., et al., *Mapping the zoonotic niche of Lassa fever in Africa.* Trans R Soc Trop Med Hyg, 2015. **109**(8): p. 483-92.

95. Monath, T.P., et al., *A hospital epidemic of Lassa fever in Zorzor, Liberia, March-April 1972.* Am J Trop Med Hyg, 1973. **22**(6): p. 773-9.

96. Frame, J.D., *Surveillance of Lassa fever in missionaries stationed in West Africa.* Bull World Health Organ, 1975. **52**(4-6): p. 593-8.

97. Jahrling, P.B., et al., *Endemic Lassa fever in Liberia. III. Characterization of Lassa virus isolates.* Trans R Soc Trop Med Hyg, 1985. **79**(3): p. 374-9.

98. Fisher-Hoch, S.P., et al., *Review of cases of nosocomial Lassa fever in Nigeria: the high price of poor medical practice.* BMJ, 1995. **311**(7009): p. 857-9.

99. Woodruff, A.W., et al., *Lassa fever in Britain: an imported case.* Br Med J, 1973. **3**(5881): p. 616-7.

100. Shlaeffer, F., E. Sikuler, and A. Keynan, *[Lassa fever--first case diagnosed in Israel]*. Harefuah, 1988. **114**(1): p. 12-4.

101. Mahdy, M.S., et al., *Lassa fever: the first confirmed case imported into Canada.* Can Dis Wkly Rep, 1989. **15**(39): p. 193-8.

102. Hirabayashi, Y., et al., *[The first imported case of Lassa fever in Japan]*. Nihon Rinsho, 1989. **47**(1): p. 71-5.

103. ProMED-mail. *Lassa Fever - South Africa Ex Nigeria. ProMED-email; 20090425.1554.*

104. Holmes, G.P., et al., *Lassa fever in the United States. Investigation of a case and new guidelines for management.* N Engl J Med, 1990. **323**(16): p. 1120-3.

105. *Lassa fever, imported case, Netherlands.* Wkly Epidemiol Rec, 2000. **75**(33): p. 265.

106. Centers for Disease, C. and Prevention, *Imported Lassa fever--New Jersey, 2004.* MMWR Morb Mortal Wkly Rep, 2004. **53**(38): p. 894-7.

107. Macher, A.M. and M.S. Wolfe, *Historical Lassa fever reports and 30-year clinical update.* Emerg Infect Dis, 2006. **12**(5): p. 835-7.

108. Kitching, A., et al., *A fatal case of Lassa fever in London, January 2009.* Euro Surveill, 2009. **14**(6).

109. Atkin, S., et al., *The first case of Lassa fever imported from Mali to the United Kingdom, February 2009.* Euro Surveill, 2009. **14**(10).

110. Grahn, A., et al., *Imported Case of Lassa Fever in Sweden With Encephalopathy and Sensorineural Hearing Deficit.* Open Forum Infect Dis, 2016. **3**(4): p. ofw198.

111. Ehlkes, L., et al., *Management of a Lassa fever outbreak, Rhineland-Palatinate, Germany, 2016.* Euro Surveill, 2017. **22**(39).

112. Hewson, R., *Lessons learnt from imported cases and onward transmission of Lassa fever in Europe support broader management of viral haemorrhagic fevers.* Euro Surveill, 2017. **22**(39).

113. The Lancet Infectious, D., *Lassa fever and global health security.* Lancet Infect Dis, 2018. **18**(4): p. 357.

114. ProMED-mail., *Lassa Fever - Niger (08): Update. ProMED-email; 20120714.1201872.*

115. Ajayi, N.A., et al., *Containing a Lassa fever epidemic in a resource-limited setting: outbreak description and lessons learned from Abakaliki, Nigeria (January-March 2012).* Int J Infect Dis, 2013. **17**(11): p. e1011-6.

116. Maxmen, A., *Deadly outbreak tests Nigerian health agency*, in *Public Health*. 2018, Nature. p. 421-422.

117. Roberts, L., *Nigeria hit by unprecedented Lassa fever outbreak.* Science, 2018. **359**(6381): p. 1201-1202.

118. ProMED-mail. *Lassa Fever - West Africa (26): Nigeria. ProMED-email; 20180509.5790856*.

119. WHO-Nigeria *[Internet] 28 February 2018. Nigeria battles its largest Lassa fever outbreak on record.* http://www.afro.who.int/news/nigeria-battles-its-largest-lassa-fever-outbreak-record. *[cited 11 May 2018]*.

120. Blasdell, K.R., et al., *Evidence of human infection by a new mammarenavirus endemic to Southeastern Asia.* Elife, 2016. **5**.

121. Marien, J., et al., *Movement Patterns of Small Rodents in Lassa Fever-Endemic Villages in Guinea.* Ecohealth, 2018.

122. Sarute, N. and S.R. Ross, *New World Arenavirus Biology.* Annu Rev Virol, 2017. **4**(1): p. 141-158.

123. Charrel, R.N. and X. de Lamballerie, *Zoonotic aspects of arenavirus infections.* Vet Microbiol, 2010. **140**(3-4): p. 213-20.

124. Monath, T.P., et al., *Lassa virus isolation from Mastomys natalensis rodents during an epidemic in Sierra Leone.* Science, 1974. **185**(4147): p. 263-5.

125. Wulff, H., A. Fabiyi, and T.P. Monath, *Recent isolations of Lassa virus from Nigerian rodents.* Bull World Health Organ, 1975. **52**(4-6): p. 609-13.

126. Olayemi, A., et al., *New Hosts of The Lassa Virus.* Sci Rep, 2016. **6**: p. 25280.

127. Lo Iacono, G., et al., *Using modelling to disentangle the relative contributions of zoonotic and anthroponotic transmission: the case of lassa fever.* PLoS Negl Trop Dis, 2015. **9**(1): p. e3398.

128. Dalldorf, G., *The Simultaneous Occurrence of the Viruses of Canine Distemper and Lymphocytic Choriomeningitis : A Correction of "Canine Distemper in the Rhesus Monkey".* J Exp Med, 1939. **70**(1): p. 19-27.

129. Bowen, G.S., et al., *Laboratory studies of a lymphocytic choriomeningitis virus outbreak in man and laboratory animals.* Am J Epidemiol, 1975. **102**(3): p. 233-40.

130. Vitullo, A.D., V.L. Hodara, and M.S. Merani, *Effect of persistent infection with Junin virus on growth and reproduction of its natural reservoir, Calomys musculinus.* Am J Trop Med Hyg, 1987. **37**(3): p. 663-9.

131. Greenwood, A.G. and S. Sanchez, *Serological evidence of murine pathogens in wild grey squirrels (Sciurus carolinensis) in North Wales.* Vet Rec, 2002. **150**(17): p. 543-6.

132. Blasdell, K.R., et al., *Host range and genetic diversity of arenaviruses in rodents, United Kingdom.* Emerg Infect Dis, 2008. **14**(9): p. 1455-8.

133. Zapata, J.C., et al., *Lymphocytic choriomeningitis virus (LCMV) infection of macaques: a model for Lassa fever.* Antiviral Res, 2011. **92**(2): p. 125-38.

134. Lukashevich, I.S., R.F. Maryankova, and F.M. Fidarov, *Reproduction of Lassa virus in different cell cultures.* Acta Virol, 1983. **27**(3): p. 282-5.

135. Jae, L.T., et al., *Lassa virus entry requires a trigger-induced receptor switch.* Science, 2014. **344**(6191): p. 1506-10.

136. Lukashevich, I.S., et al., *A live attenuated vaccine for Lassa fever made by reassortment of Lassa and Mopeia viruses.* J Virol, 2005. **79**(22): p. 13934-42.

137. Knobloch, J., et al., *Clinical observations in 42 patients with Lassa fever.* Tropenmed Parasitol, 1980. **31**(4): p. 389-98.

138. McCormick, J.B. and S.P. Fisher-Hoch, *Lassa fever.* Curr Top Microbiol Immunol, 2002. **262**: p. 75-109.

139. Kerber, R., et al., *Research efforts to control highly pathogenic arenaviruses: a summary of the progress and gaps.* J Clin Virol, 2015. **64**: p. 120-7.

140. McCormick, J.B., et al., *A case-control study of the clinical diagnosis and course of Lassa fever.* J Infect Dis, 1987. **155**(3): p. 445-55.

141. Mateer, E.J., et al., *Lassa fever-induced sensorineural hearing loss: A neglected public health and social burden.* PLoS Negl Trop Dis, 2018. **12**(2): p. e0006187.

142. Schlie, K., et al., *Viral protein determinants of Lassa virus entry and release from polarized epithelial cells.* J Virol, 2010. **84**(7): p. 3178-88.

143. Dylla, D.E., et al., *Basolateral entry and release of New and Old World arenaviruses from human airway epithelia.* J Virol, 2008. **82**(12): p. 6034-8.

144. Cosset, F.L., et al., *Characterization of Lassa virus cell entry and neutralization with Lassa virus pseudoparticles.* J Virol, 2009. **83**(7): p. 3228-37.

145. Baize, S., et al., *Lassa virus infection of human dendritic cells and macrophages is productive but fails to activate cells.* J Immunol, 2004. **172**(5): p. 2861-9.

146. Basler, C.F., *Molecular pathogenesis of viral hemorrhagic fever.* Semin Immunopathol, 2017. **39**(5): p. 551-561.

147. Russier, M., D. Pannetier, and S. Baize, *Immune responses and Lassa virus infection.* Viruses, 2012. **4**(11): p. 2766-85.

148. Lukashevich, I.S., et al., *Lassa and Mopeia virus replication in human monocytes/macrophages and in endothelial cells: different effects on IL-8 and TNF-alpha gene expression.* J Med Virol, 1999. **59**(4): p. 552-60.

149. Johnson, K.M., et al., *Clinical virology of Lassa fever in hospitalized patients.* J Infect Dis, 1987. **155**(3): p. 456-64.

150. Gunther, S., et al., *Lassa fever encephalopathy: Lassa virus in cerebrospinal fluid but not in serum.* J Infect Dis, 2001. **184**(3): p. 345-9.

151. McCormick, J.B., et al., *Lassa virus hepatitis: a study of fatal Lassa fever in humans.* Am J Trop Med Hyg, 1986. **35**(2): p. 401-7.

152. Beier, J.I., et al., *Novel mechanism of arenavirus-induced liver pathology.* PLoS One, 2015. **10**(3): p. e0122839.

153. Oldstone, M.B. and K.P. Campbell, *Decoding arenavirus pathogenesis: essential roles for alpha-dystroglycan-virus interactions and the immune response.* Virology, 2011. **411**(2): p. 170-9.

154. Weber, F. and O. Haller, *Viral suppression of the interferon system.* Biochimie, 2007. **89**(6-7): p. 836-42.

155. Borrow, P., L. Martinez-Sobrido, and J.C. de la Torre, *Inhibition of the type I interferon antiviral response during arenavirus infection.* Viruses, 2010. **2**(11): p. 2443-80.

156. Martinez-Sobrido, L., et al., *Differential inhibition of type I interferon induction by arenavirus nucleoproteins.* J Virol, 2007. **81**(22): p. 12696-703.

157. Martinez-Sobrido, L., et al., *Inhibition of the type I interferon response by the nucleoprotein of the prototypic arenavirus lymphocytic choriomeningitis virus.* J Virol, 2006. **80**(18): p. 9192-9.

158. Hayes, M. and M. Salvato, *Arenavirus evasion of host anti-viral responses.* Viruses, 2012. **4**(10): p. 2182-96.

159. Zinzula, L. and E. Tramontano, *Strategies of highly pathogenic RNA viruses to block dsRNA detection by RIG-I-like receptors: hide, mask, hit.* Antiviral Res, 2013. **100**(3): p. 615-35.

160. Xing, J., H. Ly, and Y. Liang, *The Z proteins of pathogenic but not nonpathogenic arenaviruses inhibit RIG-I-like receptor-dependent interferon production.* J Virol, 2015. **89**(5): p. 2944-55.

161. ter Meulen, J., et al., *Characterization of human CD4(+) T-cell clones recognizing conserved and variable epitopes of the Lassa virus nucleoprotein.* J Virol, 2000. **74**(5): p. 2186-92.

162. Meulen, J., et al., *Old and New World arenaviruses share a highly conserved epitope in the fusion domain of the glycoprotein 2, which is recognized by Lassa virus-specific human CD4+ T-cell clones.* Virology, 2004. **321**(1): p. 134-43.

163. Prescott, J.B., et al., *Immunobiology of Ebola and Lassa virus infections.* Nat Rev Immunol, 2017. **17**(3): p. 195-207.

164. Fehling, S.K., F. Lennartz, and T. Strecker, *Multifunctional nature of the arenavirus RING finger protein Z.* Viruses, 2012. **4**(11): p. 2973-3011.

165. Salvato, M.S. and E.M. Shimomaye, *The completed sequence of lymphocytic choriomeningitis virus reveals a unique RNA structure and a gene for a zinc finger protein.* Virology, 1989. **173**(1): p. 1-10.

166. Talmon, Y., et al., *Electron microscopy of vitrified-hydrated La Crosse virus.* J Virol, 1987. **61**(7): p. 2319-21.

167. Emonet, S.E., S. Urata, and J.C. de la Torre, *Arenavirus reverse genetics: new approaches for the investigation of arenavirus biology and development of antiviral strategies.* Virology, 2011. **411**(2): p. 416-25.

168. Meyer, B. and H. Ly, *Inhibition of Innate Immune Responses Is Key to Pathogenesis by Arenaviruses.* J Virol, 2016. **90**(8): p. 3810-3818.

169. Wolff, S., H. Ebihara, and A. Groseth, *Arenavirus budding: a common pathway with mechanistic differences.* Viruses, 2013. **5**(2): p. 528-49.

170. Riviere, Y., et al., *The S RNA segment of lymphocytic choriomeningitis virus codes for the nucleoprotein and glycoproteins 1 and 2.* J Virol, 1985. **53**(3): p. 966-8.

171. Khamina, K., et al., *Characterization of host proteins interacting with the lymphocytic choriomeningitis virus L protein.* PLoS Pathog, 2017. **13**(12): p. e1006758.

172. Capul, A.A., et al., *Arenavirus Z-glycoprotein association requires Z myristoylation but not functional RING or late domains.* J Virol, 2007. **81**(17): p. 9451-60.

173. Perez, M., D.L. Greenwald, and J.C. de la Torre, *Myristoylation of the RING finger Z protein is essential for arenavirus budding.* J Virol, 2004. **78**(20): p. 11443-8.

174. Strecker, T., et al., *The role of myristoylation in the membrane association of the Lassa virus matrix protein Z.* Virol J, 2006. **3**: p. 93.

175. Strecker, T., et al., *Lassa virus Z protein is a matrix protein and sufficient for the release of virus-like particles [corrected].* J Virol, 2003. **77**(19): p. 10700-5.

176. Urata, S. and J. Yasuda, *Cis- and cell-type-dependent trans-requirements for Lassa virus-like particle production.* J Gen Virol, 2015. **96**(Pt 7): p. 1626-35.

177. Nunberg, J.H. and J. York, *The curious case of arenavirus entry, and its inhibition.* Viruses, 2012. **4**(1): p. 83-101.

178. Qi, X., et al., *Cap binding and immune evasion revealed by Lassa nucleoprotein structure.* Nature, 2010. **468**(7325): p. 779-83.

179. Morin, B., et al., *The N-terminal domain of the arenavirus L protein is an RNA endonuclease essential in mRNA transcription.* PLoS Pathog, 2010. **6**(9): p. e1001038.

180. Perez, M. and J.C. de la Torre, *Characterization of the genomic promoter of the prototypic arenavirus lymphocytic choriomeningitis virus.* J Virol, 2003. **77**(2): p. 1184-94.

181. Kranzusch, P.J. and S.P. Whelan, *Arenavirus Z protein controls viral RNA synthesis by locking a polymerase-promoter complex.* Proc Natl Acad Sci U S A, 2011. **108**(49): p. 19743-8.

182. Ferron, F., et al., *Transcription and replication mechanisms of Bunyaviridae and Arenaviridae L proteins.* Virus Res, 2017. **234**: p. 118-134.

183. Burri, D.J., et al., *Envelope glycoprotein of arenaviruses.* Viruses, 2012. **4**(10): p. 2162-81.

184. Urata, S. and J.C. de la Torre, *Arenavirus budding.* Adv Virol, 2011. **2011**: p. 180326.

185. York, J. and J.H. Nunberg, *Myristoylation of the Arenavirus Envelope Glycoprotein Stable Signal Peptide Is Critical for Membrane Fusion but Dispensable for Virion Morphogenesis.* J Virol, 2016. **90**(18): p. 8341-50.

186. Agnihothram, S.S., J. York, and J.H. Nunberg, *Role of the stable signal peptide and cytoplasmic domain of G2 in regulating intracellular transport of the Junin virus envelope glycoprotein complex.* J Virol, 2006. **80**(11): p. 5189-98.

187. Bederka, L.H., et al., *Arenavirus stable signal peptide is the keystone subunit for glycoprotein complex organization.* MBio, 2014. **5**(6): p. e02063.

188. Eichler, R., et al., *Identification of Lassa virus glycoprotein signal peptide as atrans-acting maturation factor.* EMBO reports, 2003. **4**(11): p. 1084-1088.

189. York, J. and J.H. Nunberg, *A novel zinc-binding domain is essential for formation of the functional Junin virus envelope glycoprotein complex.* J Virol, 2007. **81**(24): p. 13385-91.

190. Albarino, C.G., et al., *Reverse genetics generation of chimeric infectious Junin/Lassa virus is dependent on interaction of homologous glycoprotein stable signal peptide and G2 cytoplasmic domains.* J Virol, 2011. **85**(1): p. 112-22.

191. York, J. and J.H. Nunberg, *Distinct requirements for signal peptidase processing and function in the stable signal peptide subunit of the Junin virus envelope glycoprotein.* Virology, 2007. **359**(1): p. 72-81.

192. Burri, D.J., et al., *Molecular characterization of the processing of arenavirus envelope glycoprotein precursors by subtilisin kexin isozyme-1/site-1 protease.* J Virol, 2012. **86**(9): p. 4935-46.

193. Schlie, K., et al., *Characterization of Lassa virus glycoprotein oligomerization and influence of cholesterol on virus replication.* J Virol, 2010. **84**(2): p. 983-92.

194. Vigerust, D.J. and V.L. Shepherd, *Virus glycosylation: role in virulence and immune interactions.* Trends Microbiol, 2007. **15**(5): p. 211-8.

195. Helenius, A. and M. Aebi, *Intracellular functions of N-linked glycans.* Science, 2001. **291**(5512): p. 2364-9.

196. Backovic, M. and F.A. Rey, *Virus entry: old viruses, new receptors.* Curr Opin Virol, 2012. **2**(1): p. 4-13.

197. Sommerstein, R., et al., *Arenavirus Glycan Shield Promotes Neutralizing Antibody Evasion and Protracted Infection.* PLoS Pathog, 2015. **11**(11): p. e1005276.

198. Wang, W., et al., *Structure-function relationship of the mammarenavirus envelope glycoprotein.* Virol Sin, 2016. **31**(5): p. 380-394.

199. Eichler, R., et al., *The role of single N-glycans in proteolytic processing and cell surface transport of the Lassa virus glycoprotein GP-C.* Virol J, 2006. **3**: p. 41.

200. Wright, K.E., et al., *Post-translational processing of the glycoproteins of lymphocytic choriomeningitis virus.* Virology, 1990. **177**(1): p. 175-83.

201. Eschli, B., et al., *Identification of an N-terminal trimeric coiled-coil core within arenavirus glycoprotein 2 permits assignment to class I viral fusion proteins.* J Virol, 2006. **80**(12): p. 5897-907.

202. Hastie, K.M., et al., *Structural basis for antibody-mediated neutralization of Lassa virus.* Science, 2017. **356**(6341): p. 923-928.

203. Hallenberger, S., et al., *Inhibition of furin-mediated cleavage activation of HIV-1 glycoprotein gp160.* Nature, 1992. **360**(6402): p. 358-61.

204. Klimstra, W.B., H.W. Heidner, and R.E. Johnston, *The furin protease cleavage recognition sequence of Sindbis virus PE2 can mediate virion attachment to cell surface heparan sulfate.* J Virol, 1999. **73**(8): p. 6299-306.

205. Day, P.M. and J.T. Schiller, *The role of furin in papillomavirus infection.* Future Microbiol, 2009. **4**(10): p. 1255-62.

206. Krzyzaniak, M.A., et al., *Host cell entry of respiratory syncytial virus involves macropinocytosis followed by proteolytic activation of the F protein.* PLoS Pathog, 2013. **9**(4): p. e1003309.

207. Bottcher-Friebertshauser, E., et al., *The hemagglutinin: a determinant of pathogenicity.* Curr Top Microbiol Immunol, 2014. **385**: p. 3-34.

208. El Najjar, F., et al., *Analysis of cathepsin and furin proteolytic enzymes involved in viral fusion protein activation in cells of the bat reservoir host.* PLoS One, 2015. **10**(2): p. e0115736.

209. Lenz, O., et al., *The Lassa virus glycoprotein precursor GP-C is proteolytically processed by subtilase SKI-1/S1P.* Proc Natl Acad Sci U S A, 2001. **98**(22): p. 12701-5.

210. Beyer, W.R., et al., *Endoproteolytic processing of the lymphocytic choriomeningitis virus glycoprotein by the subtilase SKI-1/S1P.* J Virol, 2003. **77**(5): p. 2866-72.

211. Klaus, J.P., et al., *The intracellular cargo receptor ERGIC-53 is required for the production of infectious arenavirus, coronavirus, and filovirus particles.* Cell Host Microbe, 2013. **14**(5): p. 522-34.

212. Li, S., et al., *Acidic pH-Induced Conformations and LAMP1 Binding of the Lassa Virus Glycoprotein Spike.* PLoS Pathog, 2016. **12**(2): p. e1005418.

213. Zeltina, A. and T.A. Bowden, *Human antibody pieces together the puzzle of the trimeric Lassa virus surface antigen.* Nat Struct Mol Biol, 2017. **24**(7): p. 559-560.

214. Glushakova, S.E., et al., *The fusion of artificial lipid membranes induced by the synthetic arenavirus 'fusion peptide'.* Biochim Biophys Acta, 1992. **1110**(2): p. 202-8.

215. Gallaher, W.R., C. DiSimone, and M.J. Buchmeier, *The viral transmembrane superfamily: possible divergence of Arenavirus and Filovirus glycoproteins from a common RNA virus ancestor.* BMC Microbiol, 2001. **1**: p. 1.

216. Klewitz, C., H.D. Klenk, and J. ter Meulen, *Amino acids from both N-terminal hydrophobic regions of the Lassa virus envelope glycoprotein GP-2 are critical for pH-dependent membrane fusion and infectivity.* J Gen Virol, 2007. **88**(Pt 8): p. 2320-8.

217. Igonet, S., et al., *X-ray structure of the arenavirus glycoprotein GP2 in its postfusion hairpin conformation.* Proc Natl Acad Sci U S A, 2011. **108**(50): p. 19967-72.

218. Hastie, K.M., et al., *Crystal structure of the prefusion surface glycoprotein of the prototypic arenavirus LCMV*. Nat Struct Mol Biol, 2016. **23**(6): p. 513-521.

219. York, J. and J.H. Nunberg, *Role of the stable signal peptide of Junin arenavirus envelope glycoprotein in pH-dependent membrane fusion.* J Virol, 2006. **80**(15): p. 7775-80.

220. Saunders, A.A., et al., *Mapping the landscape of the lymphocytic choriomeningitis virus stable signal peptide reveals novel functional domains.* J Virol, 2007. **81**(11): p. 5649-57.

221. Cohen-Dvashi, H., et al., *Molecular Mechanism for LAMP1 Recognition by Lassa Virus.* J Virol, 2015. **89**(15): p. 7584-92.

222. Mahmutovic, S., et al., *Molecular Basis for Antibody-Mediated Neutralization of New World Hemorrhagic Fever Mammarenaviruses.* Cell Host Microbe, 2015. **18**(6): p. 705-13.

223. Zeltina, A., et al., *Convergent immunological solutions to Argentine hemorrhagic fever virus neutralization.* Proc Natl Acad Sci U S A, 2017. **114**(27): p. 7031-7036.

224. Parsy, M.L., et al., *Crystal structure of Venezuelan hemorrhagic fever virus fusion glycoprotein reveals a class 1 postfusion architecture with extensive glycosylation.* J Virol, 2013. **87**(23): p. 13070-5.

225. Bowden, T.A., et al., *Unusual molecular architecture of the machupo virus attachment glycoprotein.* J Virol, 2009. **83**(16): p. 8259-65.

226. Abraham, J., et al., *Structural basis for receptor recognition by New World hemorrhagic fever arenaviruses.* Nat Struct Mol Biol, 2010. **17**(4): p. 438-44.

227. Shimon, A., O. Shani, and R. Diskin, *Structural Basis for Receptor Selectivity by the Whitewater Arroyo Mammarenavirus.* J Mol Biol, 2017. **429**(18): p. 2825-2839.

228. Boulant, S., M. Stanifer, and P.Y. Lozach, *Dynamics of virus-receptor interactions in virus binding, signaling, and endocytosis.* Viruses, 2015. **7**(6): p. 2794-815.

229. Li, W., et al., *Angiotensin-converting enzyme 2 is a functional receptor for the SARS coronavirus.* Nature, 2003. **426**(6965): p. 450-4.

230. Li, W., et al., *Animal origins of the severe acute respiratory syndrome coronavirus: insight from ACE2-S-protein interactions.* J Virol, 2006. **80**(9): p. 4211-9.

231. White, J.M. and G.R. Whittaker, *Fusion of Enveloped Viruses in Endosomes.* Traffic, 2016. **17**(6): p. 593-614.

232. Lozach, P.Y., J. Huotari, and A. Helenius, *Late-penetrating viruses.* Curr Opin Virol, 2011. **1**(1): p. 35-43.

233. Quirin, K., et al., *Lymphocytic choriomeningitis virus uses a novel endocytic pathway for infectious entry via late endosomes.* Virology, 2008. **378**(1): p. 21-33.

234. Johannsdottir, H.K., et al., *Host cell factors and functions involved in vesicular stomatitis virus entry.* J Virol, 2009. **83**(1): p. 440-53.

235. Kielian, M.C., M. Marsh, and A. Helenius, *Kinetics of endosome acidification detected by mutant and wild-type Semliki Forest virus.* EMBO J, 1986. **5**(12): p. 3103-9.

236. Chandran, K., et al., *Endosomal proteolysis of the Ebola virus glycoprotein is necessary for infection.* Science, 2005. **308**(5728): p. 1643-5.

237. Schornberg, K., et al., *Role of endosomal cathepsins in entry mediated by the Ebola virus glycoprotein.* J Virol, 2006. **80**(8): p. 4174-8.

238. Park, J.E., et al., *Proteolytic processing of Middle East respiratory syndrome coronavirus spikes expands virus tropism.* Proc Natl Acad Sci U S A, 2016. **113**(43): p. 12262-12267.

239. Mingo, R.M., et al., *Ebola virus and severe acute respiratory syndrome coronavirus display late cell entry kinetics: evidence that transport to NPC1+ endolysosomes is a rate-defining step.* J Virol, 2015. **89**(5): p. 2931-43.

240. Glushakova, S.E., et al., *[Lysosomotropic agents inhibit the penetration of arenaviruses into a culture of BHK-21 and Vero cells].* Vopr Virusol, 1990. **35**(2): p. 146-50.

241. Rojek, J.M. and S. Kunz, *Cell entry by human pathogenic arenaviruses.* Cell Microbiol, 2008. **10**(4): p. 828-35.

242. Rojek, J.M., et al., *Different mechanisms of cell entry by human-pathogenic Old World and New World arenaviruses.* J Virol, 2008. **82**(15): p. 7677-87.

243. Lozach, P.Y., et al., *DC-SIGN as a receptor for phleboviruses.* Cell Host Microbe, 2011. **10**(1): p. 75-88.

244. Fedeli, C., et al., *Axl Can Serve as Entry Factor for Lassa Virus Depending on the Functional Glycosylation of Dystroglycan.* J Virol, 2018. **92**(5).

245. Oppliger, J., et al., *Lassa Virus Cell Entry via Dystroglycan Involves an Unusual Pathway of Macropinocytosis.* J Virol, 2016. **90**(14): p. 6412-6429.

246. Goncalves, A.R., et al., *Role of DC-SIGN in Lassa virus entry into human dendritic cells.* J Virol, 2013. **87**(21): p. 11504-15.

247. Spiegel, M., T. Plegge, and S. Pohlmann, *The Role of Phlebovirus Glycoproteins in Viral Entry, Assembly and Release.* Viruses, 2016. **8**(7).

248. Iwasaki, M., N. Ngo, and J.C. de la Torre, *Sodium hydrogen exchangers contribute to arenavirus cell entry.* J Virol, 2014. **88**(1): p. 643-54.

249. Nanbo, A., et al., *Ebolavirus is internalized into host cells via macropinocytosis in a viral glycoprotein-dependent manner.* PLoS Pathog, 2010. **6**(9): p. e1001121.

250. Saeed, M.F., et al., *Cellular entry of ebola virus involves uptake by a macropinocytosis-like mechanism and subsequent trafficking through early and late endosomes.* PLoS Pathog, 2010. **6**(9): p. e1001110.

251. Mercer, J. and A. Helenius, *Gulping rather than sipping: macropinocytosis as a way of virus entry.* Curr Opin Microbiol, 2012. **15**(4): p. 490-9.

252. Kunz, S., *Receptor binding and cell entry of Old World arenaviruses reveal novel aspects of virus-host interaction.* Virology, 2009. **387**(2): p. 245-9.

253. Pasqual, G., et al., *Old world arenaviruses enter the host cell via the multivesicular body and depend on the endosomal sorting complex required for transport.* PLoS Pathog, 2011. **7**(9): p. e1002232.

254. Beutler, B., et al., *Genetic analysis of host resistance: Toll-like receptor signaling and immunity at large.* Annu Rev Immunol, 2006. **24**: p. 353-89.

255. Lee, B.L. and G.M. Barton, *Trafficking of endosomal Toll-like receptors.* Trends Cell Biol, 2014. **24**(6): p. 360-9.

256. Kolokoltsov, A.A., et al., *Inhibition of Lassa virus and Ebola virus infection in host cells treated with the kinase inhibitors genistein and tyrphostin.* Arch Virol, 2012. **157**(1): p. 121-7.

257. Vela, E.M., et al., *Arenavirus entry occurs through a cholesterol-dependent, non-caveolar, clathrin-mediated endocytic mechanism.* Virology, 2007. **369**(1): p. 1-11.

258. Cohen-Dvashi, H., et al., *Role of LAMP1 Binding and pH Sensing by the Spike Complex of Lassa Virus.* J Virol, 2016. **90**(22): p. 10329-10338.

259. Kampmann, T., et al., *The Role of histidine residues in low-pH-mediated viral membrane fusion.* Structure, 2006. **14**(10): p. 1481-7.

260. Hastie, K.M. and E.O. Saphire, *Lassa virus glycoprotein: stopping a moving target.* Curr Opin Virol, 2018.

261. Illick, M.M., et al., *Uncoupling GP1 and GP2 expression in the Lassa virus glycoprotein complex: implications for GP1 ectodomain shedding.* Virol J, 2008. **5**: p. 161.

262. White, J.M., et al., *Structures and mechanisms of viral membrane fusion proteins: multiple variations on a common theme.* Crit Rev Biochem Mol Biol, 2008. **43**(3): p. 189-219.

263. Apellaniz, B., et al., *The three lives of viral fusion peptides.* Chem Phys Lipids, 2014. **181**: p. 40-55.

264. Harrison, S.C., *Viral membrane fusion.* Virology, 2015. **479-480**: p. 498-507.

265. Li, Y., X. Han, and L.K. Tamm, *Thermodynamics of fusion peptide-membrane interactions.* Biochemistry, 2003. **42**(23): p. 7245-51.

266. Grove, J. and M. Marsh, *The cell biology of receptor-mediated virus entry.* J Cell Biol, 2011. **195**(7): p. 1071-82.

267. Marsh, M. and A. Helenius, *Virus entry: open sesame.* Cell, 2006. **124**(4): p. 729-40.

268. Van Breedam, W., et al., *Bitter-sweet symphony: glycan-lectin interactions in virus biology.* FEMS Microbiol Rev, 2014. **38**(4): p. 598-632.

269. Jae, L.T. and T.R. Brummelkamp, *Emerging intracellular receptors for hemorrhagic fever viruses.* Trends Microbiol, 2015. **23**(7): p. 392-400.

270. Shimojima, M., et al., *Identification of cell surface molecules involved in dystroglycan-independent Lassa virus cell entry.* J Virol, 2012. **86**(4): p. 2067-78.

271. Martinez, M.G., et al., *Utilization of human DC-SIGN and L-SIGN for entry and infection of host cells by the New World arenavirus, Junin virus.* Biochem Biophys Res Commun, 2013. **441**(3): p. 612-617.

272. Brouillette, R.B., et al., *TIM-1 Mediates Dystroglycan-Independent Entry of Lassa Virus.* J Virol, 2018.

273. Radoshitzky, S.R., et al., *Transferrin receptor 1 is a cellular receptor for New World haemorrhagic fever arenaviruses.* Nature, 2007. **446**(7131): p. 92-6.

274. Flanagan, M.L., et al., *New world clade B arenaviruses can use transferrin receptor 1 (TfR1)-dependent and -independent entry pathways, and glycoproteins from*

human pathogenic strains are associated with the use of TfR1. J Virol, 2008. **82**(2): p. 938-48.

275. Choe, H., et al., *Transferrin receptor 1 in the zoonosis and pathogenesis of New World hemorrhagic fever arenaviruses.* Curr Opin Microbiol, 2011. **14**(4): p. 476-82.

276. Spiropoulou, C.F., et al., *New World arenavirus clade C, but not clade A and B viruses, utilizes alpha-dystroglycan as its major receptor.* J Virol, 2002. **76**(10): p. 5140-6.

277. Shao, J., Y. Liang, and H. Ly, *Human Hemorrhagic Fever Causing Arenaviruses: Molecular Mechanisms Contributing to Virus Virulence and Disease Pathogenesis.* Pathogens, 2015. **4**(2): p. 283-306.

278. Cao, W., et al., *Identification of alpha-dystroglycan as a receptor for lymphocytic choriomeningitis virus and Lassa fever virus.* Science, 1998. **282**(5396): p. 2079-81.

279. Borrow, P. and M.B. Oldstone, *Characterization of lymphocytic choriomeningitis virus-binding protein(s): a candidate cellular receptor for the virus.* J Virol, 1992. **66**(12): p. 7270-81.

280. Raaben, M., et al., *NRP2 and CD63 Are Host Factors for Lujo Virus Cell Entry.* Cell Host Microbe, 2017. **22**(5): p. 688-696 e5.

281. Rambukkana, A., et al., *Role of alpha-dystroglycan as a Schwann cell receptor for Mycobacterium leprae.* Science, 1998. **282**(5396): p. 2076-9.

282. Menke, A. and H. Jockusch, *Decreased osmotic stability of dystrophin-less muscle cells from the mdx mouse.* Nature, 1991. **349**(6304): p. 69-71.

283. Weir, M.L., et al., *Dystroglycan loss disrupts polarity and beta-casein induction in mammary epithelial cells by perturbing laminin anchoring.* J Cell Sci, 2006. **119**(Pt 19): p. 4047-58.

284. Leonoudakis, D., et al., *Dystroglycan controls signaling of multiple hormones through modulation of STAT5 activity.* J Cell Sci, 2010. **123**(Pt 21): p. 3683-92.

285. Cartaud, A., et al., *Evidence for in situ and in vitro association between beta-dystroglycan and the subsynaptic 43K rapsyn protein. Consequence for acetylcholine receptor clustering at the synapse.* J Biol Chem, 1998. **273**(18): p. 11321-6.

286. Henry, M.D. and K.P. Campbell, *Dystroglycan inside and out.* Curr Opin Cell Biol, 1999. **11**(5): p. 602-7.

287. Akhavan, A., et al., *Loss of cell-surface laminin anchoring promotes tumor growth and is associated with poor clinical outcomes.* Cancer Res, 2012. **72**(10): p. 2578-88.

288. de Bernabe, D.B., et al., *Loss of alpha-dystroglycan laminin binding in epithelium-derived cancers is caused by silencing of LARGE.* J Biol Chem, 2009. **284**(17): p. 11279-84.

289. Kunz, S., et al., *Posttranslational modification of alpha-dystroglycan, the cellular receptor for arenaviruses, by the glycosyltransferase LARGE is critical for virus binding.* J Virol, 2005. **79**(22): p. 14282-96.

290. Yurchenco, P.D. and B.L. Patton, *Developmental and pathogenic mechanisms of basement membrane assembly.* Curr Pharm Des, 2009. **15**(12): p. 1277-94.

291. Leonoudakis, D., et al., *Endocytic trafficking of laminin is controlled by dystroglycan and is disrupted in cancers.* J Cell Sci, 2014. **127**(Pt 22): p. 4894-903.

292. Ervasti, J.M., A.L. Burwell, and A.L. Geissler, *Tissue-specific heterogeneity in alpha-dystroglycan sialoglycosylation. Skeletal muscle alpha-dystroglycan is a latent receptor for Vicia villosa agglutinin b4 masked by sialic acid modification.* J Biol Chem, 1997. **272**(35): p. 22315-21.

293. Ervasti, J.M. and K.P. Campbell, *A role for the dystrophin-glycoprotein complex as a transmembrane linker between laminin and actin.* J Cell Biol, 1993. **122**(4): p. 809-23.

294. Ervasti, J.M. and K.P. Campbell, *Membrane organization of the dystrophin-glycoprotein complex.* Cell, 1991. **66**(6): p. 1121-31.

295. Chiba, A., et al., *Structures of sialylated O-linked oligosaccharides of bovine peripheral nerve alpha-dystroglycan. The role of a novel O-mannosyl-type oligosaccharide in the binding of alpha-dystroglycan with laminin.* J Biol Chem, 1997. **272**(4): p. 2156-62.

296. Kunz, S., et al., *Characterization of the interaction of lassa fever virus with its cellular receptor alpha-dystroglycan.* J Virol, 2005. **79**(10): p. 5979-87.

297. Kunz, S., et al., *Molecular analysis of the interaction of LCMV with its cellular receptor [alpha]-dystroglycan.* J Cell Biol, 2001. **155**(2): p. 301-10.

298. Kanagawa, M., et al., *Molecular recognition by LARGE is essential for expression of functional dystroglycan.* Cell, 2004. **117**(7): p. 953-64.

299. Rojek, J.M., et al., *Old World arenavirus infection interferes with the expression of functional alpha-dystroglycan in the host cell.* Mol Biol Cell, 2007. **18**(11): p. 4493-507.

300. Jae, L.T., et al., *Deciphering the glycosylome of dystroglycanopathies using haploid screens for lassa virus entry.* Science, 2013. **340**(6131): p. 479-83.

301. Carette, J.E., et al., *Ebola virus entry requires the cholesterol transporter Niemann-Pick C1.* Nature, 2011. **477**(7364): p. 340-3.

302. Pillay, S. and J.E. Carette, *Hunting Viral Receptors Using Haploid Cells.* Annu Rev Virol, 2015. **2**(1): p. 219-39.

303. Carette, J.E., et al., *Haploid genetic screens in human cells identify host factors used by pathogens.* Science, 2009. **326**(5957): p. 1231-5.

304. Ng, M., et al., *Cell entry by a novel European filovirus requires host endosomal cysteine proteases and Niemann-Pick C1.* Virology, 2014. **468-470**: p. 637-46.

305. Aman, M.J., *Chasing Ebola through the Endosomal Labyrinth.* MBio, 2016. **7**(2): p. e00346.

306. Miller, E.H., et al., *Ebola virus entry requires the host-programmed recognition of an intracellular receptor.* EMBO J, 2012. **31**(8): p. 1947-60.

307. Ndungo, E., et al., *A Single Residue in Ebola Virus Receptor NPC1 Influences Cellular Host Range in Reptiles.* mSphere, 2016. **1**(2).

308. Ng, M., et al., *Filovirus receptor NPC1 contributes to species-specific patterns of ebolavirus susceptibility in bats.* Elife, 2015. **4**.

309. Li, G., et al., *The dual role of tetraspanin CD63 in HIV-1 replication.* Virol J, 2014. **11**: p. 23.

310. Clark, L.E., et al., *Vaccine-elicited receptor-binding site antibodies neutralize two New World hemorrhagic fever arenaviruses.* Nat Commun, 2018. **9**(1): p. 1884.

311. Hashiguchi, T., et al., *Structures of the prefusion form of measles virus fusion protein in complex with inhibitors.* Proc Natl Acad Sci U S A, 2018. **115**(10): p. 2496-2501.

312. Kadam, R.U. and I.A. Wilson, *Structural basis of influenza virus fusion inhibition by the antiviral drug Arbidol.* Proc Natl Acad Sci U S A, 2017. **114**(2): p. 206-214.

313. Tani, H., *Analyses of Entry Mechanisms of Novel Emerging Viruses Using Pseudotype VSV System.* Trop Med Health, 2014. **42**(2 Suppl): p. 71-82.

314. Lukashevich, I.S., *Advanced vaccine candidates for Lassa fever.* Viruses, 2012. **4**(11): p. 2514-57.

315. WHO, *Clinical management of patients with viral haemorrhagic fever*. 2016.

316. Thomas, E., M.G. Ghany, and T.J. Liang, *The application and mechanism of action of ribavirin in therapy of hepatitis C.* Antivir Chem Chemother, 2012. **23**(1): p. 1-12.

317. Olschlager, S., J. Neyts, and S. Gunther, *Depletion of GTP pool is not the predominant mechanism by which ribavirin exerts its antiviral effect on Lassa virus.* Antiviral Res, 2011. **91**(2): p. 89-93.

318. Bausch, D.G., et al., *Review of the literature and proposed guidelines for the use of oral ribavirin as postexposure prophylaxis for Lassa fever.* Clin Infect Dis, 2010. **51**(12): p. 1435-41.

319. Raabe, V. and J. Koehler, *Laboratory Diagnosis of Lassa Fever.* J Clin Microbiol, 2017. **55**(6): p. 1629-1637.

320. Bossi, P., et al., *Bichat guidelines for the clinical management of haemorrhagic fever viruses and bioterrorism-related haemorrhagic fever viruses.* Euro Surveill, 2004. **9**(12): p. E11-2.

321. Hadi, C.M., et al., *Ribavirin for Lassa fever postexposure prophylaxis.* Emerg Infect Dis, 2010. **16**(12): p. 2009-11.

322. Huggins, J.W., *Prospects for treatment of viral hemorrhagic fevers with ribavirin, a broad-spectrum antiviral drug.* Rev Infect Dis, 1989. **11 Suppl 4**: p. S750-61.

323. McCormick, J.B., et al., *Lassa fever. Effective therapy with ribavirin.* N Engl J Med, 1986. **314**(1): p. 20-6.

324. Tam, R.C., J.Y. Lau, and Z. Hong, *Mechanisms of action of ribavirin in antiviral therapies.* Antivir Chem Chemother, 2001. **12**(5): p. 261-72.

325. ter Meulen, J., et al., *Short communication: Lassa fever in Sierra Leone: UN peacekeepers are at risk.* Trop Med Int Health, 2001. **6**(1): p. 83-4.

326. Westover, J.B., et al., *Low-dose ribavirin potentiates the antiviral activity of favipiravir against hemorrhagic fever viruses.* Antiviral Res, 2016. **126**: p. 62-8.

327. Cai, X., et al., *PIKfyve, a class III PI kinase, is the target of the small molecular IL-12/IL-23 inhibitor apilimod and a player in Toll-like receptor signaling.* Chem Biol, 2013. **20**(7): p. 912-21.

328. Johansen, L.M., et al., *A screen of approved drugs and molecular probes identifies therapeutics with anti-Ebola virus activity.* Sci Transl Med, 2015. **7**(290): p. 290ra89.

329. Dyall, J., et al., *Identification of Combinations of Approved Drugs with Synergistic Activity against Ebola Virus in Cell Cultures.* The Journal of Infectious Diseases, 2018.

330. Hessvik, N.P., et al., *PIKfyve inhibition increases exosome release and induces secretory autophagy.* Cell Mol Life Sci, 2016. **73**(24): p. 4717-4737.

331. Nelson, E.A., et al., *The phosphatidylinositol-3-phosphate 5-kinase inhibitor apilimod blocks filoviral entry and infection.* PLoS Negl Trop Dis, 2017. **11**(4): p. e0005540.

332. Krausz, S., et al., *Brief report: a phase IIa, randomized, double-blind, placebo-controlled trial of apilimod mesylate, an interleukin-12/interleukin-23 inhibitor, in patients with rheumatoid arthritis.* Arthritis Rheum, 2012. **64**(6): p. 1750-5.

333. Sands, B.E., et al., *Randomized, double-blind, placebo-controlled trial of the oral interleukin-12/23 inhibitor apilimod mesylate for treatment of active Crohn's disease.* Inflamm Bowel Dis, 2010. **16**(7): p. 1209-18.

334. Kouznetsova, J., et al., *Identification of 53 compounds that block Ebola virus-like particle entry via a repurposing screen of approved drugs.* Emerg Microbes Infect, 2014. **3**(12): p. e84.

335. Jurgeit, A., et al., *Niclosamide is a proton carrier and targets acidic endosomes with broad antiviral effects.* PLoS Pathog, 2012. **8**(10): p. e1002976.

336. Wang, Y.M., et al., *Antiviral activities of niclosamide and nitazoxanide against chikungunya virus entry and transmission.* Antiviral Res, 2016. **135**: p. 81-90.

337. Wu, C.J., et al., *Inhibition of severe acute respiratory syndrome coronavirus replication by niclosamide.* Antimicrob Agents Chemother, 2004. **48**(7): p. 2693-6.

338. Rajamuthiah, R., et al., *Repurposing salicylanilide anthelmintic drugs to combat drug resistant Staphylococcus aureus.* PLoS One, 2015. **10**(4): p. e0124595.

339. Fonseca, B.D., et al., *Structure-activity analysis of niclosamide reveals potential role for cytoplasmic pH in control of mammalian target of rapamycin complex 1 (mTORC1) signaling.* J Biol Chem, 2012. **287**(21): p. 17530-45.

340. Zilbermintz, L., et al., *Identification of agents effective against multiple toxins and viruses by host-oriented cell targeting.* Sci Rep, 2015. **5**: p. 13476.

341. Wishart, D.S., et al., *DrugBank: a comprehensive resource for in silico drug discovery and exploration.* Nucleic Acids Res, 2006. **34**(Database issue): p. D668-72.

342. Johansen, L.M., et al., *FDA-approved selective estrogen receptor modulators inhibit Ebola virus infection.* Sci Transl Med, 2013. **5**(190): p. 190ra79.

343. Ekins, S. and M. Coffee, *FDA approved drugs as potential Ebola treatments.* F1000Res, 2015. **4**: p. 48.

344. Shoemaker, C.J., et al., *Multiple cationic amphiphiles induce a Niemann-Pick C phenotype and inhibit Ebola virus entry and infection.* PLoS One, 2013. **8**(2): p. e56265.

345. Fan, H., et al., *Selective inhibition of Ebola entry with selective estrogen receptor modulators by disrupting the endolysosomal calcium.* Sci Rep, 2017. **7**: p. 41226.

346. Schramm, M., et al., *Acid sphingomyelinase is required for efficient phago-lysosomal fusion.* Cell Microbiol, 2008. **10**(9): p. 1839-53.

347. Beckmann, N., et al., *Inhibition of acid sphingomyelinase by tricyclic antidepressants and analogons.* Front Physiol, 2014. **5**: p. 331.

348. Marala, R.B., et al., *Zoniporide: a potent and highly selective inhibitor of human Na(+)/H(+) exchanger-1.* Eur J Pharmacol, 2002. **451**(1): p. 37-41.

349. Pettersen, J.C., et al., *Neurotoxic effects of zoniporide: a selective inhibitor of the NA+/H+ exchanger isoform 1.* Toxicol Pathol, 2008. **36**(4): p. 608-19.

350. Murphy, E. and D.G. Allen, *Why did the NHE inhibitor clinical trials fail?* J Mol Cell Cardiol, 2009. **46**(2): p. 137-41.

351. Fleisher, L.A., et al., *Efficacy of zoniporide, an Na/H exchange ion inhibitor, for reducing perioperative cardiovascular events in vascular surgery patients.* J Cardiothorac Vasc Anesth, 2005. **19**(5): p. 570-6.

352. Pecheur, E.I., et al., *The Synthetic Antiviral Drug Arbidol Inhibits Globally Prevalent Pathogenic Viruses.* J Virol, 2016. **90**(6): p. 3086-92.

353. Teissier, E., et al., *Mechanism of inhibition of enveloped virus membrane fusion by the antiviral drug arbidol.* PLoS One, 2011. **6**(1): p. e15874.

354. Fink, S.L., et al., *The Antiviral Drug Arbidol Inhibits Zika Virus.* Nature Scientific Reports, 2018.

355. Leneva, I.A., et al., *Characteristics of arbidol-resistant mutants of influenza virus: implications for the mechanism of anti-influenza action of arbidol.* Antiviral Res, 2009. **81**(2): p. 132-40.

356. Brancato, V., et al., *Design of inhibitors of influenza virus membrane fusion: synthesis, structure-activity relationship and in vitro antiviral activity of a novel indole series.* Antiviral Res, 2013. **99**(2): p. 125-35.

357. Teissier, E. and E.I. Pecheur, *Lipids as modulators of membrane fusion mediated by viral fusion proteins.* Eur Biophys J, 2007. **36**(8): p. 887-99.

358. Boriskin, Y.S., E.I. Pecheur, and S.J. Polyak, *Arbidol: a broad-spectrum antiviral that inhibits acute and chronic HCV infection.* Virol J, 2006. **3**: p. 56.

359. Blaising, J., S.J. Polyak, and E.I. Pecheur, *Arbidol as a broad-spectrum antiviral: an update.* Antiviral Res, 2014. **107**: p. 84-94.

360. Pinschewer, D.D., et al., *Recombinant lymphocytic choriomeningitis virus expressing vesicular stomatitis virus glycoprotein.* Proc Natl Acad Sci U S A, 2003. **100**(13): p. 7895-900.

361. Rathbun, J.Y., et al., *Novel Arenavirus Entry Inhibitors Discovered by Using a Minigenome Rescue System for High-Throughput Drug Screening.* J Virol, 2015. **89**(16): p. 8428-43.

362. Martinez-Sobrido, L. and J.C. de la Torre, *Reporter-Expressing, Replicating-Competent Recombinant Arenaviruses.* Viruses, 2016. **8**(7).

363. Hoenen, T., et al., *Minigenomes, transcription and replication competent virus-like particles and beyond: reverse genetics systems for filoviruses and other negative stranded hemorrhagic fever viruses.* Antiviral Res, 2011. **91**(2): p. 195-208.

364. Hass, M., et al., *Replicon system for Lassa virus.* J Virol, 2004. **78**(24): p. 13793-803.

365. Lee, A.M., et al., *Inhibition of cellular entry of lymphocytic choriomeningitis virus by amphipathic DNA polymers.* Virology, 2008. **372**(1): p. 107-17.

366. Cashman, K.A., et al., *Evaluation of Lassa antiviral compound ST-193 in a guinea pig model.* Antiviral Res, 2011. **90**(1): p. 70-9.

367. Larson, R.A., et al., *Identification of a broad-spectrum arenavirus entry inhibitor.* J Virol, 2008. **82**(21): p. 10768-75.

368. York, J., et al., *pH-induced activation of arenavirus membrane fusion is antagonized by small-molecule inhibitors.* J Virol, 2008. **82**(21): p. 10932-9.

369. Shankar, S., et al., *Small-Molecule Fusion Inhibitors Bind the pH-Sensing Stable Signal Peptide-GP2 Subunit Interface of the Lassa Virus Envelope Glycoprotein.* J Virol, 2016. **90**(15): p. 6799-807.

370. Ngo, N., et al., *Identification and Mechanism of Action of a Novel Small-Molecule Inhibitor of Arenavirus Multiplication.* J Virol, 2015. **89**(21): p. 10924-33.

371. Cong, L., et al., *Multiplex genome engineering using CRISPR/Cas systems.* Science, 2013. **339**(6121): p. 819-23.

372. Kuscu, C. and M. Adli, *CRISPR-Cas9-AID base editor is a powerful gain-of-function screening tool.* Nat Methods, 2016. **13**(12): p. 983-984.

373. Coevoets, R., et al., *A reliable cell-based assay for testing unclassified TSC2 gene variants.* Eur J Hum Genet, 2009. **17**(3): p. 301-10.

374. Wang, S., et al., *Metabolism. Lysosomal amino acid transporter SLC38A9 signals arginine sufficiency to mTORC1.* Science, 2015. **347**(6218): p. 188-94.

375. Rohrer, J., et al., *The targeting of Lamp1 to lysosomes is dependent on the spacing of its cytoplasmic tail tyrosine sorting motif relative to the membrane.* J Cell Biol, 1996. **132**(4): p. 565-76.

376. Gerlach, T., et al., *pH Optimum of Hemagglutinin-Mediated Membrane Fusion Determines Sensitivity of Influenza A Viruses to the Interferon-Induced Antiviral State and IFITMs.* J Virol, 2017. **91**(11).

377. Kondo, N., K. Miyauchi, and Z. Matsuda, *Monitoring viral-mediated membrane fusion using fluorescent reporter methods.* Curr Protoc Cell Biol, 2011. **Chapter 26**: p. Unit 26 9.

378. Côté, M., et al., *Small molecule inhibitors reveal Niemann-Pick C1 is essential for Ebola virus infection.* Nature, 2011. **477**(7364): p. 344-8.

379. Cavrois, M., C. De Noronha, and W.C. Greene, *A sensitive and specific enzyme-based assay detecting HIV-1 virion fusion in primary T lymphocytes.* Nat Biotechnol, 2002. **20**(11): p. 1151-4.

380. Yonezawa, A., M. Cavrois, and W.C. Greene, *Studies of ebola virus glycoprotein-mediated entry and fusion by using pseudotyped human immunodeficiency virus type 1 virions: involvement of cytoskeletal proteins and enhancement by tumor necrosis factor alpha.* J Virol, 2005. **79**(2): p. 918-26.

381. Schornberg, K.L., et al., *Alpha5beta1-integrin controls ebolavirus entry by regulating endosomal cathepsins.* Proc Natl Acad Sci U S A, 2009. **106**(19): p. 8003-8.

382. Delos, S.E., et al., *Studies of the "chain reversal regions" of the avian sarcoma/leukosis virus (ASLV) and ebolavirus fusion proteins: analogous residues*

are important, and a His residue unique to EnvA affects the pH dependence of ASLV entry. J Virol, 2010. **84**(11): p. 5687-94.

383. Sorkin, A. and M. Von Zastrow, *Signal transduction and endocytosis: close encounters of many kinds.* Nat Rev Mol Cell Biol, 2002. **3**(8): p. 600-14.

384. Morris, S.J., et al., *Kinetics of pH-dependent fusion between 3T3 fibroblasts expressing influenza hemagglutinin and red blood cells. Measurement by dequenching of fluorescence.* J Biol Chem, 1989. **264**(7): p. 3972-8.

385. de Boer, S.M., et al., *Acid-activated structural reorganization of the Rift Valley fever virus Gc fusion protein.* J Virol, 2012. **86**(24): p. 13642-52.

386. Chen, J.W., et al., *Identification of two lysosomal membrane glycoproteins.* J Cell Biol, 1985. **101**(1): p. 85-95.

387. Andrejewski, N., et al., *Normal lysosomal morphology and function in LAMP-1-deficient mice.* J Biol Chem, 1999. **274**(18): p. 12692-701.

388. Eskelinen, E.-L., Y. Tanaka, and P. Saftig, *At the acidic edge: emerging functions for lysosomal membrane proteins.* Trends in Cell Biology, 2003. **13**(3): p. 137-145.

389. Cook, N.R., P.E. Row, and H.W. Davidson, *Lysosome associated membrane protein 1 (Lamp1) traffics directly from the TGN to early endosomes.* Traffic, 2004. **5**(9): p. 685-99.

390. Fisher-Hoch, S.P. and J.B. McCormick, *Lassa fever vaccine.* Expert Rev Vaccines, 2004. **3**(2): p. 189-97.

391. Gunther, S. and O. Lenz, *Lassa virus.* Crit Rev Clin Lab Sci, 2004. **41**(4): p. 339-90.

392. WHO, *Lassa Fever - Nigeria* 2018, World Health Organization: Switzerland.

393. ProMED-mail., *Lassa Fever - West Africa (29): Nigeria. ProMED-email; 20180530.5829096.*

394. Asogun, D.A., et al., *Molecular diagnostics for lassa fever at Irrua specialist teaching hospital, Nigeria: lessons learnt from two years of laboratory operation.* PLoS Negl Trop Dis, 2012. **6**(9): p. e1839.

395. Fisher-Hoch, S.P., et al., *Crimean Congo-haemorrhagic fever treated with oral ribavirin.* Lancet, 1995. **346**(8973): p. 472-5.

396. Mardani, M., et al., *The efficacy of oral ribavirin in the treatment of crimean-congo hemorrhagic fever in Iran.* Clin Infect Dis, 2003. **36**(12): p. 1613-8.

397. Vigant, F., N.C. Santos, and B. Lee, *Broad-spectrum antivirals against viral fusion.* Nat Rev Microbiol, 2015. **13**(7): p. 426-37.

398. Chopra, G., et al., *Combating Ebola with Repurposed Therapeutics Using the CANDO Platform.* Molecules, 2016. **21**(12).

399. Gehring, G., et al., *The clinically approved drugs amiodarone, dronedarone and verapamil inhibit filovirus cell entry.* J Antimicrob Chemother, 2014. **69**(8): p. 2123-31.

400. Long, J., et al., *Antiviral therapies against Ebola and other emerging viral diseases using existing medicines that block virus entry.* F1000Res, 2015. **4**: p. 30.

401. Madrid, P.B., et al., *A systematic screen of FDA-approved drugs for inhibitors of biological threat agents.* PLoS One, 2013. **8**(4): p. e60579.

402. Madrid, P.B., et al., *Evaluation of Ebola Virus Inhibitors for Drug Repurposing.* ACS Infect Dis, 2015. **1**(7): p. 317-26.

403. Blaising, J., et al., *Arbidol inhibits viral entry by interfering with clathrin-dependent trafficking.* Antiviral Res, 2013. **100**(1): p. 215-9.

404. Brooks, M.J., et al., *Antiviral activity of arbidol, a broad-spectrum drug for use against respiratory viruses, varies according to test conditions.* J Med Virol, 2012. **84**(1): p. 170-81.

405. Deng, H.Y., et al., *Efficacy of arbidol on lethal hantaan virus infections in suckling mice and in vitro.* Acta Pharmacol Sin, 2009. **30**(7): p. 1015-24.

406. Shi, L., et al., *Antiviral activity of arbidol against influenza A virus, respiratory syncytial virus, rhinovirus, coxsackie virus and adenovirus in vitro and in vivo.* Arch Virol, 2007. **152**(8): p. 1447-55.

407. Zhong, Q., et al., *Antiviral activity of Arbidol against Coxsackie virus B5 in vitro and in vivo.* Arch Virol, 2009. **154**(4): p. 601-7.

408. Postnikova, E., et al., *Testing therapeutics in cell-based assays: Factors that influence the apparent potency of drugs.* PLoS One, 2018. **13**(3): p. e0194880.

409. Ren, J., et al., *Target Identification and Mode of Action of Four Chemically Divergent Drugs against Ebolavirus Infection.* J Med Chem, 2018. **61**(3): p. 724-733.

410. Gao, L., et al., *Critical role of the STAT3 pathway in the cardioprotective efficacy of zoniporide in a model of myocardial preservation - the rat isolated working heart.* Br J Pharmacol, 2011. **162**(3): p. 633-47.

411. Tracey, W.R., et al., *Zoniporide: a potent and selective inhibitor of the human sodium-hydrogen exchanger isoform 1 (NHE-1).* Cardiovasc Drug Rev, 2003. **21**(1): p. 17-32.

412. Picazo, E. and F. Giordanetto, *Small molecule inhibitors of ebola virus infection.* Drug Discov Today, 2015. **20**(2): p. 277-86.

413. Xu, M., et al., *Identification of small-molecule inhibitors of Zika virus infection and induced neural cell death via a drug repurposing screen.* Nat Med, 2016. **22**(10): p. 1101-1107.

414. Qiu, S., et al., *Ebola virus requires phosphatidylinositol (3,5) bisphosphate production for efficient viral entry.* Virology, 2018. **513**: p. 17-28.

415. Oestereich, L., et al., *Evaluation of antiviral efficacy of ribavirin, arbidol, and T-705 (favipiravir) in a mouse model for Crimean-Congo hemorrhagic fever.* PLoS Negl Trop Dis, 2014. **8**(5): p. e2804.

416. Pecheur, E.I., et al., *Biochemical mechanism of hepatitis C virus inhibition by the broad-spectrum antiviral arbidol.* Biochemistry, 2007. **46**(20): p. 6050-9.

417. Martin, B., et al., *Filovirus proteins for antiviral drug discovery: A structure/function analysis of surface glycoproteins and virus entry.* Antiviral Res, 2016. **135**: p. 1-14.

418. Nelson, E.A., et al., *Clomiphene and Its Isomers Block Ebola Virus Particle Entry and Infection with Similar Potency: Potential Therapeutic Implications.* Viruses, 2016. **8**(8).

419. Sun, W., et al., *Synergistic drug combination effectively blocks Ebola virus infection.* Antiviral Res, 2017. **137**: p. 165-172.

420. Hulseberg, C.E., et al., *Lamp1 Increases the Efficiency of Lassa Virus Infection by Promoting Fusion in Less Acidic Endosomal Compartments.* MBio, 2018. **9**(1).

421. Zhao, Y., et al., *Toremifene interacts with and destabilizes the Ebola virus glycoprotein.* Nature, 2016. **535**(7610): p. 169-172.

422. Andrews, N.W., P.E. Almeida, and M. Corrotte, *Damage control: cellular mechanisms of plasma membrane repair.* Trends Cell Biol, 2014. **24**(12): p. 734-42.

423. Tani, H., et al., *Analysis of Lujo virus cell entry using pseudotype vesicular stomatitis virus.* J Virol, 2014. **88**(13): p. 7317-30.

424. Acciani, M., et al., *Mutational Analysis of Lassa Virus Glycoprotein Highlights Regions Required for Alpha-Dystroglycan Utilization.* J Virol, 2017. **91**(18).

425. Lavanya, M., et al., *siRNA screen for genes that affect Junin virus entry uncovers voltage-gated calcium channels as a therapeutic target.* Sci Transl Med, 2013. **5**(204): p. 204ra131.

426. Israeli, H., et al., *Mapping of the Lassa virus LAMP1 binding site reveals unique determinants not shared by other old world arenaviruses.* PLoS Pathog, 2017. **13**(4): p. e1006337.

427. Gagarinova, V.M., et al., *[The new chemical preparation arbidol: its prophylactic efficacy during influenza epidemics].* Zh Mikrobiol Epidemiol Immunobiol, 1993(5): p. 40-3.

428. Kiselev, O.I., et al., *[Clinical efficacy of arbidol (umifenovir) in the therapy of influenza in adults: preliminary results of the multicenter double-blind randomized placebo-controlled study ARBITR].* Ter Arkh, 2015. **87**(1): p. 88-96.

429. Leneva, I.A., et al., *Virus susceptibility and clinical effectiveness of anti-influenza drugs during the 2010-2011 influenza season in Russia.* Int J Infect Dis, 2016. **43**: p. 77-84.

430. Wang, M.Z., et al., *[Efficacy and safety of arbidol in treatment of naturally acquired influenza].* Zhongguo Yi Xue Ke Xue Yuan Xue Bao, 2004. **26**(3): p. 289-93.

431. Deng, P., et al., *Pharmacokinetics, metabolism, and excretion of the antiviral drug arbidol in humans.* Antimicrob Agents Chemother, 2013. **57**(4): p. 1743-55.

432. Oestereich, L., et al., *Successful treatment of advanced Ebola virus infection with T-705 (favipiravir) in a small animal model.* Antiviral Res, 2014. **105**: p. 17-21.

433. Raabe, V.N., et al., *Favipiravir and Ribavirin Treatment of Epidemiologically Linked Cases of Lassa Fever.* Clin Infect Dis, 2017. **65**(5): p. 855-859.

434. Rosenke, K., et al., *Use of Favipiravir to Treat Lassa Virus Infection in Macaques.* Emerg Infect Dis, 2018. **24**(9).

435. Uckun, F.M., et al., *Stampidine prevents mortality in an experimental mouse model of viral hemorrhagic fever caused by lassa virus.* BMC Infect Dis, 2004. **4**: p. 1.

436. Uckun, F.M., et al., *Zidampidine, an aryl phosphate derivative of AZT: in vivo pharmacokinetics, metabolism, toxicity, and anti-viral efficacy against hemorrhagic fever caused by Lassa virus.* Bioorg Med Chem, 2005. **13**(9): p. 3279-88.

437. Safronetz, D., et al., *The broad-spectrum antiviral favipiravir protects guinea pigs from lethal Lassa virus infection post-disease onset.* Sci Rep, 2015. **5**: p. 14775.

Appendices

Appendix A. Structures and dose response curves for EBOV and LASV entry inhibitors. Representative dose response curves for LASV and EBOV GP-mediated pseudovirus infection. The chemical structures for each compound were obtained from PubChem (https://pubchem.ncbi.nlm.nih.gov). Drugs exhibit potency against EBOV GP (**A**) or equivalent potency against EBOV and LASV GP (**B**). The structure of arbidol is shown in **C**, with the atomic color-coding scheme indicated beneath each molecule.

A

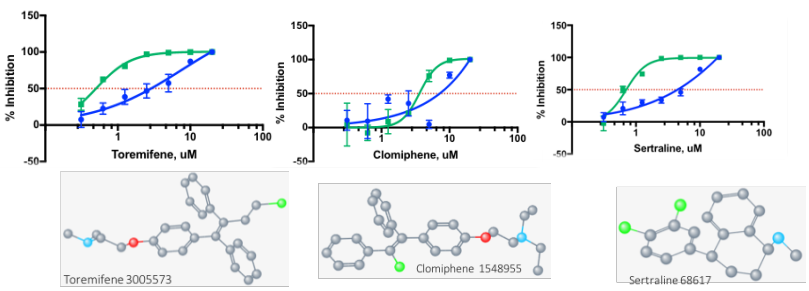

Drugs with greater (> 3-fold IC_{50} difference) potency against Ebola entry

B

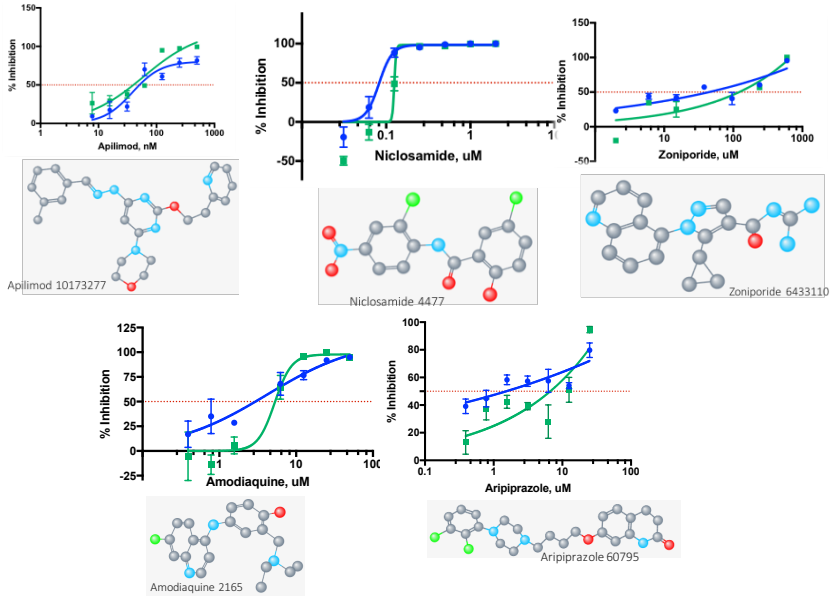

Drugs with roughly equivalent potency against Lassa and Ebola entry

C

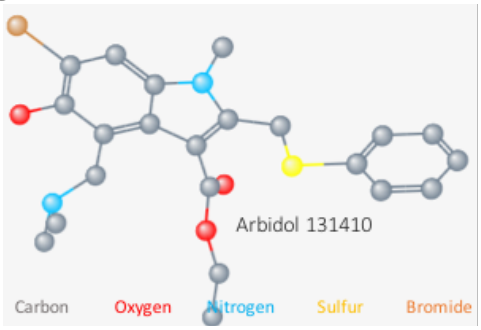

Appendix B.1. Arbidol is less cytotoxic when ethanol is used as a solvent. Triplicate wells of BSC cells were treated with the indicated concentration of arbidol, which had been prepared using either 10% ethanol (EtOH) or DMSO. Dilutions of the stock solution of arbidol (1 mg/ml; ~1.88 mM) were made in OMEM. After incubating the cells in the presence of arbidol for 24 h, the viability was determined by an ATP-based luminescence assay. Signal was normalized to mock treated cells; error bars represent standard deviation for triplicate measurements. This experiment was performed once.

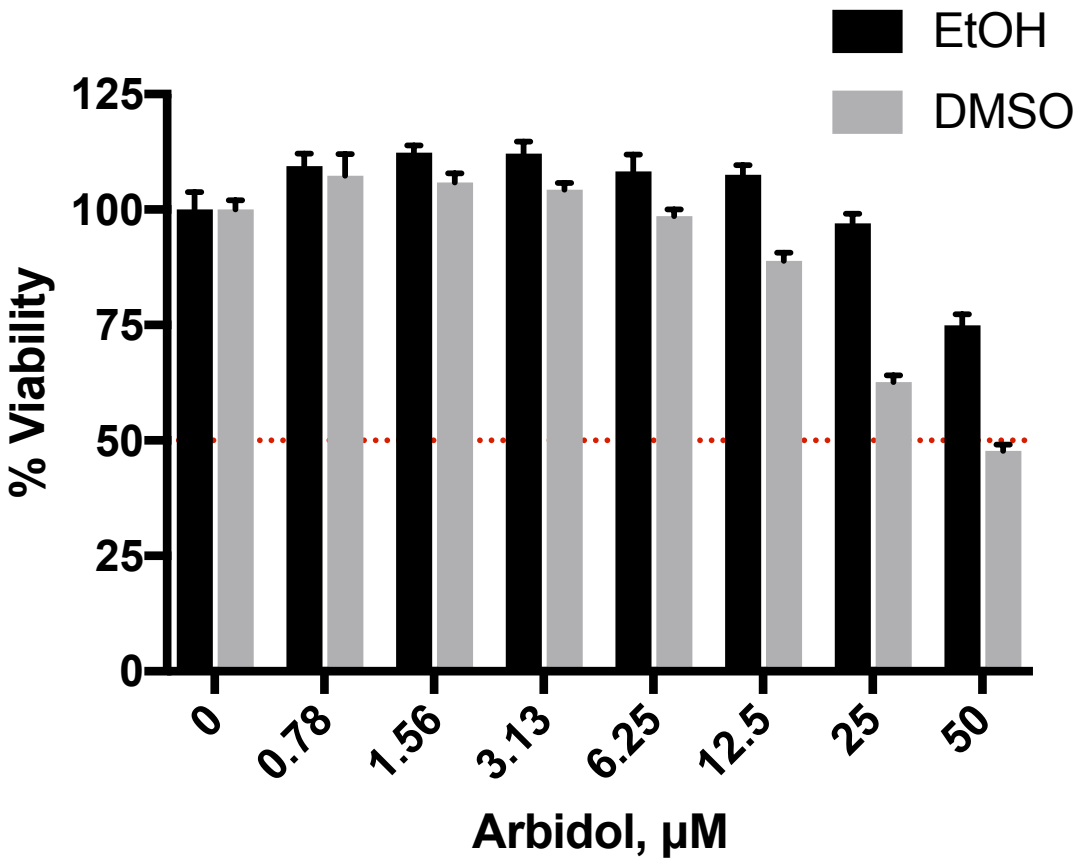
EtOH
DMSO
125
100
75
50
25
0
% Viability
0
0.78
1.56
3.13
6.25
12.5
25
50
Arbidol, μM

Appendix B.2. Visual appearance of Vero cells after prolonged exposure to arbidol. Photos are of cells under 20x magnification after sustained exposed to the indicated dose of arbidol in 10% EtOH (at 24 h intervals). In (**A**), the 10, 20, and 40 μM treatments are omitted from days 2-4 for easier viewing, but the high dose (80 μM) is included. In (**B**), the untreated cells on Day 1 (a day after seeding) is presented alongside of cells on Day 5, with either mock (10% EtOH treatment) or 80 μM arbidol. Under 80 μM arbidol treatment, the monolayer is clearly disrupted as many dead or dying cells have lifted.

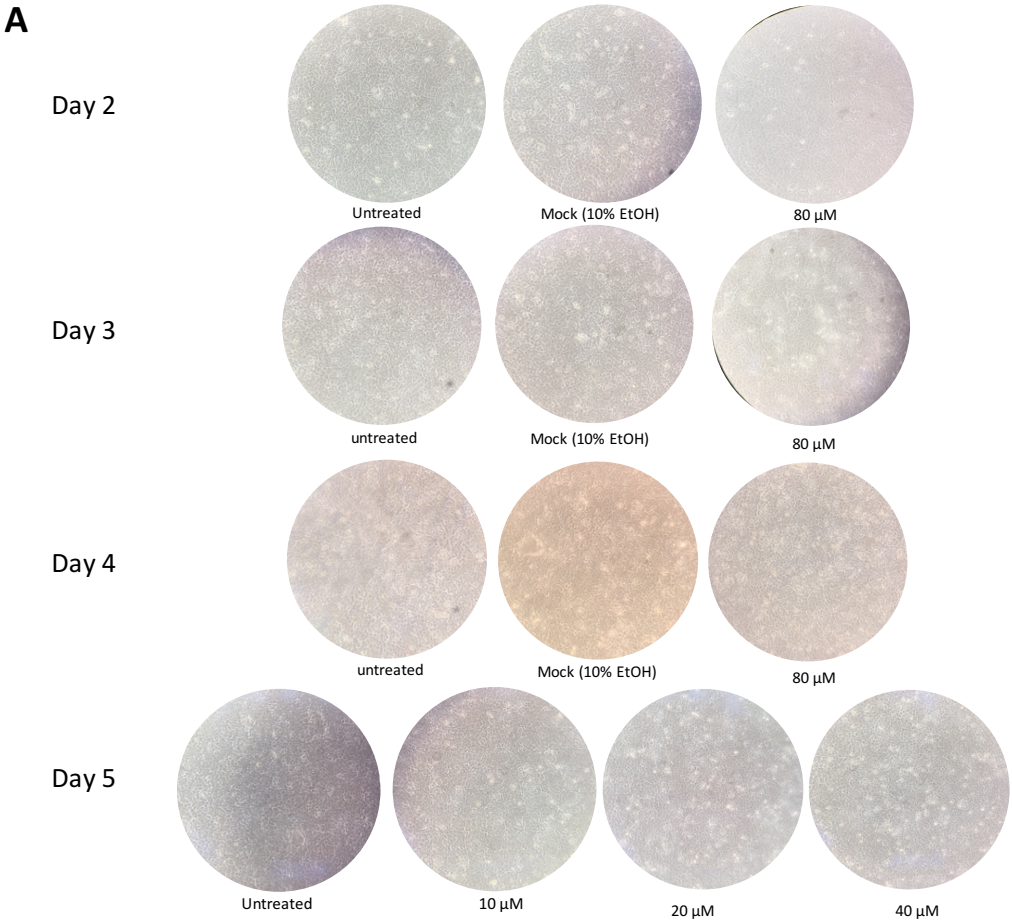
A
Day 2
Untreated
Mock (10% EtOH)
80 µM
Day 3
untreated
Mock (10% EtOH)
80 µM
Day 4
untreated
Mock (10% EtOH)
80 µM
Day 5
Untreated
10 µM
20 µM
40 µM

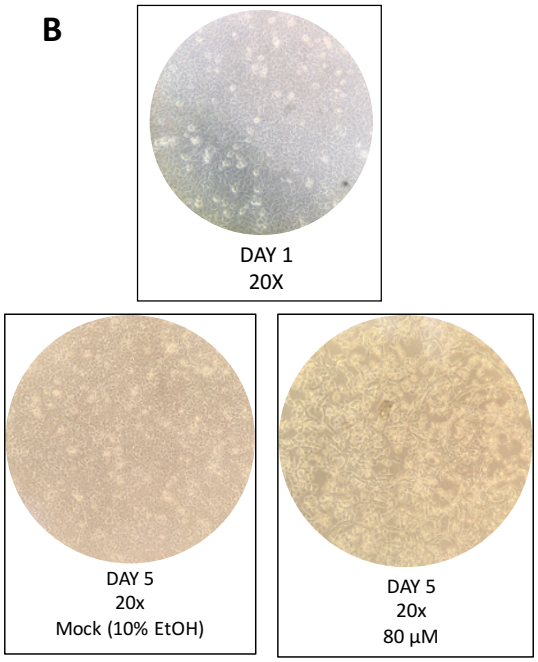
B
DAY 1
20X
DAY 5
20x
Mock (10% EtOH)
DAY 5
20x
80 µM

Appendix B.3. Temperature- and pH-dependence of LASV GP1 dissociation. Blot of pH-dependent dissociation of 44 kDa GP1 subunit (supernatant, right) from the bead-captured GP fraction (pellet, left) (**A**). GP1 dissociation after a 1 min pulse at the indicated pH is shown at three temperatures: 4, 25, 37°C (from top to bottom). The graphical plot in **B** depicts the percentage of GP1 detected in the supernatant fraction over the total amount of GP1 in both pellet and supernatant fractions. The pH-dependence of dissociation after a 1 min pH pulse at the 37°C optimal dissociation temperature is shown in **C**. Shedding of LASV GP1 is half maximal at pH ~ 6.4, as indicated by the horizontal dashed red line (**D**).

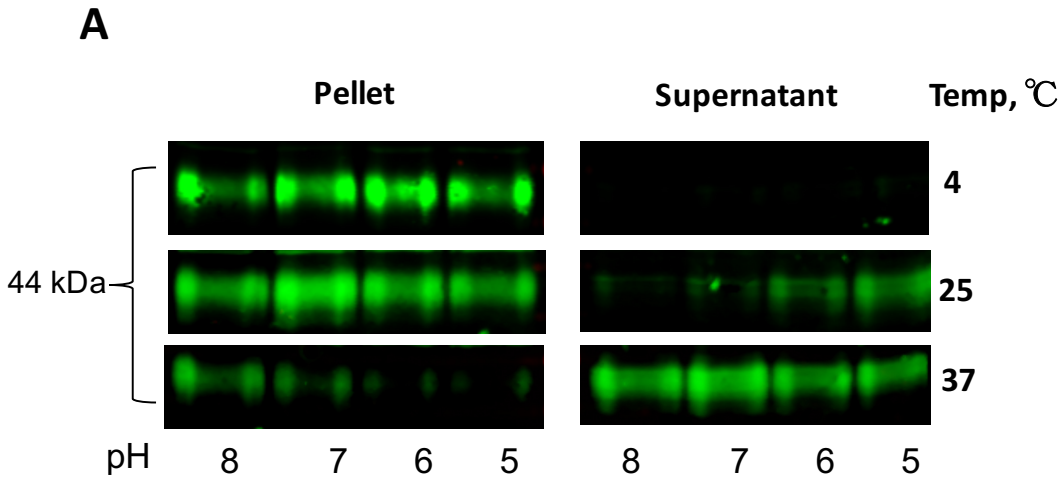
A
Pellet
Supernatant
Temp, ℃
44 kDa
4
25
37
pH
8
7
6
5
8
7
6
5

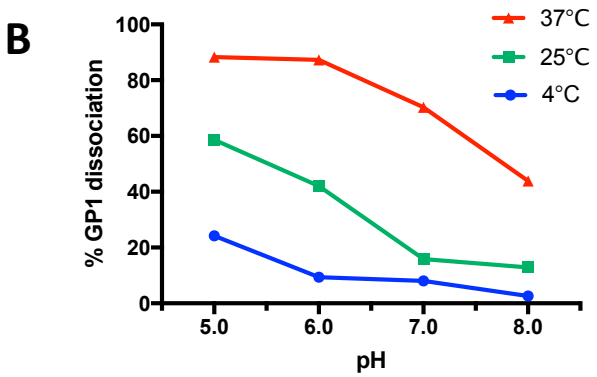
B
% GP1 dissociation
100
80
60
40
20
0
5.0
6.0
7.0
8.0
pH
37°C
25°C
4°C

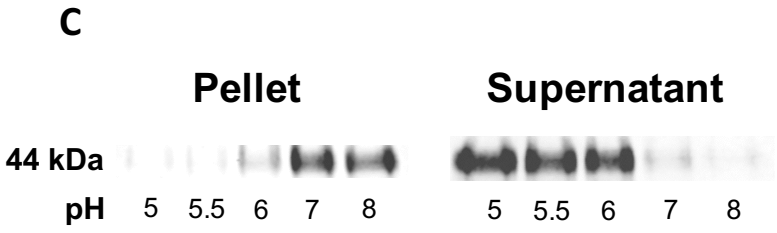
C
Pellet
Supernatant
44 kDa
pH
5
5.5
6
7
8
5
5.5
6
7
8

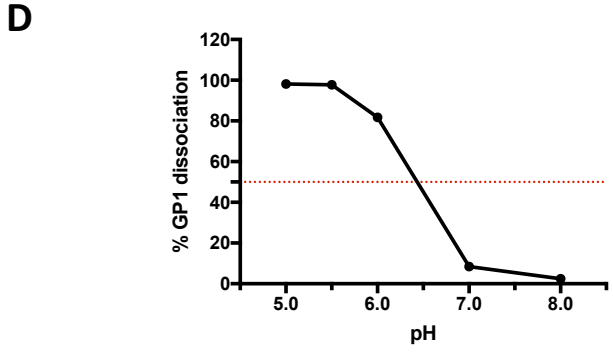
D
% GP1 dissociation
120
100
80
60
40
20
0
5.0
6.0
7.0
8.0
pH